

Breast Cancer Antiestrogen Resistance-3 (BCAR3) in mammary gland development and breast cancer

Allison Margarethe Cross
Royersford, PA

B.S. Lycoming College 2010

A Dissertation presented to the Graduate Faculty
of the University of Virginia in Candidacy for the Degree of
Doctor of Philosophy

Department of Microbiology, Immunology, and Cancer

University of Virginia
May, 2016

Abstract

Despite increased early detection and improved treatment options, breast cancer remains the second leading cause of cancer deaths among women. The majority of breast cancer mortalities are the consequence of therapeutic-resistant metastatic disease. A better understanding of the genetic alterations and signaling pathways involved in breast cancer progression and therapeutic resistance is required to identify new and better therapeutic targets to combat this disease. Breast Cancer Antiestrogen-3 (BCAR3) has been identified as an adaptor molecule that is upregulated in aggressive breast cancer cell lines, where it contributes to increased proliferation, migration, and invasion. The work presented in this thesis focuses on understanding BCAR3 signaling in breast cancer progression as well as mammary gland morphogenesis. The data presented demonstrate that BCAR3 controls adhesion turnover, migration, and invasion through interactions with the adaptor molecule p130^{Cas} (Cas). In addition, BCAR3 was found to be upregulated and differentially expressed during tumor progression in the MMTV-polyoma middle T (PyMT) mouse model of spontaneous breast cancer. Preliminary xenograft studies in mice reveal that BCAR3 expression accelerates tumor formation and controls total tumor burden in MDA-MB-231 breast tumors. Future studies are needed to determine if BCAR3 can regulate the growth of established tumors and promote metastasis, and if interactions with Cas are required for its functions *in vivo*.

Notably, many of the signaling pathways that regulate tumor progression are also involved in normal development. Thus, by gaining a better understanding of how proteins regulate normal development, we can improve our understanding of how they can be used and/or disrupted to promote cancer progression. BCAR3 expression was found to be upregulated in mammary glands of pubertal and pregnant mice. Despite the established proliferative, migratory, and invasive functions of BCAR3 in breast cancer cells, BCAR3 does not appear to promote these functions in mammary epithelial cells during mammary

morphogenesis. Preliminary studies analyzing mammary glands of BCAR3 knockout mice revealed enhanced ductal outgrowth and reduced numbers of terminal end buds during puberty, a phenotype consistent with accelerated mammary gland development. These data suggest that BCAR3 may normally function to suppress mammary gland development. Further studies are needed to determine if the putative suppressive role of BCAR3 during mammary gland development stems from a function of BCAR3 in the epithelial or stromal cells of the gland. Understanding how BCAR3 acts to suppress normal mammary gland development may provide insight into as-yet-unknown functions of BCAR3 in epithelial and non-epithelial cells.

Based on the work presented in this thesis, and the established functions of BCAR3, we propose that BCAR3 may be a useful biomarker and/or therapeutic target for breast cancer. Future studies are needed to determine if there is a correlation between BCAR3 protein expression and tumor subtype, tumor grade, metastasis, therapeutic response, and relapse-free and overall survival. These data will in turn determine whether BCAR3 could serve as biomarker for metastasis and/or sensitivity to Src and TGF- β inhibitors. Additionally, if the BCAR3/Cas complex proves to be a driver of breast tumor growth and progression, it will be important to explore novel approaches for targeting the complex, including BCAR3-specific siRNAs or small molecule and/or peptide inhibitors to block BCAR3/Cas interactions.

Table of Contents

Abstract.....	i
Table of Contents	iii
List of Figures.....	viii
List of Abbreviations	xi
Chapter 1: Introduction	1
1.1 Normal mammary gland development	2
1.2 Breast cancer development and pathology	8
1.3 Molecular and genetic classification of breast cancer.....	12
1.4 Breast cancer metastasis.....	13
1.5 Current breast cancer treatments.....	16
1.6 The BCAR3/Cas/c-Src signaling complex	17
1.6.1 BCAR3	17
1.6.2 Cas.....	22
1.6.3 c-Src.....	27
1.7 Significance and overview.....	32
Chapter 2: Breast Cancer Antiestrogen Resistance 3 (BCAR3) – p130Cas interactions promote adhesion disassembly and invasion in breast cancer cells	34
2.1 Introduction.....	34
2.2 Results	35
2.2.1 The entire cellular pool of BCAR3 is in complex with Cas in invasive breast cancer cells	35
2.2.2 Localization of BCAR3 to adhesions does not require a functional SH2 domain or direct interaction with Cas.....	38

2.2.3	Direct interaction between BCAR3 and Cas is required for efficient adhesion disassembly in BT549 breast cancer cells.....	41
2.2.4	Direct interaction between BCAR3 and Cas promotes breast tumor cell invasion in 3D and chemotaxis toward serum	54
2.2.5	BCAR3 is co-expressed with Cas in multiple subtypes of human breast tumors	64
2.3	Discussion	64
2.3.1	BCAR3 targeting to adhesions is multi-factorial	67
2.3.2	BCAR3/Cas interactions are required for efficient BCAR3-mediated adhesion disassembly, migration, invasion, and Rac1 activity	67
2.3.3	BCAR3/Cas functions as an oncogenic protein complex in invasive breast tumor cells.....	72
Chapter 3: Breast Cancer Antiestrogen Resistance 3 (BCAR3) accelerates time-to-tumor appearance and regulates tumor burden <i>in vivo</i>		
3.1	Introduction.....	73
3.2	Results	75
3.2.1	BCAR3 is upregulated and differentially expressed during tumor progression	75
3.2.2	Co-expression of BCAR3 and cyclin D1 can be observed in PyMT tumors	78
3.2.3	BCAR3 accelerates time-to-tumor appearance and increases total tumor burden <i>in vivo</i>	78
3.3	Discussion	86
3.3.1	How does BCAR3 regulate primary tumor formation?	87
3.3.2	Does BCAR3 regulate tumor growth in established tumors?	88

3.3.3	Is there a role for BCAR3 in tumor metastasis?	89
Chapter 4: Breast Cancer Antiestrogen Resistance 3 (BCAR3) is a potential negative regulator of normal mammary gland development		
		91
4.1	Introduction.....	91
4.2	Results	95
4.2.1	BCAR3 expression is upregulated during mammary gland development.....	95
4.2.2	BCAR3 is expressed but not upregulated during branching morphogenesis in mammary epithelial organoid cultures	101
4.2.3	BCAR3 knockout mice exhibit altered mammary gland development...	101
4.2.4	BCAR3 is not required for MCF10A acini formation.....	106
4.3	Discussion	119
Chapter 5: Perspectives		
		124
5.1	How does BCAR3 function as a negative regulator of mammary gland development?	125
5.1.1	Is BCAR3 loss in epithelial or stromal cells responsible for the control of ductal outgrowth during mammary gland development?	126
5.1.2	How might BCAR3 function in epithelial cells to slow mammary gland development?.....	127
5.1.3	How might BCAR3 function in stroma cells to slow mammary gland development?.....	129
5.1.4	Does BCAR3 regulate the mammary gland during pregnancy, lactation, and involution?	130
5.2	How does BCAR3 regulate tumor progression?	131

5.2.1	Is the ability of BCAR3 to tumor progression dependent on Src?	132
5.2.2	Could BCAR3 be a regulator of TGF- β signaling?	134
5.2.2.1	Cas as a regulator of canonical and non-canonical TGF- β signaling	134
5.2.2.2	Does BCAR3 regulate canonical and non-canonical signaling downstream of TGF- β in cancer cells?	135
5.2.2.3	TGF- β signaling in epithelial cells during mammary gland development	137
5.2.3	How could BCAR3 promote tumor progression independently of Src activity?	138
5.3.	Does BCAR3 promote metastasis?	139
5.4	Can BCAR3 serve as a potential biomarker and/or therapeutic target in breast cancer patients?	140
5.4.1	BCAR3 as a biomarker.....	141
5.4.2	BCAR3 as a therapeutic target.....	143
Chapter 6: Materials and Methods.....		147
6.1	Antibodies and reagents	147
6.2	Expression vectors.....	147
6.3	Cell culture.....	149
6.3.1	3D cell culture	150
6.3.2	Mammary epithelial organoid culture.....	150
6.4	Plasmid transfection, lentivirus production and infection	151
6.5	Immunoprecipitation, immunoblotting and immunofluorescence	151
6.6	Live-cell imaging and adhesion turnover analysis	152

6.7	Rac activity assays	153
6.8	Transwell migration assays.....	153
6.9	Protein degradation studies	154
6.10	Mice.....	154
6.11	Whole mounts.....	155
6.12	Immunohistochemistry	155
6.13	IVIS imaging	155
6.14	Statistical analysis	156
Appendix 1: Control of Cas expression by BCAR3		157
A1.1	Introduction	157
A1.2	Results.....	157
A1.2.1	BCAR3 promotes Cas stabilization through direct binding	157
A1.2.2	Cell line-specific control of Cas protein expression by BCAR3	158
A1.3	Discussion	163
A1.3.1	Control of BCAR3 expression by Cas	163
A1.3.2	The mechanism of Cas stabilization by BCAR3	164
A1.3.3	Differences in BCAR3 shRNA vs siRNA knockdown on Cas protein levels	165
A1.3.4	Cell line-specific control of Cas protein expression by BCAR3	165
List of References		166

List of Figures

Figure 1.1.	Structure of the terminal end bud (TEB)	3
Figure 1.2.	Schematic of mouse mammary gland development	5
Figure 1.3.	Comparison of murine and human mammary glands.....	9
Figure 1.4.	Structural features and binding partners of BCAR3	19
Figure 1.5.	Structural features and binding partners of Cas	23
Figure 1.6.	Structural features and conformations of c-Src.....	28
Figure 2.1.	The entire cellular pool of BCAR3 is in complex with Cas	36
Figure 2.2.	BCAR3 localization in adhesions does not require a functional SH2 domain or interaction with Cas	39
Figure 2.3.	Direct interaction between BCAR3 and Cas is required for efficient dissociation of BCAR3 from adhesions.....	43
Figure 2.4.	WT and L/R BCAR3 have similar half-lives.....	46
Figure 2.5.	BCAR3 is not in complex with talin or α -actinin.....	48
Figure 2.6.	Direct interaction between BCAR3 and Cas is required for efficient dissociation of talin from adhesions	50
Figure 2.7.	Direct interactions between BCAR3 and Cas are required for efficient incorporation and turnover of α -actinin in adhesions.....	52
Figure 2.8.	BCAR3/Cas interactions are required for BCAR3 dependent Rac activity	55
Figure 2.9.	BCAR3 promotes invasion of MDA-MB-231 cells in 3D Matrigel culture	57
Figure 2.10.	Direct interaction between BCAR3 and Cas is required for invasion of MDA- MB-231 cells in 3D Matrigel culture and chemotaxis toward serum	60

Figure 2.11.	Direct interaction between BCAR3 and Cas is required for invasion of Hs578T cells in 3D Matrigel culture	62
Figure 2.12.	BCAR3 is co-expressed with Cas in multiple subtypes of human breast tumors	65
Figure 2.13.	BCAR3/Cas interactions promote efficient adhesion complex disassembly and invasion	68
Figure 3.1.	BCAR3 is upregulated and differentially expressed during PyMT tumor development.....	76
Figure 3.2.	Co-expression of BCAR3 and cyclin D1 can be observed in PyMT tumors	79
Figure 3.3.	BCAR3 accelerates time-to-tumor appearance and enhances tumor burden in MDA-MB-231 xenograft tumors	82
Figure 3.4.	BCAR3 is expressed in tumors formed from shBCAR3-infected cells.....	84
Figure 4.1.	Similarities between mammary gland development and breast cancer progression	92
Figure 4.2.	BCAR3 expression is upregulated in mammary glands of mice during puberty	96
Figure 4.3.	BCAR3 expression is upregulated in mammary glands of pregnant mice	99
Figure 4.4.	BCAR3 is expressed in mammary organoids but expression is not upregulated upon FGF-stimulated branching.....	102
Figure 4.5.	BCAR3 knockout mice show altered mammary gland development during puberty	104
Figure 4.6.	MCF10A acinar morphogenesis results in formation of structures <i>in vitro</i> that closely resemble mammary alveoli <i>in vivo</i>	107

Figure 4.7.	BCAR3 expression is highest during early acinar morphogenesis and regulates acinar size	110
Figure 4.8.	BCAR3 controls proliferation and luminal clearing, but not apoptosis, in MCF10A acini.....	112
Figure 4.9.	Conditional knockdown of BCAR3 at day 4 in culture does not alter MCF10A cell proliferation in acinar structures	115
Figure 4.10.	Constitutive depletion of BCAR3 in MCF10A acini does not affect expression of proteins that regulate cell cycle progression, proliferation, survival, and polarity.....	117
Figure 4.11.	Conditional knockdown of BCAR3 in MCF10A cells prior to plating on Matrigel does not replicate effects observed upon constitutive depletion of BCAR3 in MCF10A	120
Figure A1.1.	BCAR3 promotes Cas stabilization through direct binding.....	159
Figure A1.2.	The control of Cas expression by BCAR3 is cell line specific.....	161

List of Abbreviations

AIP4 = Atrophin-1-interacting protein 4

AHD = Atypical ductal hyperplasia

ANOVA = Analysis of variance

APC/C = Anaphase-promoting complex/cyclosome

BCAR3 = Breast Cancer Antiestrogen Resistance 3

BTRF = Biorepository and Tissue Research Facility

Cas = p130^{Cas}

CHX = Cyclohexamide

CML = Chronic myeloid leukemia

C-terminal = Carboxy terminal

C-terminus = Carboxy terminus

DCIS = Ductal carcinoma in situ

Dox = Doxycycline

JNK = c-Jun N-terminal protein kinase

ECM = Extracellular matrix

EFS = Embryonal Fyn-associated substrate

EGF = Epidermal growth factor

EGFR = Epidermal growth factor receptor

EMT = Epithelial-to-mesenchymal transition

ER = Estrogen receptor

ERK = Extracellular-signal-regulated kinase

FAK = Focal adhesion kinase

FBS = Fetal bovine serum

FEA = Flat epithelial atypia

FGF = Fibroblast growth factor

GEF = Guanine-nucleotide exchange factor

GFP = Green fluorescent protein

GTP = Guanosine triphosphate

H&E = Hematoxylin and eosin

HER2 = Human epidermal growth factor receptor 2

IDC = Invasive ductal carcinoma

IGF-1 = Insulin-like growth factor 1

IGF1R = Insulin-like growth factor 1 receptor

IHC = Immunohistochemistry

IL = Interleukin

IP = Immunoprecipitation

ITS= Insulin-transferrin-sodium selenite

IVIS = *In vivo* imaging system

KO = Knockout

LN = Lymph node

MAPK = Mitogen-activated protein kinase

MEFs = Mouse embryo fibroblasts

MIN = Mammary intra-epithelial neoplasia

MMTV = Mouse mammary tumor virus

mRNA = Messenger RNA

NSP = Novel Src homology 2-containing protein

N-terminal = Amino terminal

PAK = p21 activated kinase

PI3K = Phosphoinositide 3-kinase

PDGFR = Platelet-derived growth factor receptor

PPI = Protein-protein interaction

PR = Progesterone receptor
PTP α = Protein tyrosine phosphatase alpha
PyMT = Polyoma middle T
RIPA = Radioimmunoprecipitation assay
Src = c-Src
siRNA = Small interfering RNA
SEM = Standard error of the mean
SH = Src homology
shRNA = Short hairpin RNA
TDLU = Terminal ductal-lobular unit
T β R-II = TGF β type II receptor
TEB = Terminal end bud
TGF- β = Transforming growth factor beta
TIRF = Total internal reflection fluorescence
TN = Triple negative
TNBC = Triple negative breast cancer
VEGFR = Vascular endothelial growth factor
WT = Wildtype

Chapter 1: Introduction

Breast cancer is currently the second most common cancer among women, with over 240,000 new cases expected to be diagnosed in the US during 2016 (American Cancer Society, 2016). Over the years, deaths due to breast cancer have been declining and this decline is credited to early detection, increased awareness, and improved treatment options. Despite this, breast cancer remains the second leading cause of cancer deaths among women (American Cancer Society, 2016).

The main focus of this thesis is on understanding the contribution of a molecular signaling pathway comprised of Breast Cancer Antiestrogen Resistance-3 (BCAR3), p130^{Cas} (Cas), and c-Src (Src) to breast cancer progression and mammary gland development. This chapter will begin with an overview of mammary gland development followed by a review of the molecular and genetic classifications of breast cancer. It then addresses the current state of knowledge about breast cancer metastasis and treatment options. This is followed by a detailed description of what is known about BCAR3, Cas, and Src in breast cancer and mammary gland development. The chapter concludes with an overview of the questions that the work presented in this thesis set out to answer.

1.1 Normal mammary gland development

The mammary gland is composed of a system of ducts and alveoli that are made up of a polarized bilayer of epithelial cells. The inner layer of cells that face the lumen of the ducts and alveoli are the luminal epithelial cells. These cells are surrounded by a layer of myoepithelial cells that are in contact with the laminin-rich basement membrane. The breast epithelia are embedded in the mammary stroma, which includes adipocytes, fibroblasts, immune cells, blood vessels, and extracellular matrix (ECM) components (Hansen and Bissell, 2000; Wiseman, 2002). Mammary gland morphogenesis begins

during embryogenesis but much of the development, including branching morphogenesis, occurs during adolescence (Sternlicht, 2006). A considerable amount of what we know about mammary gland development has been discerned from studying mouse mammary gland morphogenesis (Hens and Wysolmerski, 2005). The following discussion on mammary gland development will be focused on the mouse and will be followed by a description of the differences between mouse and human mammary gland development.

During embryonic development, milk lines form and placodes develop at specific locations that will give rise to the nipples. Invagination of the cells within the placode into the underlying mesenchyme results in the formation of a mammary bud that penetrates into the fat pad to establish a rudimentary ductal tree present at birth. This tree expands to fill the mammary fat pad during puberty in response to robust hormone signaling (Hens and Wysolmerski, 2005; Sternlicht, 2006). During puberty, terminal end buds (TEBs) form at the tips of the rudimentary ductal tree and begin to penetrate into the mammary fat pad (Sternlicht, 2006) (**Figure 1.1**). As the ducts elongate, the TEBs repeatedly bifurcate and invade into the surrounding fat, resulting in the formation of primary ducts. Secondary branches sprout laterally from these primary ducts. When TEBs reach the end of the fat pad, they regress and differentiate into terminal end ducts. During each estrous cycle, tertiary side branches form from the primary and secondary ducts and alveolar structures develop at the end of the tertiary branches (Sternlicht *et al.*, 2006; Lanigan *et al.*, 2007) (**Figure 1.2**).

The formation of the primary ducts by the TEBs and the development of side branches from these duct are two distinct processes. The TEBs are believed to be pushed into the stroma by rapid proliferation of the luminal epithelial cells inside the TEB. Bifurcation of the TEBs occurs following deposition of fibrous stroma at the branch site. Following bifurcation, the TEBs continue to push through the adipose tissue. Notably, there are no myoepithelial cells present at the invading front of the TEB and no evidence

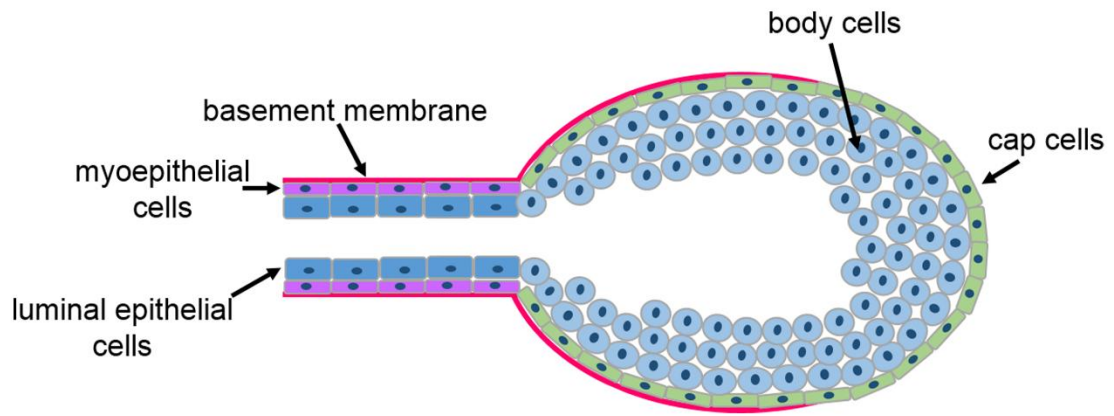


Figure 1.1. Structure of the terminal end bud (TEB)

During puberty, TEBs form at the tips of the rudimentary ductal tree and invade into the fat pad. The bilayer ducts of the developing gland are established as the TEBs move through the fat pad. The tip of the TEB consists of cap cells that are surrounded by only a thin layer of basement membrane. The cap cells at the head of the TEB generate cells of the myoepithelial lineage on the outer-side of the TEB and cells of the luminal lineage, called body cells, inside the TEB. As the TEB moves through the fat pad, the outer layer of cells, surrounded by a highly crosslinked basement membrane, differentiate into myoepithelial cells. Many of the body cells undergo apoptosis and a single layer of cells, in contact with the myoepithelial cells, differentiate into luminal epithelial cells (Smalley and Ashworth, 2003; Sternlicht, 2006).

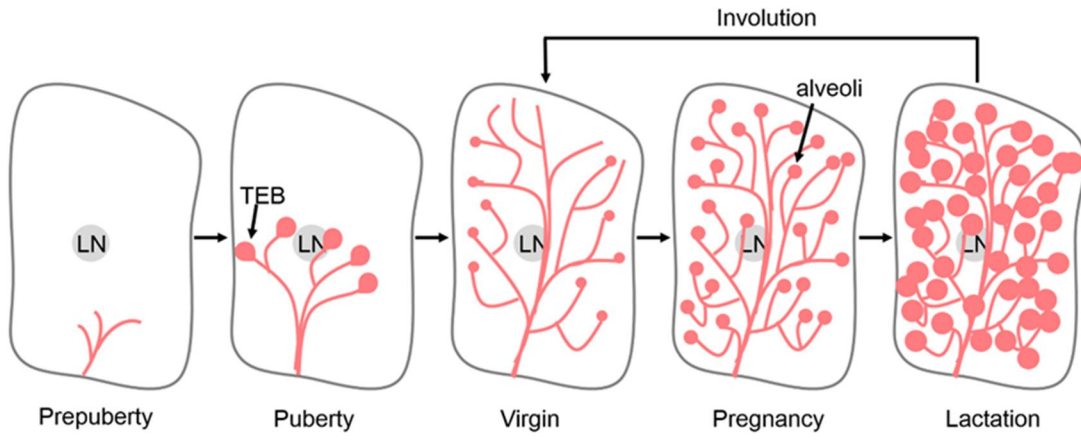


Figure 1.2. Schematic of mouse mammary gland development

Prior to puberty, a rudimentary ductal tree is present. During puberty, robust hormone signaling promotes TEBs to form at the tips of the ducts. The TEBs repeatedly bifurcate and invade into the surrounding fat, resulting in the formation of primary ducts that fill the fat pad. Secondary branches sprout laterally from these primary ducts. During pregnancy, massive amounts of proliferation occur, tertiary side branches form, and alveolar structures develop at the end of the tertiary branches. In mid-pregnancy, the newly developed alveolar buds progressively cleave and differentiate into distinct alveoli. During lactation, the alveoli, which are lined with luminal secretory cells, produce milk. Following weaning, the secretory epithelial cells formed during pregnancy die by apoptosis and the gland is remodeled to resemble that of an adult virgin gland in a process called involution (Hens and Wysolmerski, 2005; Sternlicht, 2006; Lanigan *et al.*, 2007). LN = lymph node. Figure adapted from Manavathi *et al.* (Manavathi *et al.*, 2014).

of enzymatic clearing of stroma as the TEBs progress through the fat pad. For side branches to form, the emerging bud must extend through a layer of myoepithelial cells, degrade the surrounding basement membrane, and invade through a layer of fibrous stroma (Wiseman, 2002; Hinck and Silberstein, 2005).

Following puberty, the next significant tissue remodeling of the mammary gland occurs during pregnancy. At this time, extensive proliferation occurs within the ductal tree, resulting in the formation of tertiary branches and alveolar buds. In mid-pregnancy, the newly developed alveolar buds progressively cleave and differentiate into distinct alveoli. During lactation, the alveoli, which are lined with luminal secretory cells, produce milk. Following weaning, the secretory epithelial cells formed during pregnancy die by apoptosis and the gland is remodeled to resemble that of an adult virgin gland in a process called involution (Oakes *et al.*, 2006; Lanigan *et al.*, 2007) (**Figure 1.2**).

The mouse mammary gland serves as a great model for studying mammary gland development but, despite many similarities, mammary gland development in humans is slightly different than in mice. Mice form a single ductal tree while humans form several ductal trees that merge at the nipple. Also, fetal exposure to maternal hormones in the human results in a small amount of secretory activity during late fetal development and in the newborn infant; this process is absent in mice. Following these early hormone influences, the newborn breast in humans will undergo involution and the ductal structures will remain quiescent until puberty. In mice, the rudimentary tree is destroyed in male mice during gestation while in humans, the male and female breast develop indistinguishably until puberty. During puberty, branching morphogenesis occurs in humans, as it does in mice. In humans however, the lateral branches that form lead to terminal ducts, which in turn give rise to terminal ductal-lobular units (TDLUs). These TDLUs contain numerous acini, which are embedded in a dense fibroblastic stroma that

is much more pronounced than the adipose-rich stroma found in mice (**Figure 1.3**) (Sternlicht *et al.*, 2006; Macias and Hinck, 2012).

1.2 Breast cancer development and pathology

Breast cancer can begin from any of the cell types present in the breast but 95% of human breast cancers arise from the breast epithelium and are thus referred to as adenocarcinomas (Makki, 2015). Rarely, breast cancers originate from the non-epithelial cells in the breast such as connective tissue, muscle and fat and are referred to as sarcomas (Pencavel and Hayes, 2009). Adenocarcinomas in the breast are generally divided into two subtypes, ductal carcinoma and lobular carcinoma. Both of these subtypes are believed to arise in the TDLU of the breast but differences in cell morphology distinguish between the ductal and lobule subtypes (Sgroi, 2010; Makki, 2015). Ductal carcinomas are the most common type of breast cancer, accounting for 80% of all breast cancers diagnosed in the US (Sgroi, 2010).

Ductal carcinoma consists of three characterized stages of pre-invasive disease; flat epithelial atypia (FEA), atypical ductal hyperplasia (ADH), and ductal carcinoma in situ (DCIS). FEA is described as the proliferation of luminal cells of the TDLU, resulting in multiple layers of epithelial cells with low-grade cytological atypia. At this stage, the cells do not fill up the terminal duct and acini but rather grow as single layers that enlarge the TDLU. FEA can progress to ADH, which is characterized by both low-grade cytological atypia and atypical architecture within the TDLU. A larger degree of architectural atypia and increased epithelial proliferation results in the last pre-invasive stage of breast cancer progression, DCIS (Sgroi, 2010). In DCIS, the proliferating epithelial cells fill the ducts of the breast but remained confined within the basement membrane (Sgroi, 2010).

DCIS is generally not life-threatening, but it can be a precursor to invasive carcinoma. The likelihood of DCIS progressing to invasive ductal carcinoma (IDC) is

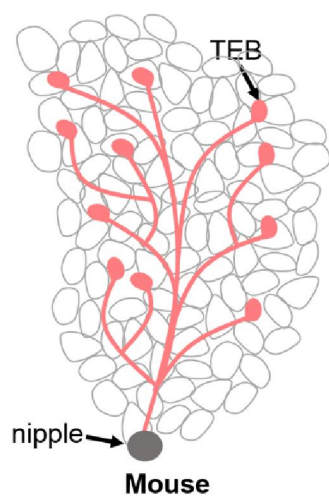
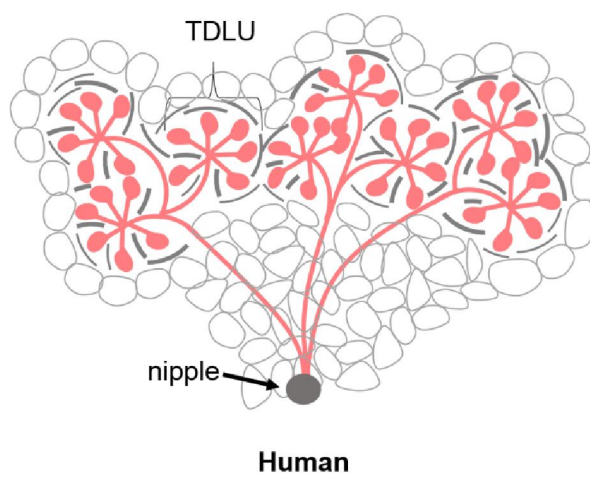
A**B**

Figure 1.3. Comparison of murine and human mammary glands

(A) The murine virgin mammary gland is comprised of a single ductal tree with TEBs that consist of a single bulbous acinar structure. The stroma of the mouse mammary gland is composed predominantly of adipose cells (gray). (B) In humans, the mammary gland consists of several ductal trees that merge at the nipple. Unlike mice, the terminal ducts in the human mammary gland give rise to terminal ductal-lobular units (TDLUs) that contain numerous acini. These acini are embedded in a dense fibroblastic stroma that is much more pronounced than the adipose-rich stroma found in mice (Lanigan *et al.*, 2007; Macias and Hinck, 2012).

proportional to the grade of the DCIS (Makki, 2015). A number of classification systems for DCIS exist but one commonly used system, the van Nuys scoring system, employs a combination of nuclear morphology and the presence or absence of necrosis to divide DCIS into three grades; low-grade, intermediate-grade, and high-grade (Leonard and Swain, 2004; Makki, 2015). In low-grade DCIS, the neoplastic cells have regular to mildly irregular nuclei and the lesions lack necrosis. Intermediate-grade DCIS is classified by the presence of regular to mildly irregular nuclei in combination with comedo necrosis. In high-grade DCIS, cells contain highly atypical, large nuclei and necrosis is generally present (Leonard and Swain, 2004).

When the proliferating neoplastic cells in a DCIS lesion undergo further genetic and epigenetic alterations that allow penetration through the myoepithelial basement membrane into the surrounding breast stroma, the cancer is considered to have progressed to IDC (Sgroi, 2010; Makki, 2015). IDC is characterized by profound heterogeneity such that 75% of IDCs fail to exhibit sufficient morphological distinctions that allow them to be classified as a specific histological subtype (Bombonati and Sgroi, 2011; Makki, 2015). The invasive tumors can be classified by grade, similar to the grading of DCIS, based upon three morphological features of the tumors: the degree of nuclear variability, tubule formation (the extent of normal ductal structures), and mitotic activity. Tumors are given a score of 1 to 3 in each of three histological categories and the scores from each category are combined to classify the tumors as grade 1, 2, or 3. Grade 1 tumors are indicated by a combined score of 2-5, grade 2 tumors have a combined score of 6-7, and tumors scored 8 to 9 are considered grade 3 (Dalton *et al.*, 1994). The tumor grades of invasive ductal carcinoma have been shown to strongly correlate with patient outcome, with patients who have grade 1 tumors experiencing significantly better survival than those with grade 2 and 3 tumors (Elston and Ellis, 1991).

1.3 Molecular and genetic classification of breast cancer

Traditionally, breast cancers have been subtyped based upon expression of 3 molecules; estrogen receptor (ER), progesterone receptor (PR), and human epidermal growth factor receptor 2 (HER2) (Dai *et al.*, 2015). However, breast cancer is a highly heterogeneous disease and, over the past decade, gene expression analysis has led to new classifications of breast cancer. Genomic studies pioneered by Perou *et al.* have resulted in the identification of four intrinsic subtypes of breast cancer; luminal A, luminal B, HER2-enriched, and basal-like (Perou *et al.*, 2000; Sørlie *et al.*, 2001; Prat and Perou, 2011). Since these original studies, a fifth intrinsic subtype of breast cancer, known as claudin-low, has been identified (Prat and Perou, 2011). Clinically, the majority of luminal A tumors are positive for ER and PR, negative for HER2 and are considered to be low grade tumors. Luminal B tumors are generally positive for ER and PR, have variable expression of HER2, and are frequently grade 2 or 3. HER2-enriched tumors are commonly negative for PR and ER and characterized as grade 2 or 3. Basal-like tumors are characterized by expression of basal markers, are typically grade 3, and are usually negative for ER, PR, and HER2 expression (Dai *et al.*, 2015; Makki, 2015). Finally, claudin-low tumors are also frequently ER, PR, and HER2 negative and exhibit a generally poor clinical outcome (Prat and Perou, 2011). With continued advances in genomic analyses, further sub-classification of breast cancers may occur.

The intrinsic subtypes identified by genomic analysis provide significant insight into tumor behaviors including responses to therapy. The microarray data used by Perou to identify the original four intrinsic subtypes has been used to create a 50 gene PCR-based assay known the PAM-50 that is now commercially available (Wallden *et al.*, 2015). In addition to identifying the luminal A, luminal B, HER2-enriched, and basal-like subtypes, this assay is used to predict risk of distant recurrence and overall survival in breast cancer patients (Kittaneh *et al.*, 2013; Wallden *et al.*, 2015; Braunstein and Taghian,

2016). Additional gene assays have been developed and used to predict survival outcome, probability of re-occurrence, and potential therapeutic benefits in breast cancer patients (Dai *et al.*, 2015; Braunstein and Taghian, 2016). Two of these commercially available assays are the Oncotype DX and the Mammaprint gene assay (Kittaneh *et al.*, 2013). The Oncotype DX is a 21 gene assay that has been used clinically to predict re-occurrence for hormone-receptor-positive early breast cancer patients on endocrine therapy (Kittaneh *et al.*, 2013). The 70 gene Mammaprint assay can be used to predict risk for developing metastasis within 10 years following surgical tumor resection in the absence of adjuvant therapy and thus it can be used to help decide whether or not adjuvant therapy should be considered to reduce that risk (Kittaneh *et al.*, 2013; Braunstein and Taghian, 2016). It is interesting to note that these gene assays share very few genes in common but have all been shown to be predictors of metastasis and survival. Notably, the main focus of this thesis is on BCAR3 and its binding partner, p130^{Cas} (Cas), neither of which are present in any of the gene assays discussed above. One reason for this could be that expression and stabilization of these proteins may be regulated at the protein rather than mRNA level.

1.4 Breast cancer metastasis

Among breast cancer patients, it is generally not the primary tumor that causes death, but rather distant metastasis (Wiechmann and Kuerer, 2008). Three years following the initial detection of a primary tumor, 10-15% of patients will develop metastatic disease. Breast cancer patients are at risk of developing metastatic disease throughout their lifetime; it is not uncommon for patients to develop metastases as many as 10 years or more after initial diagnosis. The most frequent sites of breast cancer metastasis are the bone, lung, liver and brain (Weigelt *et al.*, 2005; Soni *et al.*, 2015). As breast cancer is a highly heterogeneous disease, it is critical to determine the risk factors that control the metastatic potential of a tumor (Wiechmann and Kuerer, 2008).

The process of metastasis includes a series of steps known as the metastatic cascade. For metastasis to occur, cells in the primary tumor must locally invade the surrounding tissue and intravasate into the blood or lymphatic system. The circulating tumor cells then travel through the blood stream or the lymphatics to reach distant organs. Once the cells reach a target organ, the cells must adhere to the capillary beds within the tissue before extravasating into the organ. In order to survive and successfully seed in a distant organ, the tumor cells must be able to evade the host's immune response. The process of metastasis requires invasion and migration of the tumor cells and is highly regulated by the tumor microenvironment (TME) at the primary and metastatic sites (Scully *et al.*, 2012).

Several models of breast cancer metastasis have been proposed over the years. The traditional model of metastasis suggested that metastatic potential was acquired late in tumorigenesis and only by a subpopulation of tumor cells (Weigelt *et al.*, 2005). Additional models of breast cancer metastasis include, but are not limited to, the stem cell model, parallel evolution model, and random dissemination model. In the stem cell model, it is proposed that tumors contain rare cells with indefinite proliferative potential, known as cancer stem cells. These cells are believed to drive tumor formation, growth, and metastasis (Weigelt *et al.*, 2005). The parallel evolution model suggests that metastatic disease evolves independently from the primary tumor (Weigelt *et al.*, 2005). The random dissemination model suggests that tumor metastases are the random presentation of disseminating cells. This model argues that all disseminating cells have the capacity to form metastatic tumors, and the cells that successfully form metastatic tumors are the ones that randomly lodge in the capillary bed of an organ that provides a favorable microenvironment (Weigelt *et al.*, 2005; Vogelstein *et al.*, 2013).

Several recent findings challenge the idea that metastases arise from rare cells within a tumor gaining the ability to metastasize. An analysis of pairs of human breast

carcinomas and metastases that develop years later showed that the primary and metastatic tumors have highly similar transcriptomes (Weigelt *et al.*, 2003). In a larger study analyzing many different adenocarcinoma types, some of the primary tumors were found to share the same gene expression profile as the metastatic tumors and those were associated with poor prognosis (Ramaswamy *et al.*, 2003). Strikingly, almost all of the mutations present in metastatic lesions can be found in a large number of cells in the primary tumors (Vogelstein *et al.*, 2013). These findings, along with the ability of gene expression assays to predict the likelihood of metastasis (Kittaneh *et al.*, 2013), suggest that the ability to metastasize may be acquired early during tumor development.

It is important to note that tumor progression and metastasis is believed to be regulated by more than just genetic changes/mutations in the tumors cells. The tumor cells are surrounded by ECM, blood vessels, fibroblast, and various immune cells that collectively make up the tumor microenvironment (TME). The interaction between the tumor cells and the TME plays an important role in mediating both primary tumor growth as well as multiple steps of the metastatic cascade (Weigelt *et al.*, 2005; Sleeman *et al.*, 2012). For example, cancer-associated fibroblasts control primary tumor behavior through secretion of ECM components and by regulation of angiogenesis and immune responses (Quail and Joyce, 2013). Tumor associated macrophages augment invasion of tumor cells by supplying growth factors, regulating production of fibrillar collagen, and enhancing proteolytic ECM remodeling (Quail and Joyce, 2013). Once tumor cells have extravasated into the vasculature, the interaction of tumor cells with platelets helps the cells evade immune cell recognition and enhance their survival (Quail and Joyce, 2013). Furthermore, tumor cells are thought to be able to “prime” metastatic sites by secreting soluble factors such as growth factors. In response to these factors, tumor-associated cells including myeloid-derived suppressive cells and macrophages cluster at metastatic

locations and create an environment conducive to tumor cell adhesion, growth and invasion (Psaila and Lyden, 2009; Condamine *et al.*, 2015).

1.5 Current breast cancer treatments

The current treatment for breast cancer depends on multiple prognostic factors and usually involves surgery in combination with neoadjuvant and/or adjuvant therapy. Neoadjuvant, or “before” surgery, therapy is generally used to debulk tumors to improve surgical outcomes. It can also be used to facilitate breast conservation surgery when patients have large tumors in comparison to their breast. Once tumors are removed, patients may or may not undergo adjuvant, or “after surgery,” treatment. The decision on whether or not patients should receive adjuvant therapy, and the type of therapy they receive, is dependent on a number of factors including lymph node status, tumor grade, hormone receptor and HER2 expression status. Additionally, the multi-gene assays described above can be useful in determining the potential benefit of adjuvant therapy in individual patients (Bourdeanu and Liu, 2015). Patients who present with hormone receptor-positive tumors are treated with chemotherapy as well as targeted hormone therapy post-surgery. Patients who present with HER2-positive tumors are generally treated with a HER2-targeted therapy such as trastuzumab in combination with chemotherapy post-surgery (Bourdeanu and Liu, 2015). For patients with triple negative tumors, there are currently no FDA approved targeted therapies and patients are generally treated with adjuvant chemotherapy (Mohamed *et al.*, 2013). A great deal of effort is being devoted to the identification of novel therapeutic targets for triple negative breast cancer, but the large amount of heterogeneity in these tumors has proven a major obstacle for attaining this goal (Mohamed *et al.*, 2013).

Two of the major challenges in breast cancer treatment are therapeutic resistance and metastasis. Despite the availability and success of targeted therapies for hormone-

positive and HER2 over-expressing breast cancers, many patients experience acquired or de-novo resistance to these therapies (Mohamed *et al.*, 2013). Primary breast tumors are generally not life-threatening; approximately 90% of breast cancer mortalities are the consequence of therapeutic-resistant metastatic disease (Soni *et al.*, 2015). It is believed that 20-50% of patients diagnosed with primary breast cancer will eventually develop metastatic disease and another 6% of patients will present with metastatic disease at the time of diagnosis (Lu *et al.*, 2009). A better understanding of the genetic alterations and signaling pathways that contribute to breast cancer progression and therapeutic resistance is needed in order to develop more effective targeted therapies for both primary and metastatic disease. In this thesis, the ability of BCAR3 and the BCAR3/Cas complex to promote breast cancer progression is investigated and the possibility that the complex could serve as a potential therapeutic target for breast cancer patients is explored.

1.6 The BCAR3/Cas/c-Src signaling complex

The main focus of this thesis is on the adaptor molecular, Breast Cancer Antiestrogen Resistance-3 (BCAR3). BCAR3 is upregulated in breast cancer cell lines, where it interacts with Cas (Schrecengost *et al.*, 2007). Interaction between BCAR3 and Cas promotes Src binding to Cas and subsequent Src-mediated tyrosine phosphorylation of the Cas substrate domain. The BCAR3/Cas/Src complex is present in focal adhesions and has been shown to promote breast cancer cell proliferation, migration, and invasion *in vitro* (Riggins *et al.*, 2003; Makkinje *et al.*, 2009; Schuh *et al.*, 2010; Wallez *et al.*, 2014) (Chapter 2).

1.6.1 BCAR3

BCAR3 is a member of the novel Src homology 2 (SH2) (NSP)-containing protein family that includes two other proteins, NSP1 and NSP3/SHEP1. BCAR3 is composed of

an amino-terminal SH2 domain and a carboxy-terminal guanine-nucleotide exchange factor (GEF)-like domain with sequence homology to the CDC25 family of GEFs (**Figure 1.4**). The SH2 and GEF-like domains are connected by a serine/proline-rich linker region. SH2 domains bind to protein motifs containing phosphorylated tyrosine residues (Vervoort *et al.*, 2007). Thus far, BCAR3 has only been reported to interact with one protein through its SH2 domain, protein tyrosine phosphatase α (PTP α) (Sun *et al.*, 2012). BCAR3 binds to its only other known binding partner, Cas, through its C-terminal GEF-like domain. Notably, despite sequence homology to the GEF domain of CDC25, the BCAR3 GEF-like domain has a “closed” conformation that appears to lack catalytic activity (Mace *et al.*, 2011).

According to the Human Protein Atlas, BCAR3 protein is expressed at low to moderate levels in many normal tissues and is expressed in several cell types including glandular cells, epithelial cells, endothelial cells, myocytes, fibroblast, macrophages, and lymphocytes. BCAR3 is also expressed in multiple types of cancer, including breast, cervical, and skin cancer (Human Protein Atlas). This thesis focuses on the role of BCAR3 in normal breast development and in breast cancer. *In vitro* studies have shown that BCAR3 expression is upregulated in invasive breast cancer cell lines compared to cell lines with low migratory and invasive potential (Near *et al.*, 2007; Schrecengost *et al.*, 2007). Analysis of breast cancer genomic datasets using the CBioPortal for Cancer Genomics reveals that the most common alteration of the gene encoding BCAR3 in invasive breast cancer is amplification (Cerami *et al.*, 2012; Gao *et al.*, 2013). There is only one published study analyzing the relationship between BCAR3 expression and progression-free survival in breast cancer patients. This study reported that high BCAR3 mRNA levels correlated with increased progression-free survival in patients with ER+ breast cancer who received tamoxifen treatment (Guo *et al.*, 2014). This is surprising considering BCAR3 was first identified in a screen for genes whose overexpression

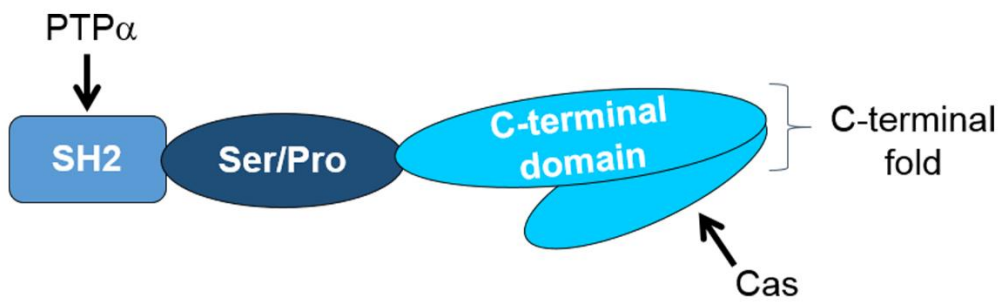


Figure 1.4. Structural features and binding partners of BCAR3

BCAR3 is composed of an amino-terminal SH2 domain, a serine/proline-rich linker, and a carboxy-terminal guanine-nucleotide exchange factor (GEF)-like domain with sequence homology to the CDC25 family of GEFs. BCAR3 has only two established binding partners; protein tyrosine phosphatase α (PTP α) binds to the SH2 domain and Cas binds to the C-terminal domain (Vervoort *et al.*, 2007; Sun *et al.*, 2012). The C-terminal domain of BCAR3 adopts the overall structural fold conformation present in CDC25-homology domains, but it is locked in a “closed” conformation that appears to render it incapable of enzymatic activity (Mace *et al.*, 2011).

conferred antiestrogen resistance in breast cancer cell lines (VanAgthoven *et al.*, 1998). However, it is possible that expression of BCAR3 may be regulated at the protein rather than mRNA level and a detailed analysis of the relationship between BCAR3 protein expression, breast cancer subtypes, and survival outcomes has yet to be published.

Since its identification as a gene product whose overexpression conferred antiestrogen resistance in breast cancer cell lines, BCAR3 has been reported to control other features of breast cancer cell behaviors, including proliferation, motility, and invasion (VanAgthoven *et al.*, 1998). *In vitro*, BCAR3 has been shown to control proliferation through activation of the cyclin D1 promoter (Near *et al.*, 2007). BCAR3 depletion in invasive breast cancer cell lines reduces cell spreading, lamellipodia formation, migration and invasion while overexpression in less invasive breast cancer cell lines promotes these phenotypes (Riggins *et al.*, 2003; Schrecengost *et al.*, 2007; Schuh *et al.*, 2010; Wilson *et al.*, 2013). As BCAR3 has no catalytic activity, the ability of BCAR3 to function in the cellular processes described above is believed to be dependent on interactions with its binding partners. In particular, the interaction between BCAR3 and Cas is thought to control many of the established functions of BCAR3. This interaction results in increased Cas/Src complexes and Src kinase activity, which in turn results in phosphorylation of the substrate domain of Cas and signaling downstream of the Cas/Src complex (Riggins *et al.*, 2003; Schrecengost *et al.*, 2007; Schuh *et al.*, 2010). The direct interaction between BCAR3 and Cas has been reported to be required for BCAR3-mediated Cas phosphorylation, membrane ruffling, anti-estrogen resistance, and cyclin D1 expression (Wallez *et al.*, 2014).

To date, there is no published work on BCAR3 function in mouse models of breast cancer, but BCAR3 knockout (KO) mice have been produced and provide some insight into the role of BCAR3 during development. Near *et al.* reported that BCAR3 KO mice develop normally with the exception of post-natal rupture of the ocular lens. These mice

nursed normally and showed no defects in mammary gland development as analyzed by H&E staining of fixed glands (Near *et al.*, 2009). These data suggest that BCAR3 expression is largely dispensable for normal embryonic and mammary development.

1.6.2 Cas

Cas is a scaffolding protein belonging to the Cas family of proteins that also includes Nedd9/HEF1, Cass4/HEPL, and Embryonal Fyn-associated Substrate (EFS) (Wallez *et al.*, 2012). Cas contains an amino terminal SH3 domain, followed by a proline-rich region, a large “substrate binding domain” containing 15 repeats of a YxxP sequence, a serine-rich region, and a C-terminal domain (**Figure 1.5**). The Cas C-terminal domain includes a proline-rich region that binds to the SH3 domain of Src, a tyrosine-containing sequence that, when phosphorylated, binds to the SH2 domain of Src, and a helix-loop-helix motif. In addition to Src, Cas has many binding partners including but not limited to focal adhesion kinase (FAK), Pyk2, Crk, and the other NSP family members in addition to BCAR3 (Defilippi *et al.*, 2006).

The Cas protein is expressed in almost all normal tissues and in a large variety of cancers, including breast (Human Protein Atlas). Analysis of breast cancer genomic datasets using the CBioPortal for Cancer Genomics reveals that the gene encoding Cas can be amplified, mutated or deleted in invasive breast cancers (Cerami *et al.*, 2012; Gao *et al.*, 2013). Cas overexpression, though seen in a large subset of human breast tumors, does not correlate with tumor size or lymph node status (Tornillo *et al.*, 2014). However, high levels of Cas protein expression correlates with HER2 expression, increased risk of resistance to tamoxifen therapy, and decreased relapse-free and overall survival in patients with primary breast tumors (Dorssers *et al.*, 2004; Wallez *et al.*, 2012).

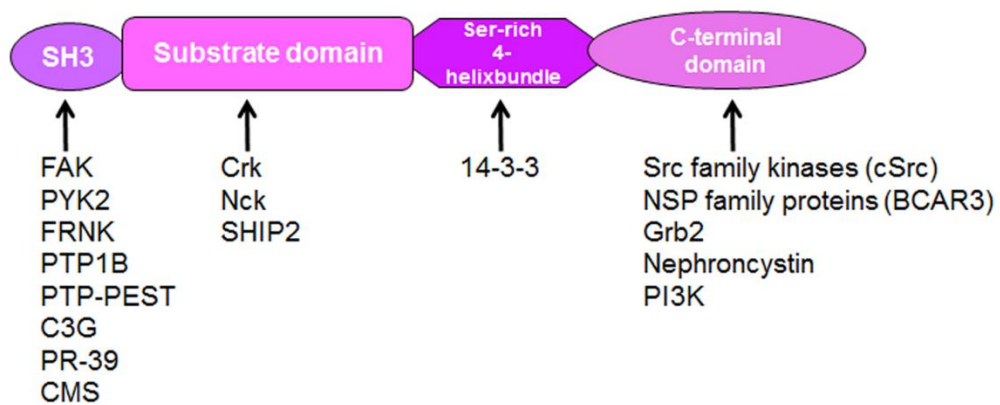


Figure 1.5. Structural features and binding partners of Cas

Cas contains an amino-terminal SH3 domain, followed by a proline-rich region, a substrate binding domain containing 15 repeats of a YxxP motif, a serine-rich region, and a C-terminal domain. Cas is a scaffolding protein with many binding partners, including but not limited to Src, FAK, Pyk2, Crk, and NSP family members such as BCAR3 (Defilippi *et al.*, 2006). Figure adapted from Bouton *et al.* (Bouton *et al.*, 2001).

In vitro studies show that Cas regulates cell migration, survival, and apoptosis. Cas is present in focal adhesions, which form upon integrin engagement with the ECM. In response to integrin engagement, the substrate domain of Cas is phosphorylated by Src, FAK, and potentially PyK2 (Bouton *et al.*, 2001). The ability of Cas to promote cell migration has been closely linked to Src-mediated phosphorylation of its substrate-binding domain. Tyrosine phosphorylation of Cas by Src allows for Cas to interact with Crk and recruit the nucleotide exchange factor, Dock180, which serves as an activator of the Rho family GTPase Rac1. At adhesion sites, Cas thus drives localized activation of Rac1, which in turn promotes actin polymerization, resulting in lamellipodia formation and migration (Raftopoulou and Hall, 2004; Defilippi *et al.*, 2006). Cas also promotes survival and proliferation by mediating signaling through ECM-engaged integrins as well as through growth factor and hormone receptors. The survival and proliferation effects of Cas signaling are facilitated by activation of the small GTPases Ras and Rac as well as c-Jun N-terminal protein kinase (JNK) and extracellular-signal-regulated kinase 1/2 (ERK1/2) (Defilippi *et al.*, 2006). In addition to the involvement of Cas in ECM-mediated integrin signaling, Cas promotes Src-dependent anchorage-independent growth through its interaction with Src (Defilippi *et al.*, 2006). Finally, Cas is capable of mediating apoptosis. Upon ECM detachment, UV irradiation and other pro-apoptotic stimuli, caspase 3 and other proteases induce the cleavage of Cas. The resultant C-terminal 31-kDa cleavage fragment is reported to promote cell death. One mechanism proposed to explain this function is the translocation of the cleavage fragment to the nucleus where it binds to the transcription factor E2A (Defilippi *et al.*, 2006). The interaction between the Cas cleavage fragment and E2A has been shown to prevent E2A-mediated transcription of the CDK inhibitor p21; p21 expression protects cells from apoptosis (Mahyar-Roemer and Roemer, 2001; Defilippi *et al.*, 2006).

Mouse models have shed light on the role of Cas in breast cancer. Upregulation of Cas alone in mouse mammary glands results in ductal hyperplasia, but in coordination with other oncogenic stimuli, Cas promotes tumor growth and invasion (Cabodi *et al.*, 2006; Guerrero *et al.*, 2012). FAK is reported to control tumor progression in MMTV-polyoma middle T (PyMT) mice, and this regulation is dependent on its interaction with Cas (Pylayeva *et al.*, 2009; Tornillo *et al.*, 2014). In a TGF- β driven xenograft model of breast cancer, Cas depletion results in a reduction in tumor cell proliferation, growth, and metastasis (Wendt *et al.*, 2009). Furthermore, Cas overexpression accelerates time-to-tumor appearance in MMTV-HER2/Neu transgenic mice (Cabodi *et al.*, 2006). This ability of Cas to augment HER2 oncogenic transformation is particularly interesting in light of the fact that Cas expression correlates with HER2 expression in breast cancer patients (Dorssers *et al.*, 2004).

Due to the fact that a global Cas deletion is embryonic lethal (Honda *et al.*, 1998), the role for Cas in normal mammary gland development has not been well studied. Nonetheless, the established functions of Cas suggest that it may play a critical role in normal mammary gland development. Cas is a well-established mediator of integrin signaling, which is essential for normal TEB formation, ductal growth, and branching (Lanigan *et al.*, 2007). Cas expression promotes activation of Src kinase and Rac1 (Schuh *et al.*, 2010; Wilson *et al.*, 2013). Studies in Src-deficient mice showed that Src is important for promoting ductal outgrowth and TEB formation (Kim, Laing, & Muller, 2005), and *in vitro* studies suggest that Rac1 may promote initiation of ductal branching during normal mammary gland morphogenesis (Ewald *et al.*, 2008). Taken together, these data support a role for Cas signaling in the regulation of normal mammary gland development.

1.6.3 Src

c-Src (Src) is one of eleven members of the Src family of non-receptor protein tyrosine kinases. The amino terminus of Src consists of a “Src homology 4” (SH4) domain that is attached to a 14-carbon myristoyl group. This is followed by a unique segment, an SH3 domain, an SH2 domain, a protein-tyrosine kinase domain (the SH1 domain), and a short carboxy-terminal tail (Roskoski, 2004) (**Figure 1.6A**). Src exists in an inactive “closed” conformation or an active “open” conformation (**Figure 1.6B**). The closed conformation of Src prevents binding of proteins to the SH2 and SH3 domains and renders the protein catalytically inactive. This conformation is established by interactions between phosphorylated tyrosine 527 (located close to the C-terminus) and the SH2 domain, and the SH3 domain with a linker region located between the SH2 and kinase domains. The open conformation of Src is induced by dephosphorylation of tyrosine 527 and/or binding of the SH2 and SH3 domains with cellular proteins. In this open conformation, Src auto-phosphorylates itself on tyrosine 416, resulting in stabilized activation of the kinase (Burnham *et al.*, 2000; Roskoski, 2004). Of particular interest in this thesis is the capability of Cas to activate Src through bipartite binding to the SH2 and SH3 domain (Burnham *et al.*, 2000).

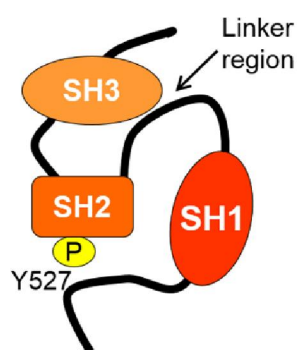
Src is a ubiquitously expressed protein, but both its expression and, to a greater extent, its activation are increased in many human cancers including breast cancer (Irby and Yeatman, 2000; Roskoski, 2004). Abnormal Src expression and/or activity in cancers has been linked to cell transformation, the epithelial-to-mesenchymal transition (EMT), and cancer development and progression (Liu *et al.*, 2015). The only gene alteration for Src that is reported for invasive breast cancers in genomic datasets is amplification (Cerami *et al.*, 2012; Gao *et al.*, 2013). In a large cohort of invasive breast cancer patients, high levels of Src expression were found to correlate with decreased survival, increased tumor grade, and ER and HER2 positivity. Furthermore, Src activation (determined by

A



B

“closed” auto-inhibitory conformation



“open” active conformation

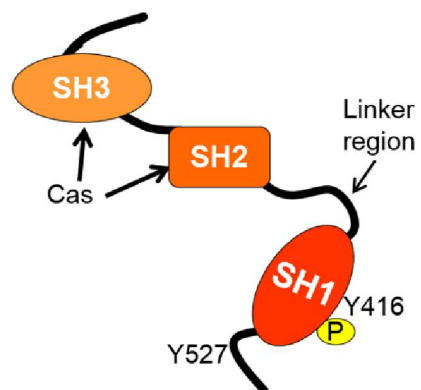


Figure 1.6. Structural features and conformations of cSrc

(A) Src begins with a 14-carbon myristoyl group attached to the SH4 domain, followed by a unique segment, an SH3 domain, an SH2 domain, a protein-tyrosine kinase domain (the SH1 domain), and a short carboxy-terminal tail (Roskoski, 2004). (B) Src can exist in an inactive “closed” conformation or an active “open” conformation. The inactive conformation of Src is established by 1) interaction between phosphorylated tyrosine residue 527 (located close to the C-terminus) and the SH2 domain and 2) interaction between the SH3 domain and a linker region located between the SH2 and SH1 domains. The open conformation of Src is established by dephosphorylation of tyrosine 527 and/or binding of the SH2 and SH3 domains with cellular proteins such as Cas. In this open conformation, Src can auto-phosphorylate itself on tyrosine 416, resulting in stabilized activation of the kinase (Burnham *et al.*, 2000; Roskoski, 2004).

phosphorylation of tyrosine 416) was found to associate with shorter disease-specific survival, increased tumor size and grade, ER negativity, and HER2 positivity (Elsberger *et al.*, 2009).

Src controls many cellular functions, including growth, motility, survival and angiogenesis. Src is activated by a variety of mechanisms including, but not limited to, direct or indirect interaction with receptor tyrosine kinases and integrin receptors (Irby and Yeatman, 2000). Downstream of receptor tyrosine kinases and integrins, Src regulates many signaling pathways including PI3K/AKT, Ras/Raf/MEK/ERK, and JNK. For example, Src activity mediates ER and epidermal growth factor receptor (EGFR)-dependent activation of mitogen-activated protein kinase (MAPK). Src activation following integrin engagement results in Src-FAK and Src-Cas interactions, ultimately leading to actin polymerization and cell migration. Src has also been shown to upregulate vascular endothelial growth factor receptor (VEGFR) expression, which is critical for both normal and malignant angiogenesis (Finn, 2008).

Mouse models highlight the importance of Src in breast cancer progression as well as in normal mammary gland development. Studies using global Src KO mice demonstrated the requirement for Src signaling in normal mammary gland development. These mice exhibit decreased ductal outgrowth and lower numbers of TEBs during puberty. This phenotype is believed to be, at least in part, due to a defect in the ability of the mammary epithelial cells to respond to estrogen signaling (Kim *et al.*, 2005). In MMTV-PyMT and MMTV-HER2/Neu spontaneous mouse models of breast cancer, Src activity is elevated in primary tumors as well as metastases (Irby and Yeatman, 2000). In addition to being overexpressed in PyMT-induced mouse mammary tumors, Src expression is required for tumor formation in this model (Guy *et al.*, 1994). Furthermore, Src activity was found to promote colonization of MDA-MB-231 breast cancer cells in the bone

following cardiac injection into nude mice, supporting a role of Src in controlling breast cancer metastasis (Myoui *et al.*, 2003).

Due to the established role of Src in tumor growth, progression, and metastasis in many cancers, several Src inhibitors have been developed for clinical use. Dasatinib is a small molecule inhibitor with activity toward Src family kinases as well as Bcr-Abl, c-Kit, platelet-derived growth factor receptor (PDGFR), and ephrin receptor kinases (Finn, 2008; Montero *et al.*, 2011). Dasatinib is currently an approved treatment for chronic myeloid leukemia (CML) and is in phase II clinical trials for the treatment of several solid tumors including colorectal, pancreatic, liver, melanoma, and breast cancer. In breast cancer, research has been focused on identifying patients who will best respond to dasatinib treatment. Despite evidence for the role of Src in HER2 and EGFR signaling, breast cancer cell lines overexpressing HER2 or EGFR were found to be less sensitive to growth inhibition by dasatinib (Finn, 2008). In contrast, basal/triple negative breast cancer cell lines were found to be sensitive to growth inhibition by dasatinib (Finn, 2008). Huang *et al.* used gene expression data from 23 breast cancer cell lines to develop a 6 gene model to predict sensitivity to dasatinib (Huang *et al.*, 2007). Notably, BCAR3, Cas, and even Src were not among the 6 genes found to predict sensitivity to dasatinib. This seems surprising considering the established ability of BCAR3 and Cas to regulate Src activity *in vitro* (Burnham *et al.*, 2000; Riggins *et al.*, 2003; Schuh *et al.*, 2010; Wallez *et al.*, 2014). It is important to note, however, that gene expression data may not be an ideal way to identify these molecules as markers for dasatinib sensitivity due to the fact that their expression and activity may be regulated at the protein rather than mRNA level. Nonetheless, using the 6 gene model, Huang *et al.* predicted that breast cancer patients with basal/triple negative disease would respond to dasatinib, consistent with the data described above showing sensitivity of triple negative cell lines to Src inhibition (Huang *et*

al., 2007). These data suggest that Src inhibitors may serve as viable therapeutics in this subset of breast cancers (Huang *et al.*, 2007).

1.7 Significance and overview

The main focus of this dissertation is on the adaptor molecule BCAR3. Our group and others have shown that BCAR3 expression is upregulated in invasive breast cancer cell lines, where it promotes cell proliferation, migration, and invasion (Near *et al.*, 2007; Schrecengost *et al.*, 2007; Schuh *et al.*, 2010; Wilson *et al.*, 2013; Wallez *et al.*, 2014). BCAR3 has no known catalytic activity and its effects on proliferation, migration, and invasion are believed to be dependent on interaction with its binding partners. BCAR3 has two established binding partners, Cas and PTP α . Initial studies by Borre *et al.* suggested that BCAR3 promotes resistance to antiestrogens, lamellipodia formation and migration in the absence of direct Cas binding (Vanden Borre *et al.*, 2011). However, it has since been proven that the BCAR3 point mutation used in these studies to inhibit the interaction between BCAR3 and Cas did not completely disrupt this interaction. Since this study, direct interaction between BCAR3 and Cas has been shown to be necessary for BCAR3-dependent Cas phosphorylation, cyclin D1 activation in the presence of antiestrogens, and lamellipodia formation (Wallez *et al.*, 2014). In chapter 2 of this thesis, we set out to further explore the requirement for BCAR3/Cas interactions in BCAR3-mediated functions by determining whether direct binding between BCAR3 and Cas played a role in adhesion disassembly, cellular migration, and invasion.

As discussed above, BCAR3 has been shown to promote Cas signaling and Src kinase activity, as well as cell proliferation, migration and invasion (Near *et al.*, 2007; Riggins *et al.*, 2003; Schuh *et al.*, 2010; Wallez *et al.*, 2014; Wilson *et al.*, 2013). Despite the ability of BCAR3 to regulate these pathways and the associated biological processes that control breast cancer progression, there are no published studies analyzing BCAR3

as a potential promoter of tumor growth and progression *in vivo*. In chapter 3, we analyze BCAR3 expression in a spontaneous mouse model of breast cancer and explore the ability of BCAR3 to promote the growth of MDA-MB-231 xenograft tumors. Data included in this chapter provide the first evidence supporting a role for BCAR3 in controlling tumor formation *in vivo*.

Finally, we explored the role of BCAR3 in mammary gland morphogenesis. Many signaling pathways and mechanisms are common to normal breast morphogenesis and breast cancer development/progression{Formatting Citation}. BCAR3 has well established roles in controlling cellular proliferation, migration and invasion, all mechanisms shown to be important for normal mammary gland morphogenesis. Despite this, it has previously been reported that BCAR3 KO mice develop normally, with no reported defects in mammary gland function (Near *et al.*, 2009). However, there are cases in which mice with fairly significant defects in mammary gland development fail to exhibit a concomitant impairment of function (Chen, Diacovo, Grenache, Santoro, & Zutter, 2002; Lilla & Werb, 2010). In chapter 4, we set out to determine if BCAR3 was involved in mammary gland development by analyzing BCAR3 expression during breast morphogenesis and performing whole mount analysis of mammary glands from BCAR3 KO mice. While preliminary, data presented in this chapter suggest that BCAR3 may function as a negative regulator of mammary gland development. *In vitro* 3D culture models are presented that begin to address the mechanism behind this proposed function.

While the work presented in this thesis provides new insights into BCAR3 function in mammary gland development and breast tumorigenesis, it also raises many questions. In chapter 5, we explore these questions and propose future experiments to elucidate the mechanisms through which BCAR3 controls mammary gland morphogenesis and breast cancer. We also explore the possibility that BCAR3 may serve as a biomarker and/or therapeutic target in breast cancer patients.

Chapter 2: Breast Cancer Antiestrogen Resistance 3 (BCAR3) – p130Cas interactions promote adhesion disassembly and invasion in breast cancer cells

**This chapter is adapted from Cross et al., Oncogene, 2016*

2.1 Introduction

Cell motility is an essential feature of processes involved in development and tissue repair as well as in pathological states such as inflammation and cancer. Previous work from our group and others has shown that BCAR3 promotes migration and invasion in breast cancer cell lines (Schrecengost *et al.*, 2007; Wilson *et al.*, 2013). One of the first steps in cell migration is the formation of nascent adhesions at the leading edge of a migrating cell (Parsons *et al.*, 2010). These nascent adhesions either undergo disassembly (turnover), or they mature into focal complexes and focal adhesions. Adhesion turnover is initiated when there is a lack of tension to reinforce the adhesion. This is mediated through adaptor molecules and kinases that function in adhesions to locally activate Rac1 and inhibit RhoA GTPase signaling, thereby reducing tension and promoting adhesion disassembly (Webb *et al.*, 2004; Broussard *et al.*, 2008). In order for the cell to move forward, adhesions in the rear of the cell must also undergo disassembly. BCAR3 has been shown to promote Rac1 activity and adhesion disassembly in invasive breast cancer cells (Wilson *et al.*, 2013). However, the mechanism(s) through which BCAR3 contributes to these activities remained to be elucidated. As previously discussed, BCAR3 has no known catalytic activity and many of its functions, including promoting Cas phosphorylation, Src activity, cyclin D1 activation, and lamellipodia formation, require Cas binding (Mace *et al.*, 2011; Wallez *et al.*, 2014).

In this study, we sought to determine the role of the BCAR3/Cas complex in BCAR3-mediated adhesion dynamics, migration, and invasion of breast cancer cells. We found that all of the BCAR3 in invasive breast cancer cells is present in a complex with

Cas and that both proteins co-localize in focal adhesions. BCAR3 entry into adhesions did not require a direct interaction with Cas or an intact SH2 domain. However, the kinetics of BCAR3 dissociation from adhesions was impaired in the absence of Cas binding. This paralleled a similar delay in the dissociation of other adhesion proteins, indicating that BCAR3/Cas interactions play an important role in adhesion complex disassembly. The BCAR3/Cas complex was also found to be important for BCAR3-dependent Rac1 activation, migration, and invasion in 3D matrices. Finally, BCAR3 and Cas were found to be co-expressed in multiple subtypes of human breast tumors. Collectively, these data highlight the importance of a functional BCAR3/Cas complex in invasive breast cancer cells.

2.2 Results

2.2.1 The entire cellular pool of BCAR3 is in complex with Cas in invasive breast cancer cells

Given the evidence of a strong functional relationship between BCAR3 and Cas, we measured the steady-state levels of BCAR3/Cas complexes in invasive breast cancer cells. Lysates from BT549 and MDA-MB-231 cells were subjected to serial immunoprecipitations with either Cas or BCAR3 antibodies (**Figure 2.1**). BCAR3 was present in Cas immune complexes (**Figure 2.1A, lanes 5-6 and 12-13**) and coincidentally lost from the lysates following immune depletion of Cas (**Figure 2.1A, lanes 2-4 and 9-11**), indicating that the majority of BCAR3 present in BT549 and MDA-MB-231 cells is in complex with Cas. In contrast, although Cas was also present in BCAR3 immune complexes (**Figure 2.1B, lanes 5 and 12**), significant amounts of Cas remained in the lysates following immune depletion of BCAR3 (**Figure 2.1B, lanes 2-4 and 9-11**). Together, these data show that, while a substantial pool of Cas is free of BCAR3, the majority of BCAR3 in invasive breast cancer cells is in complex with Cas. Based on these

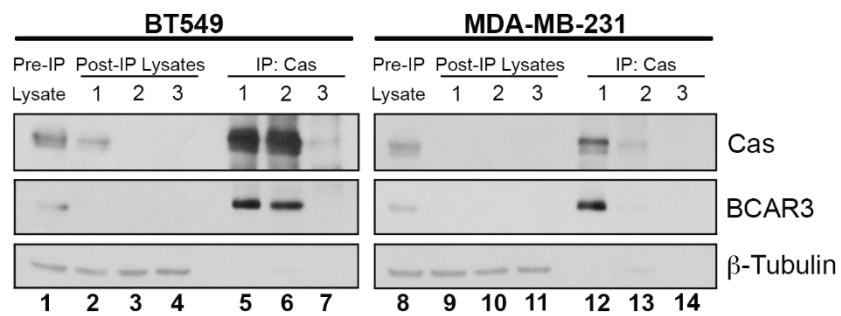
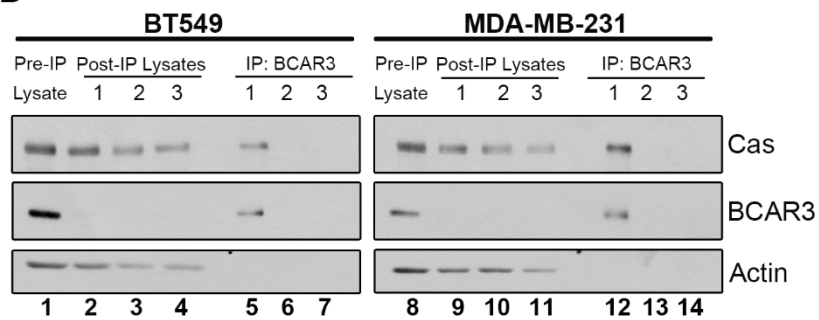
A**B**

Figure 2.1. The entire cellular pool of BCAR3 is in complex with Cas

BT549 and MDA-MB-231 cell lysates were subjected to three serial Cas (A) or BCAR3 (B) immunoprecipitations (IP). Pre-IP lysates were separated on 8% SDS-PAGE (lanes 1 and 8) together with the proteins present in the IPs (lanes 5-7, 12-14) and post-IP lysates (2-4, 9-11). Proteins were immunoblotted with antibodies recognizing the designated proteins. The pre-IP lysate is 10% of the amount of protein used for the initial IP. *Figure provided by Dr. Michael Guerrero.*

dynamics, it is likely that the interaction between these molecules is critical for the biological functions of BCAR3.

2.2.2 Localization of BCAR3 to adhesions does not require a functional SH2 domain or direct interaction with Cas

As previously discussed, BCAR3 and Cas play substantial roles in motility and invasion. BCAR3 has been reported to localize to vinculin-containing adhesions in mouse embryo fibroblasts (MEFs) (Sun *et al.*, 2012). To determine whether BCAR3 also localizes to adhesions in human breast cancer cell lines, GFP-BCAR3 was expressed in BT549 invasive breast cancer cells and adhesions were visualized by total internal reflection fluorescence (TIRF) microscopy. Similar to MEFs, GFP-BCAR3 was present in adhesions in BT549 cells (**Figure 2.2A, panel a**). Additionally, GFP-BCAR3 co-localized with endogenous Cas in these adhesions (**Figure 2.2A, panels a-c**).

To determine which domains of BCAR3 are required for localization to adhesions, we generated functional domain mutants and expressed them in BT549 cells (**Figure 2.2B**). Since the SH2 domain was previously demonstrated to be critical for BCAR3 localization to adhesions in MEFs (Sun *et al.*, 2012), we first investigated whether a mutant of this domain (R171V GFP-BCAR3) could localize to adhesions in breast cancer cells. This molecule was found to be present in adhesions and, like wildtype (WT) BCAR3, it co-localized with endogenous Cas (**Figure 2.2A, panels d-f**). This shows that the SH2 domain of BCAR3 is not the sole determinant of adhesion targeting in breast cancer cells. Since a direct interaction between BCAR3 and Cas was reported to be important for their reciprocal stability (Wallez *et al.*, 2014), and all of the BCAR3 in these cells is bound to Cas (**Figure 2.1**), we next asked whether localization of BCAR3 to adhesions requires association with Cas. This was addressed using a BCAR3 molecule containing two point mutations, L744E and R748E, which were recently shown to prevent the interaction

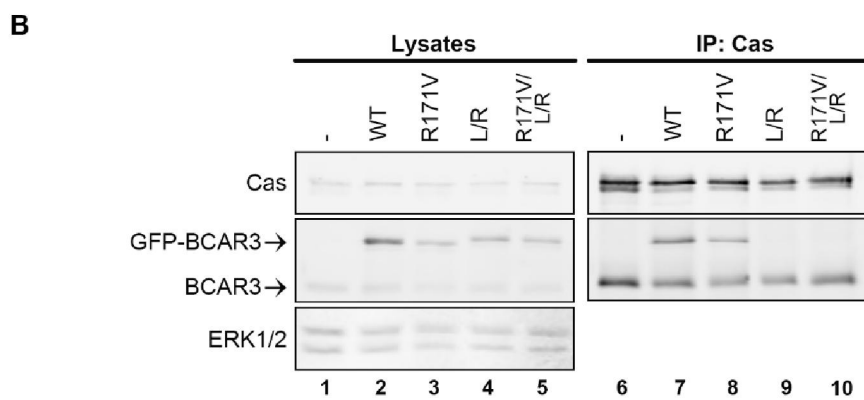
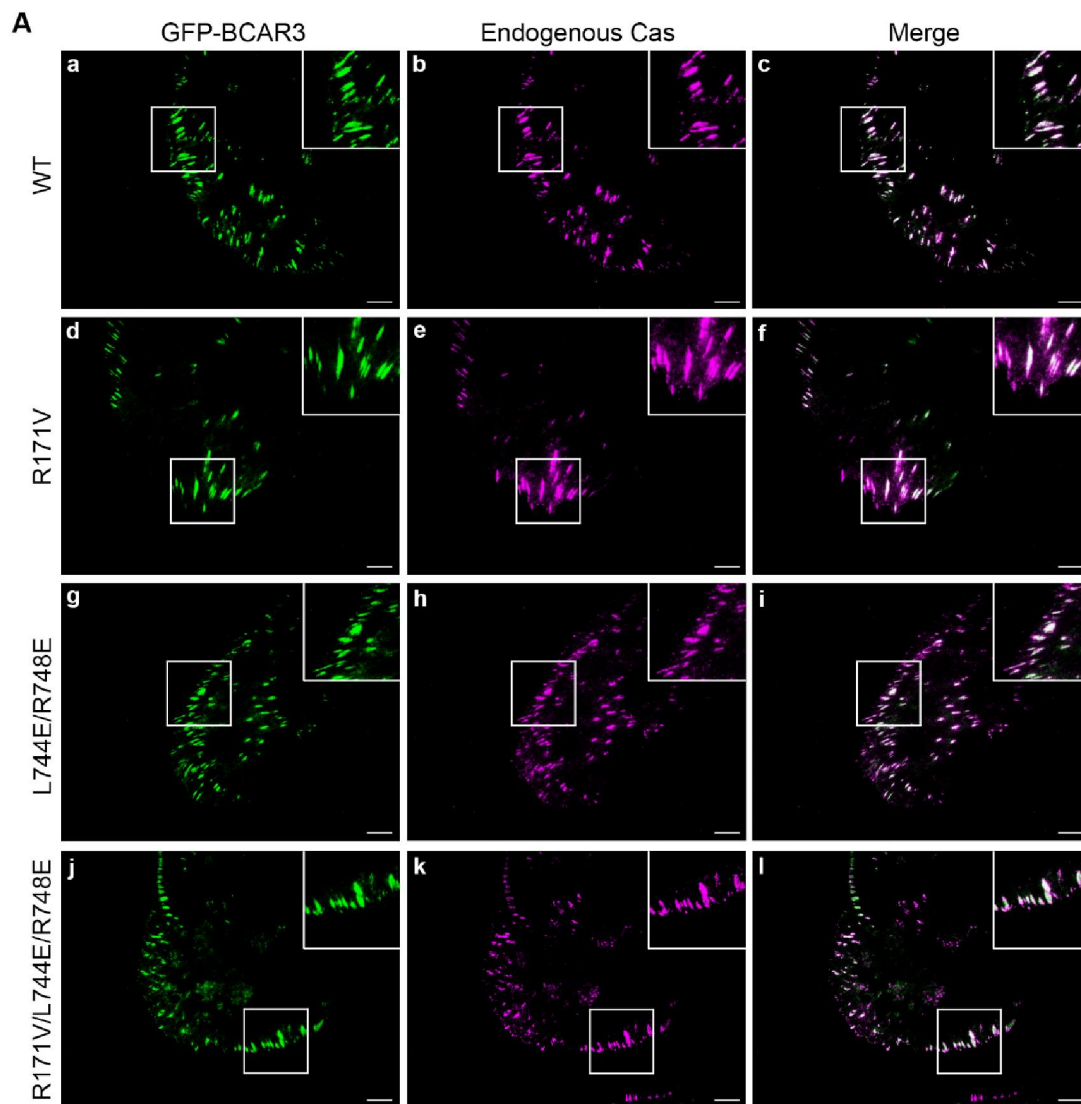


Figure 2.2. BCAR3 localization in adhesions does not require a functional SH2 domain or interaction with Cas

(A) BT549 cells were transfected with plasmids encoding WT GFP-BCAR3, R171V GFP-BCAR3, L744E/R748E GFP-BCAR3 or R171V/L744E/R748E GFP-BCAR3. Cells were incubated for 24 hours prior to plating on 10 μ g/ml fibronectin-coated coverslips for 4 hours. Cells were fixed, stained with polyclonal Cas antibodies (panels b, e, h, k), and subjected to TIRF microscopy to visualize adhesions. Merged images are shown in the right panels and insets show higher magnifications of the designated areas. *Panel A provided in collaboration with Dr. Ashley Wilson.* (B) BT549 cells were transfected with plasmids encoding GFP, WT GFP-BCAR3, R171V GFP-BCAR3, L744E/R748E GFP-BCAR3 or R171V/L744E/R748E GFP-BCAR3 and lysed in a non-denaturing buffer 24 hours post-transfection. Total cell protein and Cas immune complexes (generated from 50X more protein than the lysates) were immunoblotted with antibodies to detect the indicated proteins. Left and right panels are identical exposures from the same film.

between BCAR3 and Cas (Wallez *et al.*, 2014). To verify that these point mutations abrogated Cas binding, Cas immune complexes were isolated from BT549 cells expressing WT GFP-BCAR3 or L744E/R748E GFP-BCAR3 (**Figure 2.2B**). As expected, endogenous BCAR3 (lower bands in lower panel, lanes 6-10) and WT GFP-BCAR3 (upper band, lane 7) were present in Cas immune complexes. However, L744E/R748E GFP-BCAR3 (L/R) failed to interact with Cas (lane 9). Despite the fact that this mutant was unable to bind to Cas, it was present in adhesions and co-localized with endogenous Cas (**Figure 2.2A, panels g-i**). This demonstrates that BCAR3 localization to adhesions does not require direct association with Cas.

While neither the SH2 domain nor the Cas-binding domain were found to be solely responsible for BCAR3 localization to adhesions, these data do not discount the possibility that both domains could contain adhesion-targeting activity. To test this, a triple BCAR3 mutant (R171V/L744E/R748E GFP-BCAR3) that lacks both a functional SH2 domain and the Cas-binding site was expressed in BT549 cells. This molecule failed to associate with Cas (**Figure 2.2B, lane 10**); however, as was the case for the individual mutants, the triple mutant was present in adhesions and co-localized with Cas (**Figure 2.2A, panels j-l**). Together, these data show that, even though PTP α (through the SH2 domain) and/or Cas (through the C-terminus) may facilitate BCAR3 localization to adhesions, other mechanisms must be available in the absence of these interactions to recruit BCAR3 to adhesion sites in breast cancer cells.

2.2.3 Direct interaction between BCAR3 and Cas is required for efficient adhesion disassembly in BT549 breast cancer cells

While BCAR3 localization to adhesions does not require a direct association with Cas, BCAR3 function may be dependent on this interaction. In a previous study, BCAR3 was shown to promote adhesion disassembly in invasive breast cancer cells (Wilson *et*

al., 2013). To test whether this function is dependent on BCAR3/Cas interactions, live TIRF imaging was performed on BT549 cells that were co-transfected with plasmids encoding mCherry-tagged Cas and either WT or L744E/R748E GFP-BCAR3. Under these conditions, both WT and L744E/R748E GFP-BCAR3 co-localized with Cas in dynamic adhesions (**Figure 2.3**). To quantify adhesion turnover, adhesions at peripheral, protruding edges of a cell were selected for analysis. Time-lapse images show incorporation (arrowheads) and dissociation (arrows) of BCAR3 and Cas into and from representative adhesions co-expressing Cas and either WT (**Figure 2.3A**) or L744E/R748E GFP-BCAR3 (**Figure 2.3B**). By measuring fluorescence intensity over time (**Figures 2.3C and 3D**), BCAR3 and Cas were found to incorporate into adhesions at similar rates (**Figure 2.3E, compare bars 1 and 3**). This was independent of the ability of BCAR3 to bind to Cas, as L744E/R748E GFP-BCAR3 entered adhesions at a rate similar to that of WT BCAR3 (**Figure 2.3E, compare bars 1 and 2**). Moreover, when Cas was co-expressed with mutant BCAR3, it entered adhesions at a similar rate to when it was co-expressed with WT GFP-BCAR3 (**Figure 2.3E, compare bars 3 and 4**). Together, these data demonstrate that BCAR3 can efficiently incorporate into adhesions without being directly bound to Cas.

Using a similar approach to measure adhesion disassembly, we found that BCAR3 and Cas dissociate from adhesions at similar rates (**Figure 2.3F, compare bars 1 and 3**). However, the rate of L744E/R748E GFP-BCAR3 dissociation was significantly reduced compared to WT GFP-BCAR3 (**Figure 2.3F, compare bars 1 and 2**), and dissociation of Cas from these adhesions was similarly impaired (**Figure 2.3F, compare bars 3 and 4**). This suggests that direct binding between BCAR3 and Cas is required for efficient dissociation of BCAR3 and Cas from adhesions.

The reduced dissociation rate of Cas and L744E/R748E GFP-BCAR3 from adhesions could be the result of a specific delay in the dissociation of Cas and mutant

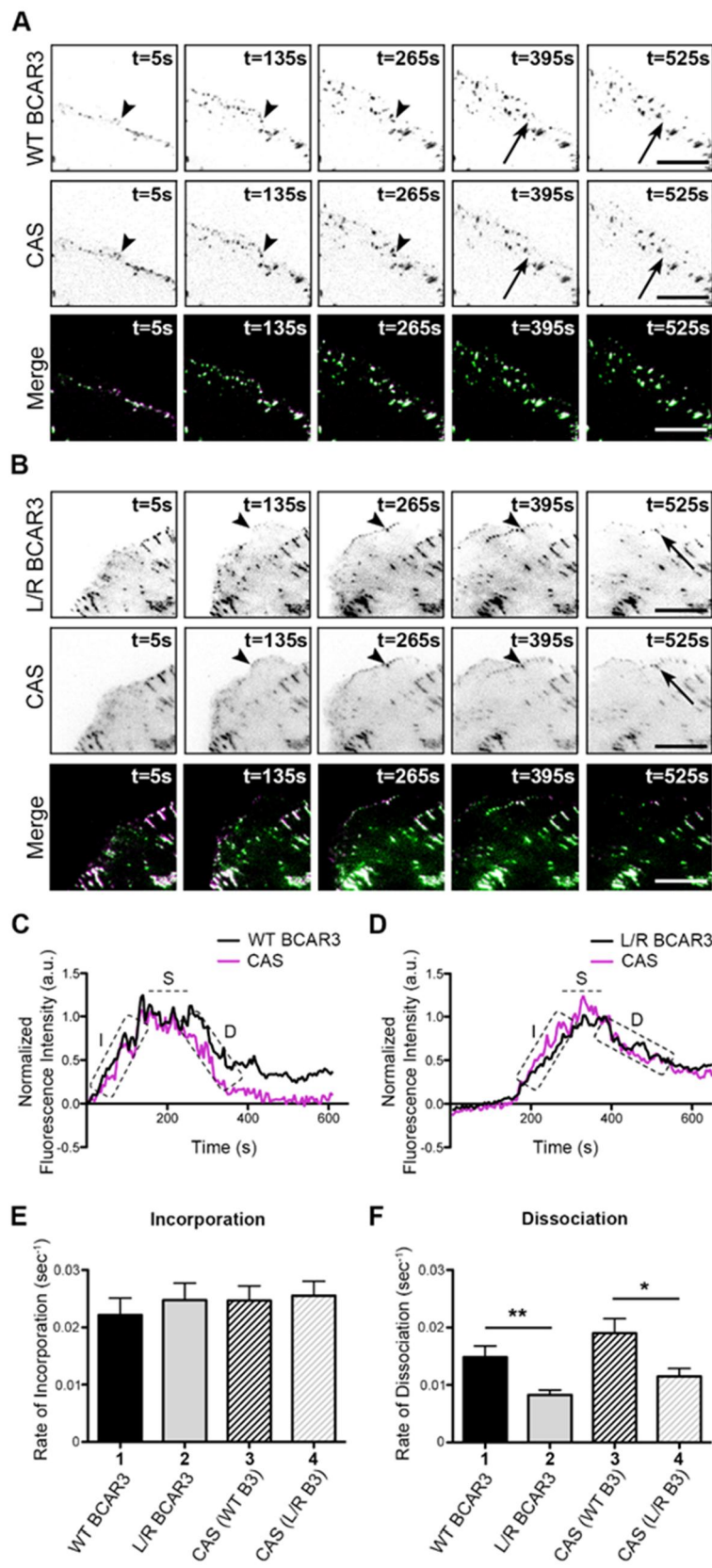


Figure 2.3. Direct interaction between BCAR3 and Cas is required for efficient dissociation of BCAR3 from adhesions

BT549 breast cancer cells were co-transfected with plasmids encoding WT or L744E/R748E (L/R) GFP-BCAR3 and mCherry-Cas, incubated for 24 hours, and then plated on 2 μ g/ml fibronectin-coated glass-bottomed TIRF dishes for 30-40 minutes prior to visualizing adhesion dynamics via live-imaging TIRF microscopy. (A, B) Representative time-lapse images show incorporation into adhesions (arrowheads) and dissociation (arrows) of the indicated proteins over the specified time course. Scale bars = 100 μ m. (C, D) Representative fluorescence intensity time tracings of BCAR3 (black) and Cas (magenta) present in adhesions from cells expressing WT (C) or L744ER748E (D) GFP-BCAR3. Dashed boxes/line indicate the incorporation (I), stability (S), and dissociation (D) phases of adhesion dynamics. (E, F) Quantitative analysis of the incorporation (E) and dissociation (F) rates of WT GFP-BCAR3 (bar 1), L744E/R748E (L/R) GFP-BCAR3 (bar 2), Cas co-expressed with WT GFP-BCAR3 (bar 3), and Cas co-expressed with L744E/R748E (L/R) GFP-BCAR3 (bar 4). Data presented are the mean \pm SEM of \geq 35 adhesions from 3 WT and L744E/R748E GFP-BCAR3 expressing cells from 3 independent experiments. Statistical analysis performed using a Kruskal-Wallis one-way ANOVA and a Dunn's Multiple Comparison post-test. *, $p < 0.05$, **, $p < 0.01$. *Figure provided by Dr. Ashley Wilson.*

BCAR3 from the adhesions, a more generalized stabilization of adhesion proteins in the adhesion complexes, or a reduction in the turnover rate of mutant BCAR3 and Cas. The latter possibility seems unlikely, as ectopic WT and L744E/R748E BCAR3 were found to have similar half-lives (**Figure 2.4**). Moreover, these half-lives, as well as the half-life of Cas (data not shown), were found to be over 20 hours, which is far greater than the 10-12 minute timespan of the videos used to quantify adhesion disassembly.

To distinguish between the first two possibilities, we examined the adhesion dynamics of another well-established adhesion protein, talin, in the presence of WT or L744E/R748E GFP-BCAR3. Unlike Cas, talin does not associate with WT BCAR3 (**Figure 2.5**). Live TIRF imaging was performed to visualize adhesion dynamics in cells expressing mCherry-talin and either WT or L744E/R748E GFP-BCAR3, and adhesion turnover was quantified as described above (**Figure 2.6**). As before, the incorporation of BCAR3 into adhesions was not dependent on its ability to bind to Cas (**Figure 2.6E, compare bars 1 and 2**), but its rate of dissociation from adhesions was significantly reduced in the absence of Cas binding (**Figure 2.6F, compare bars 1 and 2**). The rates at which BCAR3 and talin entered and left adhesions were not significantly different (**Figures 2.6E and 2.6F, bars 1 and 3**). However, as was the case for Cas, the rate at which talin dissociated from adhesions was significantly reduced in the presence of L744E/R748E GFP-BCAR3 (**Figure 2.6F, compare bars 3 and 4**). This was also the case for a third adhesion protein, α -actinin (**Figure 2.7**), which similarly does not interact with BCAR3 (**Figure 2.5**).

It is important to note that, for all of the adhesion proteins analyzed, the reduced rate at which they dissociated from adhesions in the presence of L744E/R748E BCAR3 was similar to the rate at which the mutant BCAR3 molecule left adhesions (**Figures 2.3F, 2.6F, and 2.7F, compare bars 2 and 4**). This is consistent with a stabilization of the entire adhesion complex under these conditions, suggesting that a direct interaction

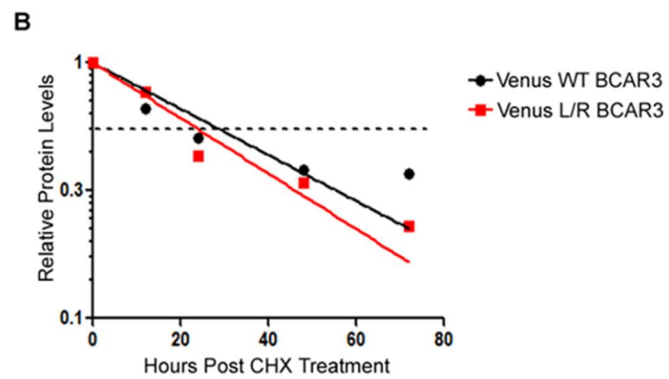
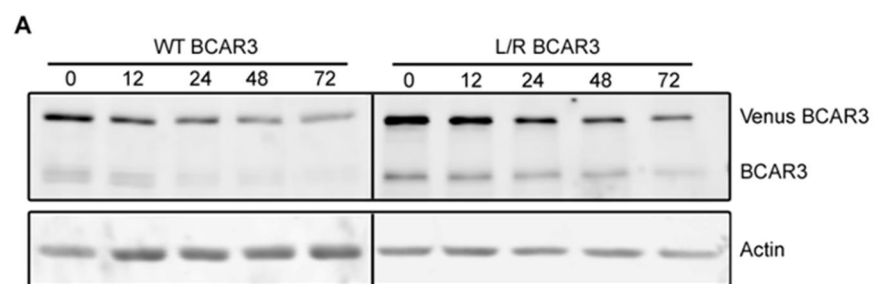


Figure 2.4. WT and L/R BCAR3 have similar half-lives

(A) BT549 cells were infected with lentiviruses encoding WT Venus-BCAR3 or L744E/R748E (L/R) Venus-BCAR3 and plated in 6-well dishes at 100,000 cells per well. One day after plating, cells were treated with 25 μ g/ml cyclohexamide (CHX) and lysed at the indicated times. Proteins were immunoblotted with antibodies recognizing the designated proteins. Representative blots are shown. (B) Protein levels from the representative blots were normalized to the 0 hour time point and plotted as an exponential decay nonlinear regression.

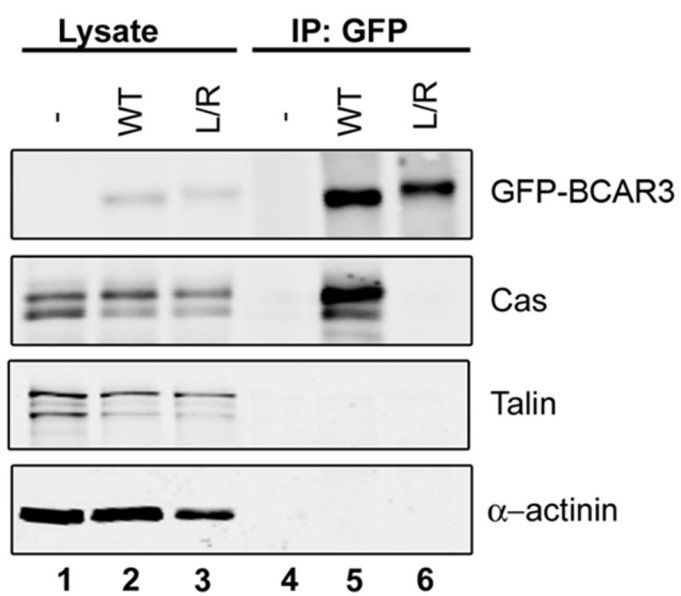


Figure 2.5. BCAR3 is not in complex with talin or α -actinin

BT549 cells were transfected with plasmids encoding GFP (-), WT GFP-BCAR3, or L744E/R748E GFP-BCAR3 and lysed 24 hours post-transfection. Total cell protein and GFP immune complexes (generated from 50X more protein than the lysates) were immunoblotted with antibodies to detect the indicated proteins. *Figure provided by Ms. Keena Thomas.*

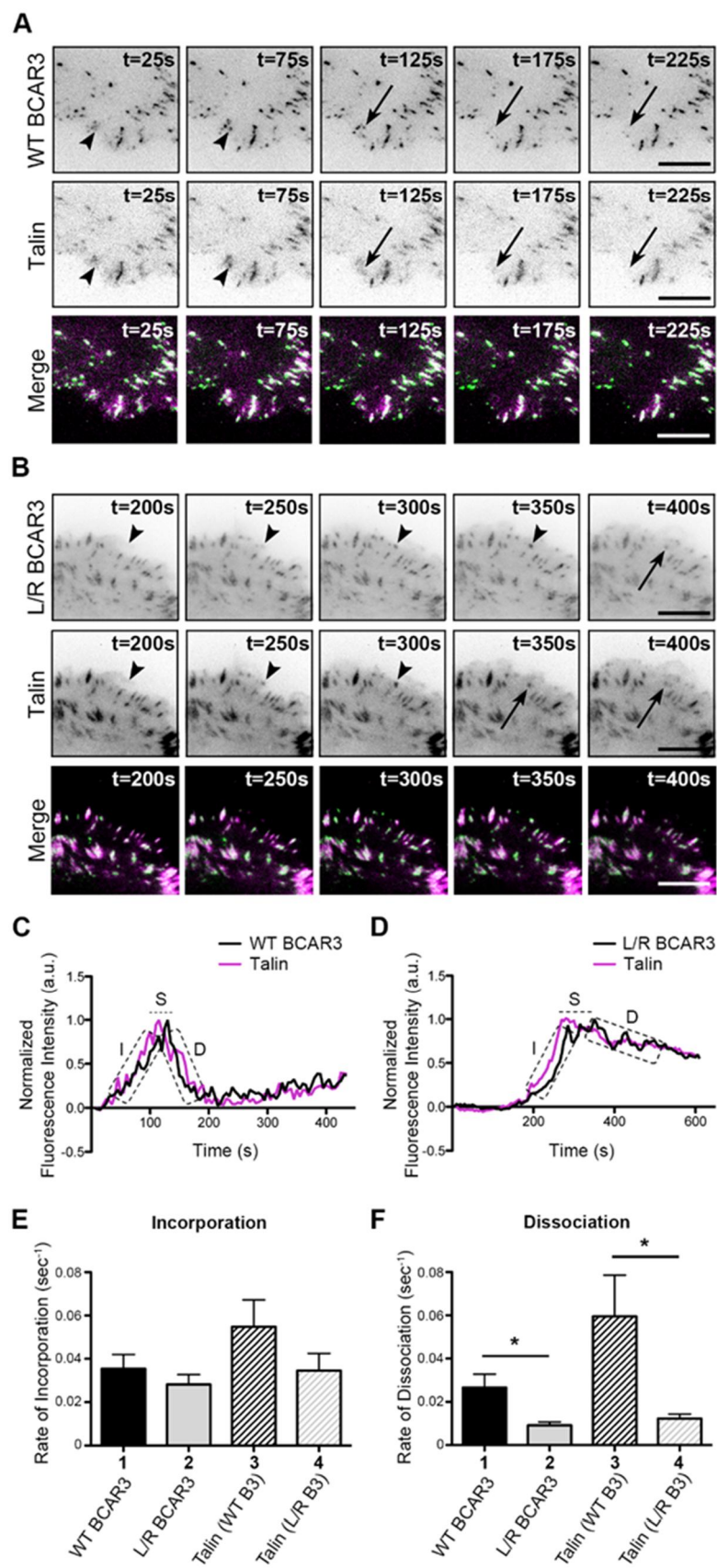


Figure 2.6. Direct interaction between BCAR3 and Cas is required for efficient dissociation of talin from adhesions

BT549 invasive breast cancer cells were co-transfected with plasmids encoding WT or L744E/R748E (L/R) GFP-BCAR3 and mCherry-talin, incubated for 24 hours, and then plated on 2 μ g/ml fibronectin-coated glass-bottomed TIRF dishes for 30-40 minutes prior to visualizing adhesion dynamics via live-imaging TIRF. (A, B) Representative time-lapse images show incorporation into adhesions (arrowheads) and dissociation (arrows) of the indicated proteins over the specified time course. Scale bars = 100 μ m. (C, D) Representative fluorescence intensity time tracings of BCAR3 (black) and talin (magenta) present in adhesions from cells expressing WT (C) or L744E/R748E (L/R) GFP-BCAR3 (D). Dashed boxes/line indicate the incorporation (I), stability (S), and dissociation (D) phases of adhesion dynamics. (E, F) Quantitative analysis of the incorporation (E) and dissociation (F) rates of WT GFP-BCAR3 (bar 1), L744E/R748E (L/R) GFP-BCAR3 (bar 2), Talin co-expressed with WT GFP-BCAR3 (bar 3), and Talin co-expressed with L744E/R748E (L/R) GFP-BCAR3 (bar 4). Data presented are the mean \pm SEM of \geq 14 adhesions from 5 separate WT BCAR3/talin or 3 separate L744E/R748E BCAR3/talin movies generated from 3 independent experiments. Statistical analysis performed using a Kruskal-Wallis one-way ANOVA and a Dunn's Multiple Comparison post-test. *, $p < 0.05$.

Figure provided by Dr. Ashley Wilson.

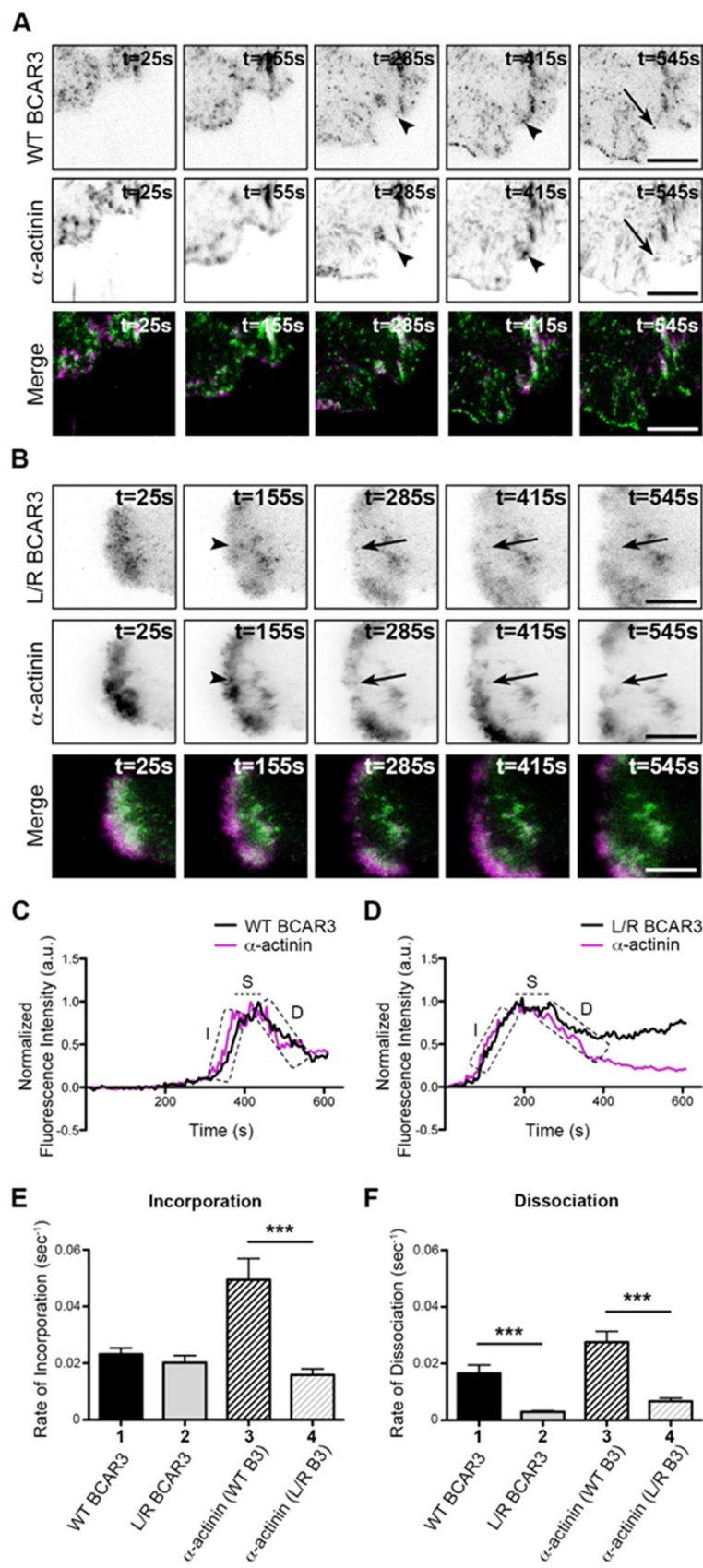


Figure 2.7. Direct interactions between BCAR3 and Cas are required for efficient incorporation and turnover of α -actinin in adhesions

BT549 breast cancer cells were co-transfected with plasmids encoding WT or L744E/R748E (L/R) GFP-BCAR3 and mCherry- α -actinin, incubated for 24 hours, and then plated on 2 μ g/ml fibronectin-coated glass-bottomed TIRF dishes for 30-40 minutes prior to visualizing adhesion dynamics via live-imaging TIRF. (A, B) Representative time-lapse images show incorporation into adhesions (arrowheads) and dissociation (arrows) of the indicated proteins over the specified time course. Scale bars = 100 μ m. (C, D) Representative fluorescence intensity time tracings of BCAR3 (black) and α -actinin (magenta) present in adhesions from cells expressing WT (C) or L744E/R748E (L/R) GFP-BCAR3 (D). Dashed boxes/line indicate the incorporation (I), stability (S), and dissociation (D) phases of adhesion dynamics. (E, F) Quantitative analysis of the incorporation (E) and dissociation (F) rates of WT GFP-BCAR3 (bar 1), L744E/R748E (L/R) GFP-BCAR3 (bar 2), α -actinin co-expressed with WT GFP-BCAR3 (bar 3), and α -actinin co-expressed with L744E/R748E (L/R) GFP-BCAR3 (bar 4). Data presented are the mean \pm SEM of ≥ 13 adhesions from 4 separate WT BCAR3/ α -actinin or 2 separate L744E/R748E BCAR3/ α -actinin movies generated from 3 independent experiments. Statistical analysis performed using a Kruskal-Wallis one-way ANOVA and a Dunn's Multiple Comparison post-test. ***, $p < 0.001$. *Figure provided by Dr. Ashley Wilson.*

between BCAR3 and Cas is required for efficient adhesion complex disassembly and turnover.

Our previous work showed that loss of BCAR3 in breast cancer cells resulted in a reduction of Rac1 activity coincident with an increase in RhoA activity, stress fiber stabilization and slower adhesion turnover (Wilson *et al.*, 2013). Because proper control of adhesion dynamics by BCAR3 required an intact Cas binding site, we hypothesized that the ability of BCAR3 to promote Rac1 activity may be dependent on its association with Cas. To test this hypothesis, active GTP-bound Rac1 was measured in extracts from BT549 cells expressing WT or L744E/R748E GFP-BCAR3 (**Figure 2.8**). Overexpression of WT BCAR3, but not the Cas binding mutant, was found to increase Rac1 activity in the cell. Together, these data show that the BCAR3/Cas complex promotes increased Rac1 activation and adhesion disassembly/turnover in breast cancer cell lines.

2.2.4 Direct interaction between BCAR3 and Cas promotes breast tumor cell invasion in 3D and chemotaxis toward serum

Previous studies have shown that BCAR3 promotes breast tumor cell motility and invasion (Schrecengost *et al.*, 2007; Wilson *et al.*, 2013). Considering that adhesion turnover is a critical facet of motility/invasion, and that BCAR3 promotes adhesion disassembly through its interaction with Cas (see above), we hypothesized that BCAR3-mediated breast tumor cell invasion and migration would similarly be dependent upon the ability of BCAR3 to bind to Cas. To test this hypothesis, stable MDA-MB-231 cells were generated that express either empty vector (pLKO) or one of two BCAR3-targeted short hairpin RNAs (shBCAR3-1 and shBCAR3-2) (**Figure 2.9A**). Each cell line was seeded in 3D Matrigel cultures to assess whether BCAR3 controlled invasion of MDA-MB-231 cells in this model. As has been reported previously for parental MDA-MB-231 cells (Kenny *et al.*, 2007), control cells formed highly invasive structures when grown in 3D Matrigel

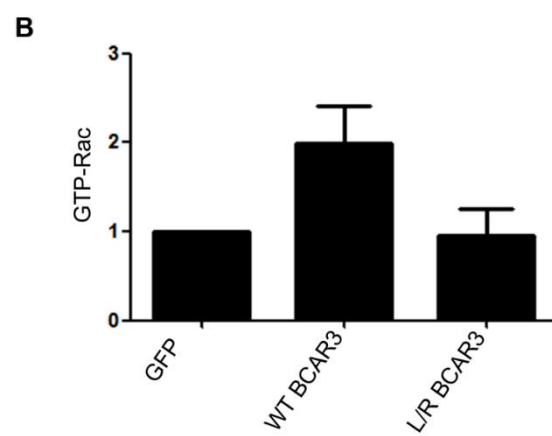
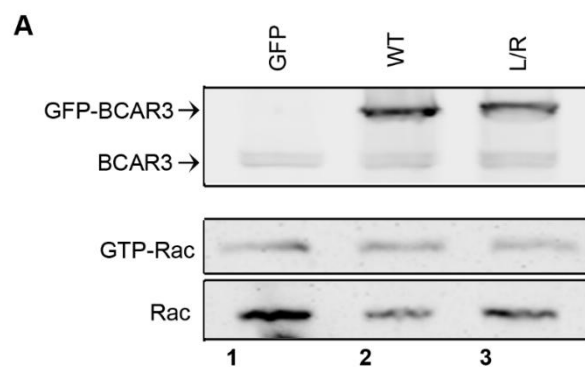


Figure 2.8. BCAR3/Cas interactions are required for BCAR3 dependent Rac activity

BT549 cells were transfected with plasmids encoding GFP, WT GFP-BCAR3, or L744E/R748E GFP-BCAR3 and incubated for 24 hours. Cells were held in suspension for 90 minutes, then plated on 10 μ g/ml fibronectin for 1 hour. (A) GTP-bound Rac1 was isolated from whole cell lysates by incubation with PAK-1-binding domain agarose. Bound proteins (middle panel) and total Rac1 (bottom panel) were detected by immunoblotting with a Rac1 antibody, and BCAR3 expression was confirmed with a BCAR3-specific antibody (top panel). (B) Quantification of the relative GTP-Rac1 level is shown. Data presented are the mean \pm SEM of 3 independent experiments.

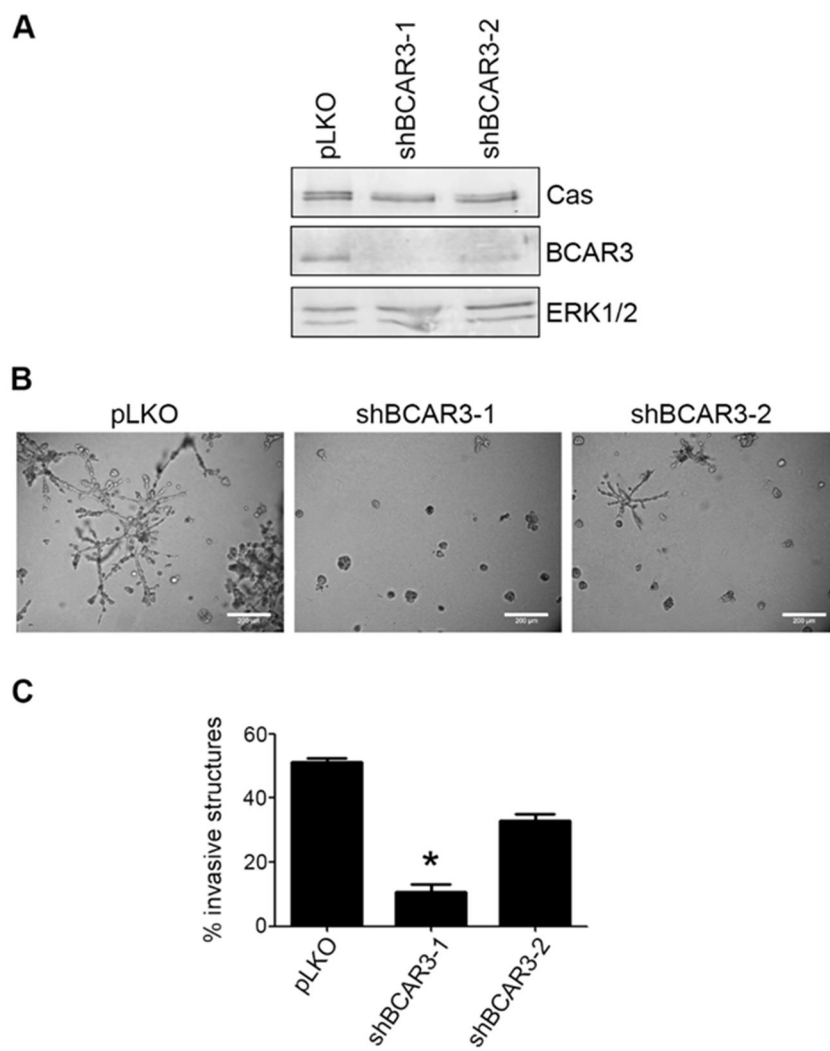


Figure 2.9. BCAR3 promotes invasion of MDA-MB-231 cells in 3D Matrigel culture

(A) MDA-MB-231 cells stably expressing empty vector (pLKO), shBCAR3-1, or shBCAR3-2 lentiviral constructs were grown in 3D Matrigel culture for 8 days. Representative immunoblot is shown confirming knockdown of BCAR3 with both shRNA constructs. (B, C) Representative phase images (B) and quantification of invasive structures (C) are shown. Data presented are the mean \pm SEM of 3 independent experiments, performed in quadruplicate. Statistical analysis performed using a Kruskal-Wallis one-way ANOVA and a Dunn's Multiple Comparison post-test. Scale bars = 200 μ m. *, $p < 0.05$ relative to pLKO.

culture (**Figure 2.9B and C**). In contrast, knockdown of BCAR3 with shBCAR3-1 resulted in a significant reduction in the percentage of invasive structures observed at day 8 in culture (**Figure 2.9B and C**). Cells infected with the second shRNA construct (shBCAR3-2) that resulted in a less robust knockdown of BCAR3 (**Figure 2.9A**) exhibited an intermediate invasive phenotype (**Figure 2.9B and C**). To assess whether BCAR3/Cas interactions were necessary for BCAR3-mediated invasion, the stable shBCAR3-1 cell line was infected with the lentiviral vector pLV-Venus (**Figure 2.10A, lane 3**) or shRNA-resistant wobble versions of pLV-Venus WT BCAR3 (lane 4) or the Cas binding mutant of BCAR3 (L744E/R748E, L/R) (lane 5). The expected Cas-binding capabilities of these molecules were confirmed through analysis of Cas immune complexes (lanes 7-10). Each cell line was seeded in 3D Matrigel cultures to evaluate whether BCAR3/Cas interactions were necessary for BCAR3-mediated invasion. Again, control cells formed highly invasive structures when grown in 3D Matrigel culture (**Figure 2.10B, panel a**) and knockdown of BCAR3 resulted in a significant reduction in the percentage of invasive structures observed at day 8 in culture (**Figure 2.10B, panel b and Figure 2.10C**). The reduced invasive phenotype exhibited by cells expressing shBCAR3 was rescued by expression of WT BCAR3 protein but not the empty vector or Cas-binding mutant (**Figure 2.10B, panel d and e and Figure 2.10C**). This requirement for direct BCAR3/Cas binding in BCAR3-mediated invasion was confirmed with a second cell line, Hs578T (**Figure 2.11**). To determine the importance of direct binding between BCAR3 and Cas in promoting BCAR3 mediated migration, the MDA-MB-231 cells described above were plated in a modified Boyden chamber and allowed to migrate toward serum for 6 hours. Knockdown of BCAR3 resulted in a loss of migration as previously described (Schrecengost *et al.*, 2007) (**Figure 2.10D, bars 1, 2**). The reduced migration observed in cells expressing shBCAR3 was similarly observed in cells re-expressing the empty vector and the Cas binding mutant of BCAR3 (**Figure 2.10D, bars 3 and 5**) but not in cells re-expressing WT

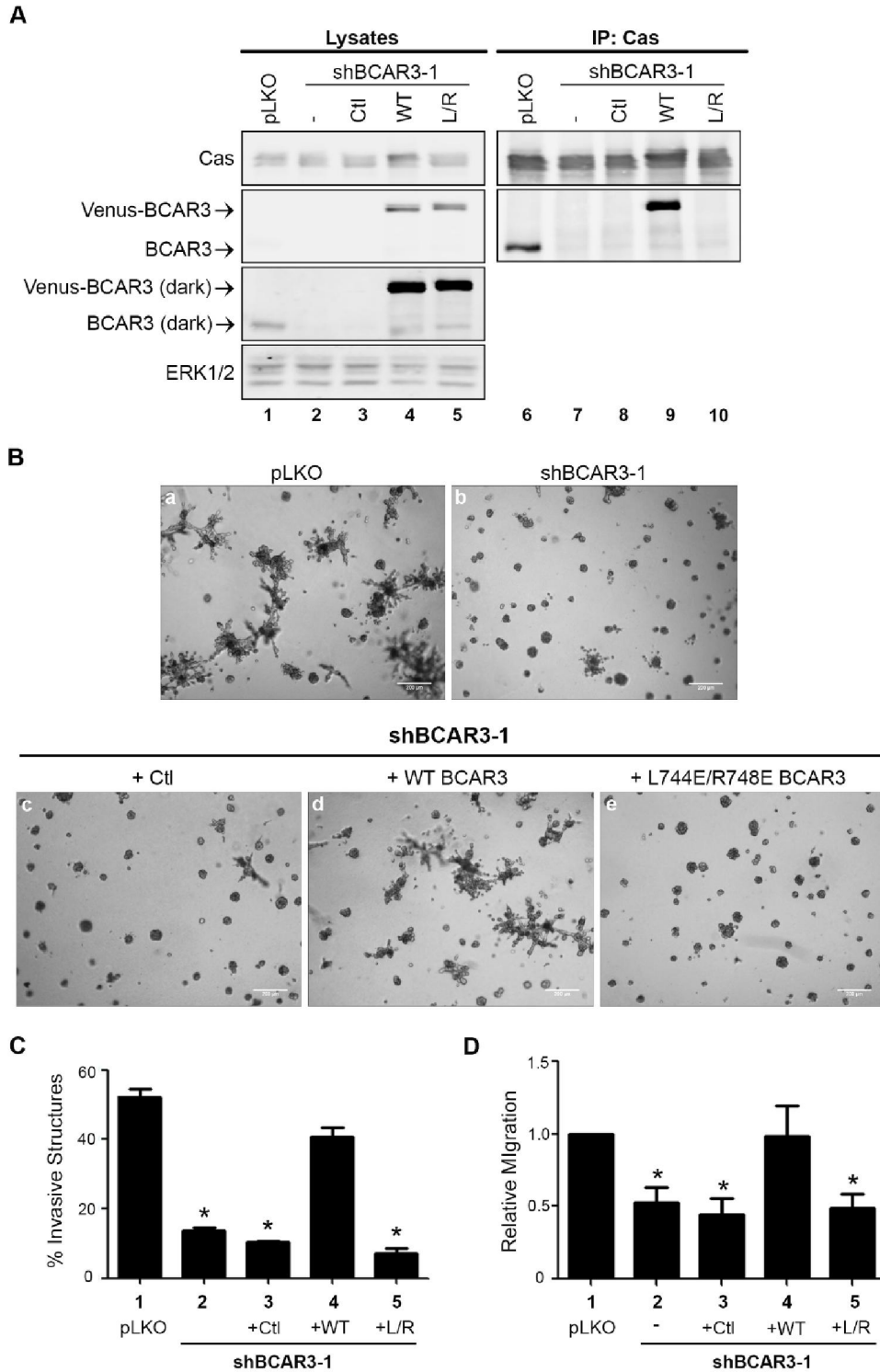
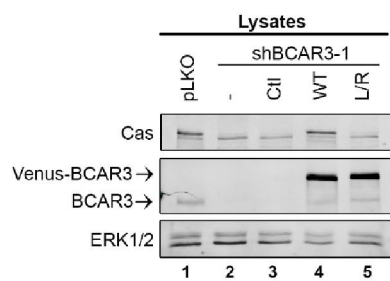


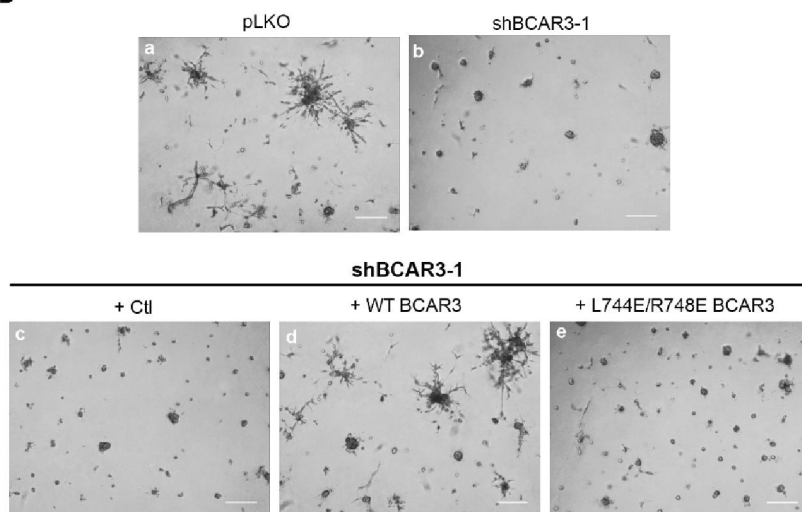
Figure 2.10. Direct interaction between BCAR3 and Cas is required for invasion of MDA-MB-231 cells in 3D Matrigel culture and chemotaxis toward serum

(A) MDA-MB-231 cells stably expressing empty vector (pLKO) or shBCAR3-1 lentiviral constructs were infected with lentiviruses encoding 3rd-base wobble variants of WT Venus-BCAR3 or L744E/R748E (L/R) Venus-BCAR3 or empty vector (pLV-Venus; Ctl). Total cell protein and Cas immune complexes were immunoblotted with antibodies to detect the indicated proteins. Left and right panels are identical exposures from the same film. (B, C) The cells described in panel A were grown in 3D Matrigel culture for 8 days. Representative phase images (B) and quantification of invasive structures (C) are shown. Data presented are the mean \pm SEM of 3 independent experiments, performed in quadruplicate. Statistical analysis performed using a Kruskal-Wallis one-way ANOVA and a Dunn's Multiple Comparison post-test. Scale bars = 200 μ m. *, $p < 0.05$ relative to pLKO. (D) The cells described in panel A were serum-starved overnight and plated (2.5×10^4) in the top of a Boyden chamber (6.5 mm, 8.0- μ m Transwell Costar membrane; Corning Incorporated). Cells were allowed to migrate toward 10% serum for 6 hours and the cells that migrated to the lower chamber were counted. Data presented are the mean \pm SEM of 7 independent experiments. Statistical analyses performed using a one-way ANOVA and the Dunnett post-test. *, $p < 0.05$ relative to pLKO.

A



B



C

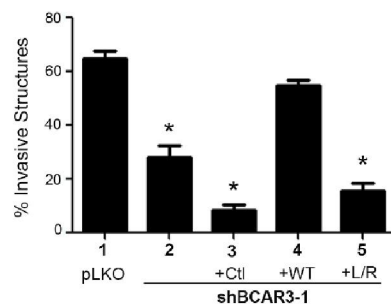


Figure 2.11. Direct interaction between BCAR3 and Cas is required for invasion of Hs578T cells in 3D Matrigel culture

(A) Hs578T cells stably expressing empty vector (pLKO) or shBCAR3-1 lentiviral constructs were infected with lentiviruses encoding 3rd-base wobble variants of WT Venus-BCAR3, L744E/R748E (L/R) Venus-BCAR3 or empty vector (pLV-Venus; Ctl). Total cell protein was immunoblotted with antibodies to detect the indicated proteins. (B, C) The cells described in panel A were grown in 3D Matrigel culture for 6 days. Representative phase images (B) and quantification of invasive structures (C) are shown. Data presented are the mean \pm SEM of 6-7 replicates per condition from one experiment. Scale bars = 200 μ m. Statistical analysis performed using a Kruskal-Wallis one-way ANOVA and a Dunn's Multiple Comparison post-test. *, $p < 0.05$ relative to pLKO.

BCAR3 (bar 4). Collectively, these data show that BCAR3 promotes both chemotaxis toward serum and invasion through its interactions with Cas.

2.2.5 BCAR3 is co-expressed with Cas in multiple subtypes of human breast tumors

Considering the strong functional relationship between BCAR3 and Cas in breast cancer cell lines *in vitro*, we next sought to determine whether there was evidence for a similar functional association in human breast tumors. Sequential sections of tumor tissue were stained with hematoxylin and eosin (H&E) or antibodies recognizing BCAR3 or Cas. BCAR3 expression was found to be low to non-detectable in normal breast tissue (**Figure 2.12, top panels**) but upregulated in multiple breast tumor subtypes (bottom 3 panels). Moreover, BCAR3 was found to be co-expressed with Cas in localized regions of tumor tissue (see insets), suggesting that these two molecules may indeed function as a unit in breast cancers.

2.3 Discussion

BCAR3 expression is upregulated in invasive breast cancer cell lines and has been shown to promote migration and invasion in these cells (Near *et al.*, 2007; Schrecengost *et al.*, 2007; Wilson *et al.*, 2013). Work from the Pasquale group demonstrated that direct binding between BCAR3 and Cas is required for enhanced Src activity and Cas phosphorylation (Wallez *et al.*, 2014). In the current study, we sought to further elucidate the importance of BCAR3/Cas complexes in BCAR3-dependent functions, particularly those associated with cell motility and invasion. The functional nature of this protein complex is underscored by our finding that all of the BCAR3 is in complex with Cas in invasive breast cancer cells.

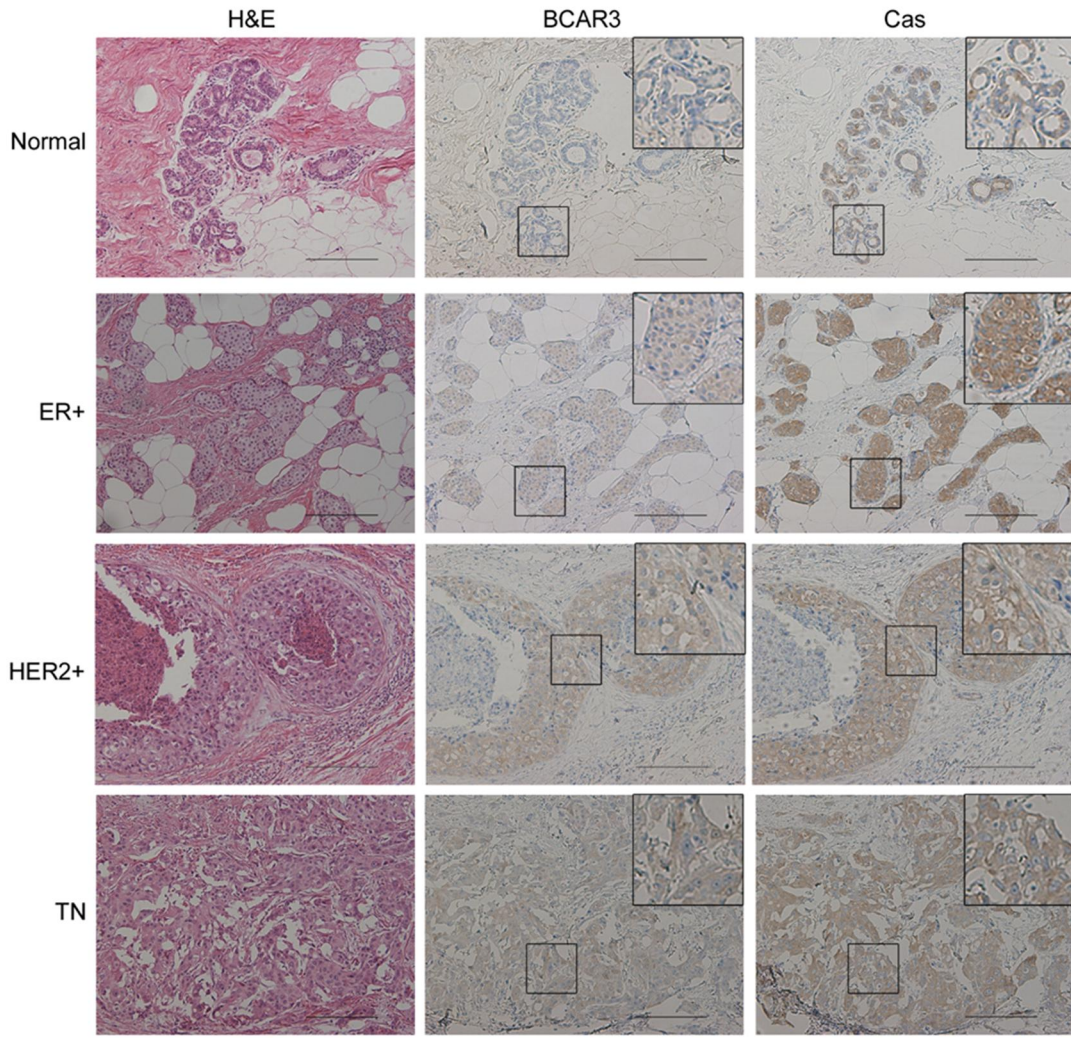


Figure 2.12. BCAR3 is co-expressed with Cas in multiple subtypes of human breast tumors

Sequential sections of human tissue were stained with hematoxylin and eosin (H&E) (left panels) or immunostained with BCAR3 (middle panels) or Cas (right panels) antibodies. Insets show higher magnifications of the designated areas. Scale bars=50 μ M.

2.3.1 BCAR3 targeting to adhesions is multi-factorial

Since all of the BCAR3 in BT549 and MDA-MB-231 breast cancer cells is present in BCAR3/Cas complexes, it is formally possible that, in the absence of any perturbation, endogenous BCAR3 enters adhesions together with Cas. However, there must also be Cas-independent mechanisms for adhesion targeting of BCAR3 since ectopically expressed L744E/R748E GFP-BCAR3 readily localized to adhesions despite its inability to associate with Cas (**Figure 2.13A**). The SH2 domain has been reported to mediate BCAR3 targeting in MEFs through its interaction with PTP α (Sun *et al.*, 2012); however, the SH2 domain was dispensable for adhesion targeting in our system. Moreover, the dual SH2/Cas binding mutant (R171V/L744E/R748E GFP-BCAR3) also localized to adhesions, indicating that there are other focal adhesion targeting mechanisms that contribute to BCAR3 localization to these sites, at least in the absence of Cas and PTP α interactions. It is unlikely that this targeting activity is a direct consequence of talin and α -actinin, as neither protein was present in WT or L744E/R748E GFP-BCAR3 immune complexes (**Figure 2.5**). Whether other adhesion proteins are responsible for adhesion targeting of ectopic BCAR3 molecules in these circumstances remains to be determined.

2.3.2 BCAR3/Cas interactions are required for efficient BCAR3-mediated adhesion disassembly, migration, invasion, and Rac1 activity

The data presented above provide the first mechanistic insight into how BCAR3 promotes adhesion disassembly and invasion of breast cancer cells. Under conditions in which BCAR3/Cas complexes were able to form (i.e. WT BCAR3), we observed rapid dissociation of multiple proteins from adhesions. However, when BCAR3/Cas interactions were blocked (i.e. L744E/R748E BCAR3), the rate of adhesion disassembly was significantly reduced. This suggests that the BCAR3/Cas complex contributes to adhesion disassembly. Furthermore, our data argue that the Cas-binding mutant of BCAR3 acts as

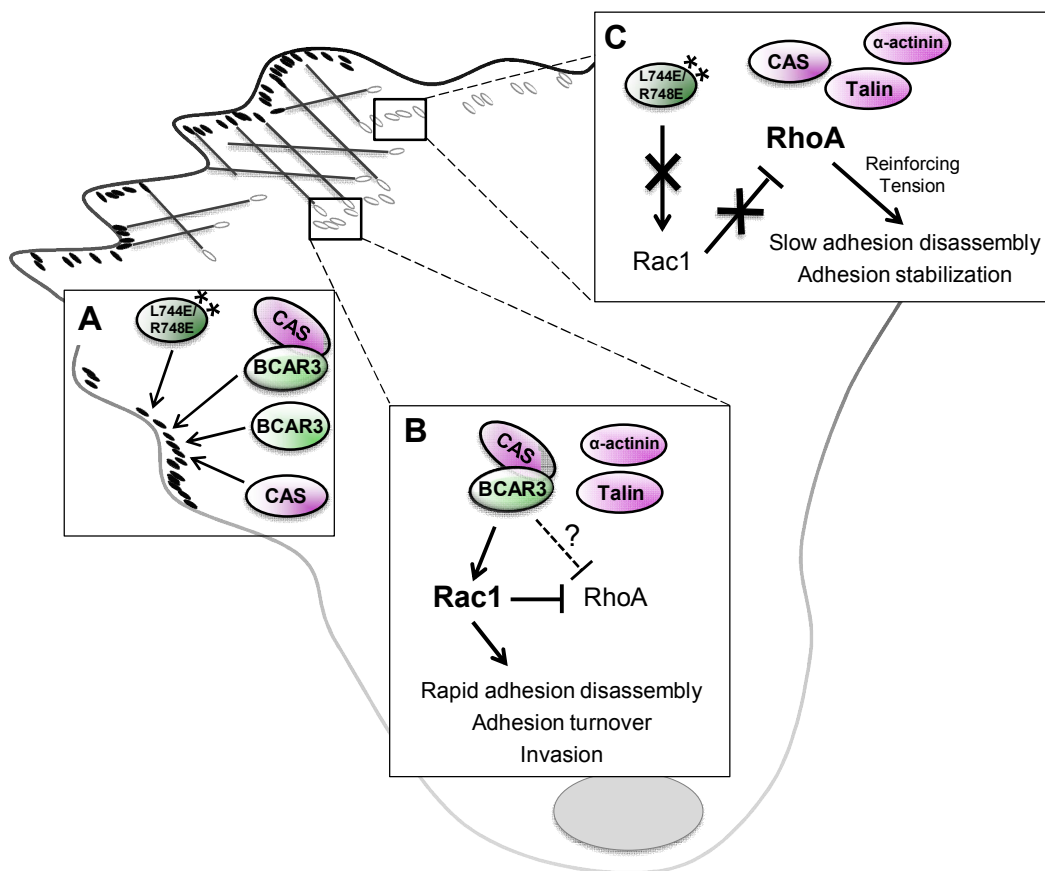


Figure 2.13. BCAR3/Cas interactions promote efficient adhesion complex disassembly and invasion

(A) BCAR3 can efficiently incorporate into adhesions in the absence of a functional Cas binding and/or SH2 domain. (B) Under conditions where BCAR3/Cas interactions are enabled (i.e. WT BCAR3), rapid disassembly of multiple adhesion proteins is observed. We propose BCAR3/Cas complexes promote localized activation of Rac1 and/or suppression of RhoA under these conditions, therefore initiating rapid adhesion turnover and invasion. (C) When BCAR3/Cas interactions are prevented (i.e. L744E/R748E BCAR3), local Rac1 activation is diminished, leading to a possible rise in localized RhoA-mediated tension, which provides the reinforcement necessary to stabilize adhesions and slow the rate of disassembly. *Figure provided in collaboration with Dr. Ashley Wilson.*

to dominantly inhibit endogenous WT BCAR3 protein, as the delay in adhesion dissociation observed in the presence of the Cas-binding mutant of BCAR3 phenocopies the previously published defect in adhesion turnover observed upon BCAR3 knockdown (Wilson *et al.*, 2013). The ability of the Cas-binding mutant to act as a dominant negative may be due to its ability to bind to another protein needed for BCAR3 function and prevent its interaction with WT BCAR3. Another possibility is that the Cas-binding mutant of BCAR3 blocks the localization of WT BCAR3 to adhesions and thus prevents its function at these sites.

Recent studies have shown that the ability of BCAR3 to induce membrane ruffling/lamellipodia in 2D also requires Cas binding (Wallez *et al.*, 2014). Data presented in this report expand on these findings by showing that interactions between BCAR3 and Cas are required for the invasive phenotype of breast cancer cells in 3D as well as chemotaxes toward serum. Finally, BCAR3 expression in cells grown on plastic promotes Src-mediated Cas phosphorylation in breast cancer cells, leading to Cas/Crk coupling and Rac1 activation (Klemke *et al.*, 1998; Akakura *et al.*, 2005; Schrecengost *et al.*, 2007; Cabodi *et al.*, 2010; Sun *et al.*, 2012; Wilson *et al.*, 2013). We show here that BCAR3-dependent Rac1 activation also requires interaction with Cas. On 3D matrices, Rac1 activity promotes a mesenchymal phenotype, while elevated RhoA signaling promotes more rounded cell morphology (Yamazaki *et al.*, 2009). It is therefore interesting to speculate that BCAR3/Cas-dependent Rac1 activity may be critical for its ability to promote an invasive phenotype in 3D culture. Whether the adhesion turnover functions of BCAR3/Cas observed in 2D contribute to the BCAR3-dependent invasive phenotype in 3D remains to be determined, particularly since adhesions that form in 2D and 3D may differ significantly in protein composition, dynamics, and regulation (Harunaga and Yamada, 2011; Petrie and Yamada, 2012).

The co-localization of BCAR3 and Cas in adhesions suggests that BCAR3/Cas-mediated Rac1 activation is likely to occur at these sites. This activity, coincident with the possible suppression of RhoA in adhesions, could account for the faster rate of adhesion disassembly and turnover observed when WT GFP-BCAR3 and Cas are expressed in the cells (**Figure 2.13B**). Although the Cas-binding mutant of BCAR3 was also seen to efficiently localize to adhesions, it failed to promote Rac1 activity. In the absence of BCAR3-Cas interactions (or upon depletion of BCAR3 as was the case in our previous study), we speculate that the inability to locally activate Rac1, together with a possible rise in RhoA-mediated tension, provides the reinforcement necessary to stabilize adhesions and reduce the rate of disassembly (**Figure 2.13C**). This model is supported by work from the Lerner group, who showed that deletion of the C-terminus of BCAR3 abrogated both Cas binding and Rac1 activation (Vanden Borre *et al.*, 2011). They also showed that a mutant of BCAR3 containing a single point mutation in the Cas-binding domain was still able to promote Rac1 activity despite its apparent inability to bind to Cas. It has since been shown, however, that this point mutation may not completely abrogate Cas binding in the cell (Wallez *et al.*, 2014).

In conclusion, we favor a model wherein BCAR3 promotes Rac1 activation, adhesion disassembly, and an invasive phenotype through its binding to Cas, and that interfering with the interaction between these proteins short-circuits signaling network(s) responsible for these activities (**Figure 2.13**). An alternative explanation for the data presented in the current study is that L744E/748E BCAR3 may function independently of Cas to inactivate other molecules/pathways whose functions are critical for these outcomes. We consider this to be unlikely, however, largely because expression of the Cas-binding mutant of BCAR3 phenocopies the effects of BCAR3 knockdown that were reported in our previous study (Wilson *et al.*, 2013) with respect to the adhesion turnover defect and diminished Rac1 activation.

2.3.3 BCAR3/Cas functions as an oncogenic protein complex in invasive breast tumor cells

Our finding that the majority of BCAR3 in BT549 and MDA-MB-231 cells is associated with Cas suggests that the function of BCAR3 in these cells is dependent on the BCAR3/Cas complex. This is further supported by the data presented above showing that BCAR3 is low to non-detectable in normal breast tissue but is co-expressed with Cas in multiple breast tumor subtypes. It should be noted that our analysis of BCAR3 expression in normal breast tissue contradicts reports in the Human Protein Atlas which show that BCAR3 is expressed at moderate levels in normal breast tissue. One explanation for this discrepancy may be the low number of normal breast tissue samples we analyzed for BCAR3 expression. Moreover, the number of normal breast tissues that were analyzed in the Human Protein Atlas was not reported, nor was the percentage of samples that were found to express BCAR3 at moderate levels. Notably, our immunohistochemical staining for BCAR3 was performed by the Biorepository and Tissue Research Facility at UVA and the staining was thoroughly validated using control and BCAR3-depleted cell pellets.

Despite strong evidence for BCAR3 as a potent regulator of cell adhesion and invasion in breast cancer cells, the fact that a global knockout of BCAR3 fails to cause any major developmental or phenotypic abnormalities at birth (Near *et al.*, 2009) indicates that its expression is largely dispensable for morphogenesis. BCAR3 expression is upregulated in invasive breast cancer cell lines (Near *et al.*, 2007; Schrecengost *et al.*, 2007), and it is in this context that BCAR3 appears to play a critical role in adhesion turnover and invasion. Together, these data suggest that BCAR3/Cas and/or its downstream effectors may prove to be effective therapeutic targets for tumors that co-express these molecules, particularly because BCAR3 is non-essential for development.

Chapter 3: Breast Cancer Antiestrogen Resistance 3 (BCAR3) accelerates time-to-tumor appearance and regulates tumor burden *in vivo*

3.1 Introduction

Much of the work done *in vitro* analyzing BCAR3 function suggests that BCAR3 may play an important role in breast tumor progression *in vivo*. BCAR3 protein expression is upregulated in invasive breast cancer cell lines, where it has been shown to enhance cell migration and invasion (Schrecengost *et al.*, 2007; Wilson *et al.*, 2013; Wallez *et al.*, 2014). In addition to the role BCAR3 plays in cancer cell motility, BCAR3 has been reported to regulate proliferation through increased cyclin D1 expression (Near *et al.*, 2007). The ability of BCAR3 to promote these phenotypes is dependent on its direct binding with Cas (Wallez *et al.*, 2014) (Chapter 2). *In vivo*, BCAR3 is seen to be co-expressed with Cas in multiple subtypes of breast cancer (Chapter 2, Figure 2.12). In comparison, low to non-detectable levels of BCAR3 protein are present in normal breast epithelium (Chapter 2, Figure 2.12). Thus, it is interesting to speculate that BCAR3 co-expression with Cas may drive proliferation, migration, and invasion of breast tumor cells *in vivo* as well as *in vitro*, and in so doing, regulate tumor growth and progression.

Despite *in vitro* data suggesting BCAR3 may control tumor growth or progression, high BCAR3 mRNA expression in ER+ breast tumors has been reported to be associated with increased progression-free survival (Guo *et al.*, 2014). It is important to note, however, that this relationship between BCAR3 mRNA and survival was only present in ER+ tumors. Furthermore, the correlation between mRNA and protein abundance is relatively poor (Maier *et al.*, 2009), and there are no reported studies analyzing BCAR3 protein expression in relation to patient survival in breast cancer.

The hypothesis that BCAR3 protein expression may promote tumor growth and/or progression is supported by the observation that BCAR3 protein augments Src kinase

activity and controls the stability and signaling downstream of Cas (Schuh *et al.*, 2010; Wallez *et al.*, 2014) (Appendix 1). Both Cas protein levels and Src activity have been reported to control breast cancer progression *in vivo*. Cas is overexpressed in human breast cancers, and its expression is correlated with decreased relapse-free survival and increased mortality (Tornillo *et al.*, 2014). Additionally, Cas has been shown to control tumor progression in several mouse models of breast cancer. For example, overexpression of Cas in MMTV-HER2-Neu transgenic mice accelerates the time-to-tumor-appearance while Cas depletion in a TGF- β driven model of mammary tumorigenesis significantly reduces tumor outgrowth (Cabodi *et al.*, 2006, Wendt, Smith, & Schiemann, 2009). Furthermore, overexpression of the phosphorylated substrate domain of Cas in MMTV-polyoma middle T (PyMT) mice accelerates tumor growth and promote metastasis (Zhao *et al.*, 2013; Kumbrink *et al.*, 2016). Src activity enhances cell growth, proliferation, angiogenesis, invasion, and metastasis (Finn, 2008). Src activity is upregulated in a significant number of breast cancer tumors and in the MMTV-PyMT mouse model of breast cancer, where it is required for both mammary tumorigenesis and metastasis (Guy *et al.*, 1994; Irby and Yeatman, 2000).

As BCAR3 influences cell proliferation, migration, invasion, Src activity and Cas phosphorylation *in vitro* (Near *et al.*, 2007; Schrecengost *et al.*, 2007; Schuh *et al.*, 2010; Wilson *et al.*, 2013) (Chapter 2), we set out to determine whether it had a role in tumor growth. We found that BCAR3 expression was upregulated and differentially expressed in the MMTV-PyMT model of breast cancer. In some regions of the early MMTV-PyMT mouse tumors, BCAR3 was seen to be co-expressed with cyclin D1 but further studies are needed to determine if BCAR3 promotes cyclin D1 expression *in vivo*. In an MDA-MB-231 xenograft tumor model, loss of BCAR3 was shown to significantly delay time-to-tumor-appearance and decrease total tumor burden. Additional studies need to be

completed to understand how BCAR3 promotes tumor formation and regulates tumor burden. Furthermore, it will be important to evaluate if BCAR3 also controls metastasis.

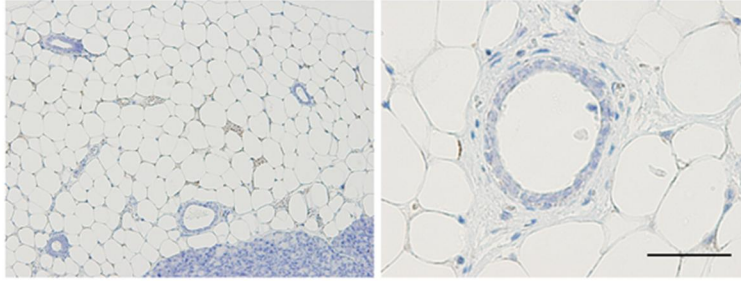
3.2 Results

3.2.1 BCAR3 is upregulated and differentially expressed during tumor progression

Despite *in vitro* data demonstrating that BCAR3 controls tumor cell proliferation, migration and invasion, the ability of BCAR3 to promote tumor progression *in vivo* has not been studied (Near *et al.*, 2007; Schrecengost *et al.*, 2007; Wilson *et al.*, 2013) (Chapter 2). To gain a better understanding about whether BCAR3 plays a role in tumor progression, BCAR3 expression was measured in tumors that form spontaneously in MMTV-PyMT mice as a consequence of expression of the PyMT oncoprotein in mammary epithelial cells. The tumors that form in these mice progress through four identifiable stages that are comparable to human breast disease; hyperplasia, adenoma/mammary intra-epithelial neoplasia (MIN), early carcinoma, and late carcinoma (Lin *et al.*, 2003). In addition to the morphological similarities between tumors that form in the MMTV-PyMT mice and human breast tumor progression, the pattern of expression of biomarkers is also similar to those seen in human disease (Lin *et al.*, 2003).

To analyze BCAR3 expression during MMTV-PyMT tumor progression, immunohistochemical (IHC) staining was performed on mammary glands isolated from MMTV-PyMT mice during the adenoma/MIN, early carcinoma, and late carcinoma stages of tumor development. Analysis of transgene-negative mice showed that BCAR3 was not expressed in the epithelial cells of non-transformed ducts (**Figure 3.1A**). During the adenoma/MIN and early carcinoma stages, BCAR3-positive cells were found to localize to the outer edge of the tumor acini (**Figure 3.1B, panels a and b**). By the late carcinoma stage, BCAR3-expressing cells were located throughout the tumor, but the expression level per cell appeared to be reduced compared to the amount of BCAR3 present in the

A



B

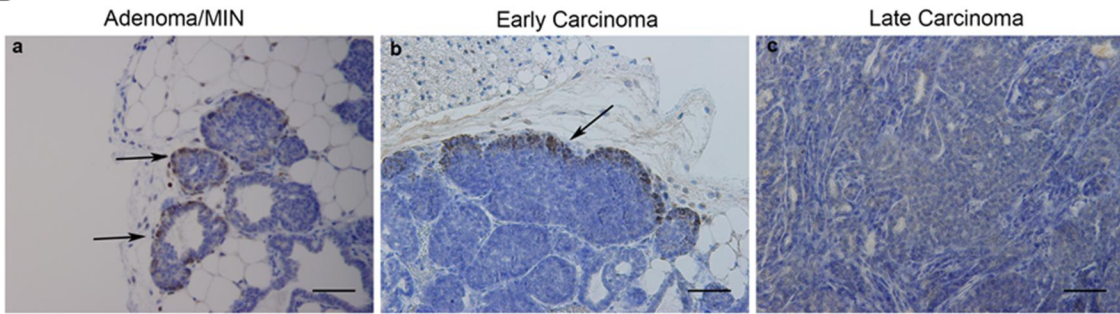


Figure 3.1. BCAR3 is upregulated and differentially expressed during PyMT tumor development

Mammary gland 1 was isolated from transgene-negative (A) or transgene-positive MMTV-PyMT mice during various stages of tumor development (B). Tumor sections were immunostained with BCAR3 antibodies. Arrows point to localized expression of BCAR3 at the outer edge of the tumor acini during adenoma/MIN and early carcinoma. Scale bars=50 μ M.

high-expressing cells seen in the earlier stages of tumor development (**Figure 3.1B, panel c**). These data demonstrate that BCAR3 expression is upregulated in tumor compared to normal tissue and that BCAR3 is expressed differentially during tumor progression in MMTV-PyMT mice.

3.2.2 Co-expression of BCAR3 and cyclin D1 can be observed in PyMT tumors

The localized expression of BCAR3 at the outer edge of the tumor acini observed in PyMT adenomas (**Figure 3.1B**) is strikingly similar to the pattern of cyclin D1 expression in these tumors reported by Lin *et al.* (Lin *et al.*, 2003). This is particularly interesting in light of the fact that Near *et al.* showed that BCAR3 expression activates the cyclin D1 promoter *in vitro* (Near *et al.* 2007). To determine if BCAR3 promotes cyclin D1 expression in PyMT tumors, we first looked for co-expression of these proteins in serial sections of PyMT adenomas. We found that a subset of the adenomas that expressed high levels of cyclin D1 also stained positively for BCAR3 (**Figure 3.2**). However, it should be noted that many regions of the tumors contained high cyclin D1 levels with little to no BCAR3, indicating that co-expression of these molecules could be the result of a stochastic rather than an active process. Our analysis of BCAR3 and cyclin D1 expression in these mice was limited to the adenoma/MIN stage of tumor development and will need to be expanded to include early and late carcinomas. These preliminary data thus suggest a possible relationship between BCAR3 and cyclin D1 but further studies are needed to determine if BCAR3 is co-expressed and regulates cyclin D1 expression *in vivo*.

3.2.3 BCAR3 accelerates time-to-tumor-appearance and increases total tumor burden in vivo

Considering the *in vitro* data demonstrating that BCAR3 promotes proliferation migration, and invasion (Riggins *et al.*, 2003; Schrecengost *et al.*, 2007; Schuh *et al.*,

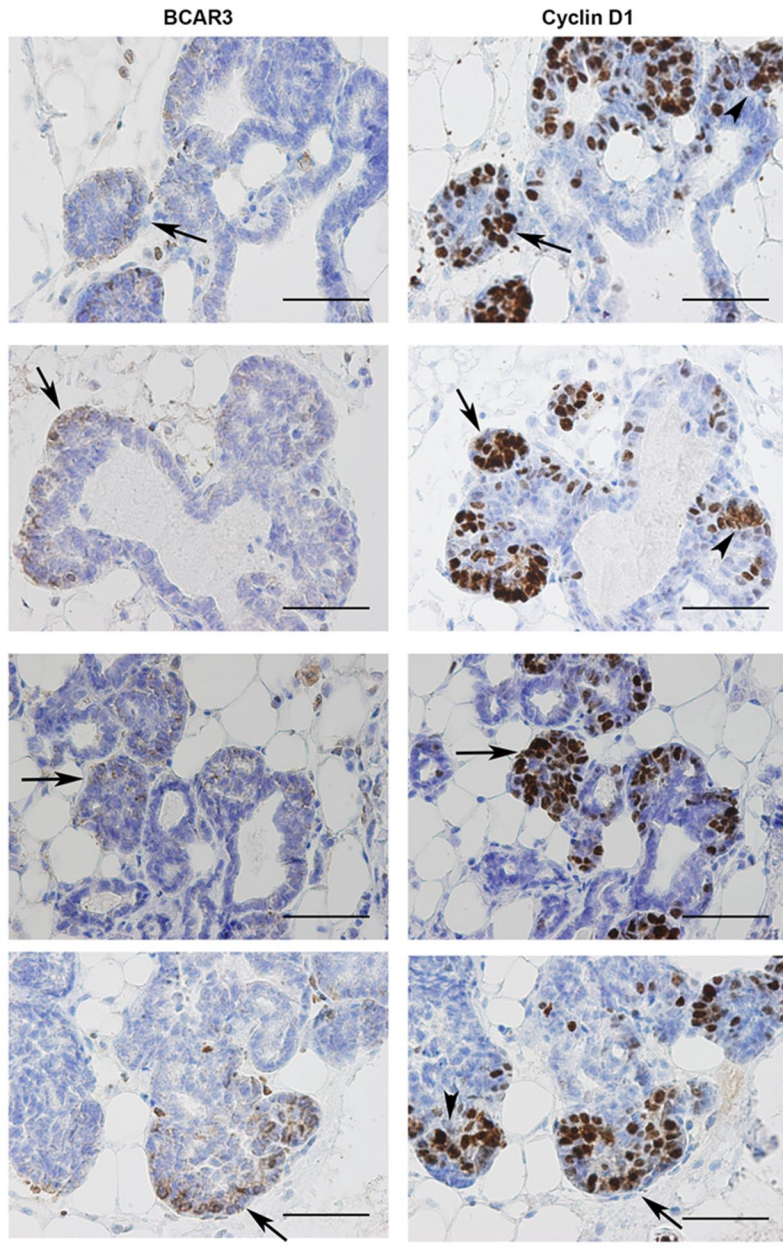


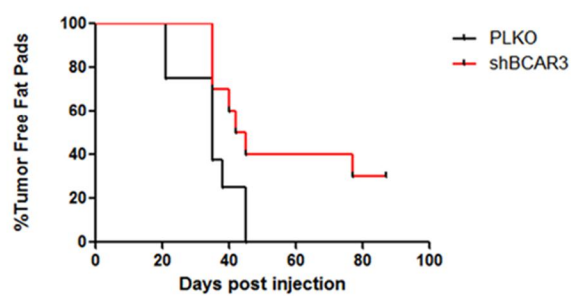
Figure 3.2. Co-expression of BCAR3 and cyclin D1 can be observed in PyMT tumors

Mammary gland 1 was isolated from MMTV-PyMT mice during the adenoma/MIN stage of tumor development. Sequential sections of tissue were immunostained with BCAR3 (left panels) or cyclin D1 (right panels) antibodies. Arrows indicate areas of co-expression and arrowheads indicate areas that are positive for cyclin D1 expression but have low to non-detectable BCAR3 expression. Scale bars=50 μ M.

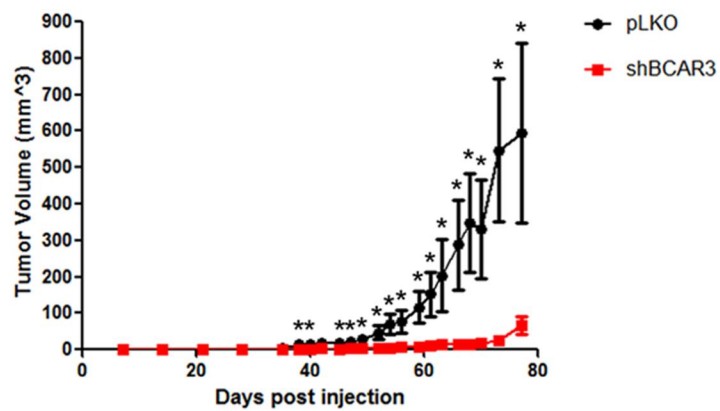
2010; Wilson *et al.*, 2013; Wallez *et al.*, 2014) (Chapter 2), and the upregulation and differential expression of BCAR3 in PyMT tumors, we set out to determine if BCAR3 promotes tumor growth *in vivo* by analyzing the effects of BCAR3 knockdown on MDA-MB-231 tumor xenografts. Stable MDA-MB-231 cells expressing either an empty vector (pLKO) or a BCAR3-targeted shRNA were infected with a luciferase-expressing virus, pLenti-PGK-Blast-V5-LUC, and injected bilaterally into mammary gland 5 of nude mice. Mice were monitored weekly using an *in vivo* imaging system (IVIS) and tumor caliper measurements were taken twice weekly once tumors became palpable. Tumors formed in all of the fat pads injected with the control cells by 42 days post-injection, while 30% of fat pads injected with cells depleted of BCAR3 remained tumor-free at 84 days post-injection (**Figure 3.3A**). Beginning on day 38 and continuing through day 77 post-injection (with the exception of day 42), there was a significant reduction in tumor burden as measured by caliper in the fat pads of mice injected with BCAR3-depleted cells compared to mice injected with control cells (**Figure 3.3B**). This difference in tumor burden was also observed by IVIS imaging (**Figure 3.3C**). IVIS imaging further revealed that, in the three fat pads that failed to form palpable tumors following injection with shBCAR3-expressing cells, no luciferase-expressing tumor cells were evident by day 28 despite the presence of luciferase-expressing tumor cells 7 days post-injection (data not shown). These fat pads remained free of luciferase-expressing tumor cells throughout the remainder of the experiment as indicated by IVIS imaging at day 77 (**Figure 3.3 C, panel b**).

Prior to injection into the mouse, analysis of lysates from cells expressing the empty vector (pLKO) or BCAR3-targeted shRNA confirmed efficient depletion of BCAR3 in the shBCAR3-expressing cells (**Figure 3.4A**). To determine whether BCAR3 expression remained knocked down in the tumors that ultimately formed from shBCAR3-expressing cells, individual tumors were isolated at week 12 or earlier (if tumor volume reached 1500mm³), fixed and paraffin embedded, and immunostained for BCAR3. Despite

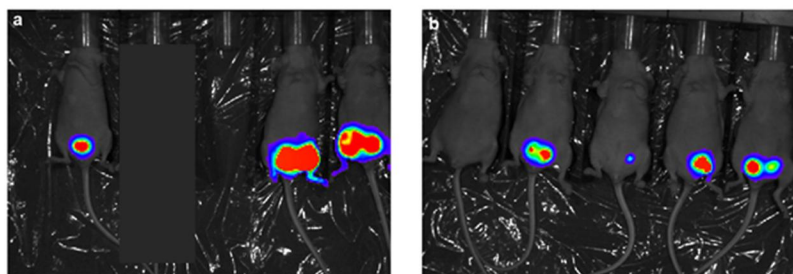
A



B



C



C

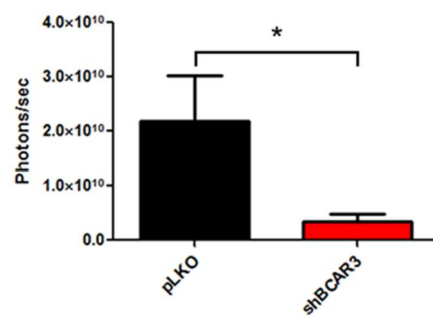


Figure 3.3. BCAR3 accelerates time-to-tumor-appearance and enhances tumor burden in MDA-MB-231 xenograft tumors

MDA-MB-231 cells stably expressing luciferase and either empty vector (pLKO) or a BCAR3 targeted shRNA (shBCAR3-1) were bilaterally injected into mammary gland 5 of nude mice n=10 mice (5 pLKO, 5 shBCAR3). (A) The time-to-palpable tumor for each fat pad was plotted on Kaplan and Meier curves for 8 fat pads in the pLKO condition and 10 fat pads in the shBCAR3 condition. Two fat pads were excluded from the pLKO condition as they were not successfully injected with cells. $p < 0.05$ by log-rank (Mantel-Cox) analysis. (B) Tumor volume per fat pad (determined by caliper measurement twice weekly) over the time course of the experiment. Data presented are the mean \pm SEM of 7 tumors from pLKO-injected mice and 10 from shBCAR3-injected mice. Three fat pads were excluded from the pLKO condition due to unsuccessful injection of cells into two fat pads and early sacrifice of a mouse due to the presence of tumor cells in the peritoneal cavity. *, $p < 0.05$ by unpaired t-test. (C) Tumor burden per mouse, as determined by IVIS imaging. Images captured from mice at day 77 injected with pLKO-expressing cells (panel a) or shBCAR3-expressing cells (panel b). Quantification of IVIS images at day 77 is shown in panel c. Data presented are the mean \pm SEM of 3 mice injected with pLKO cells and 5 mice injected with shBCAR3 cells. Two mice were excluded due to the presence of non-mammary tumors that arose when the cells were not injected correctly into the fat pads. *, $p < 0.05$ by unpaired t-test.

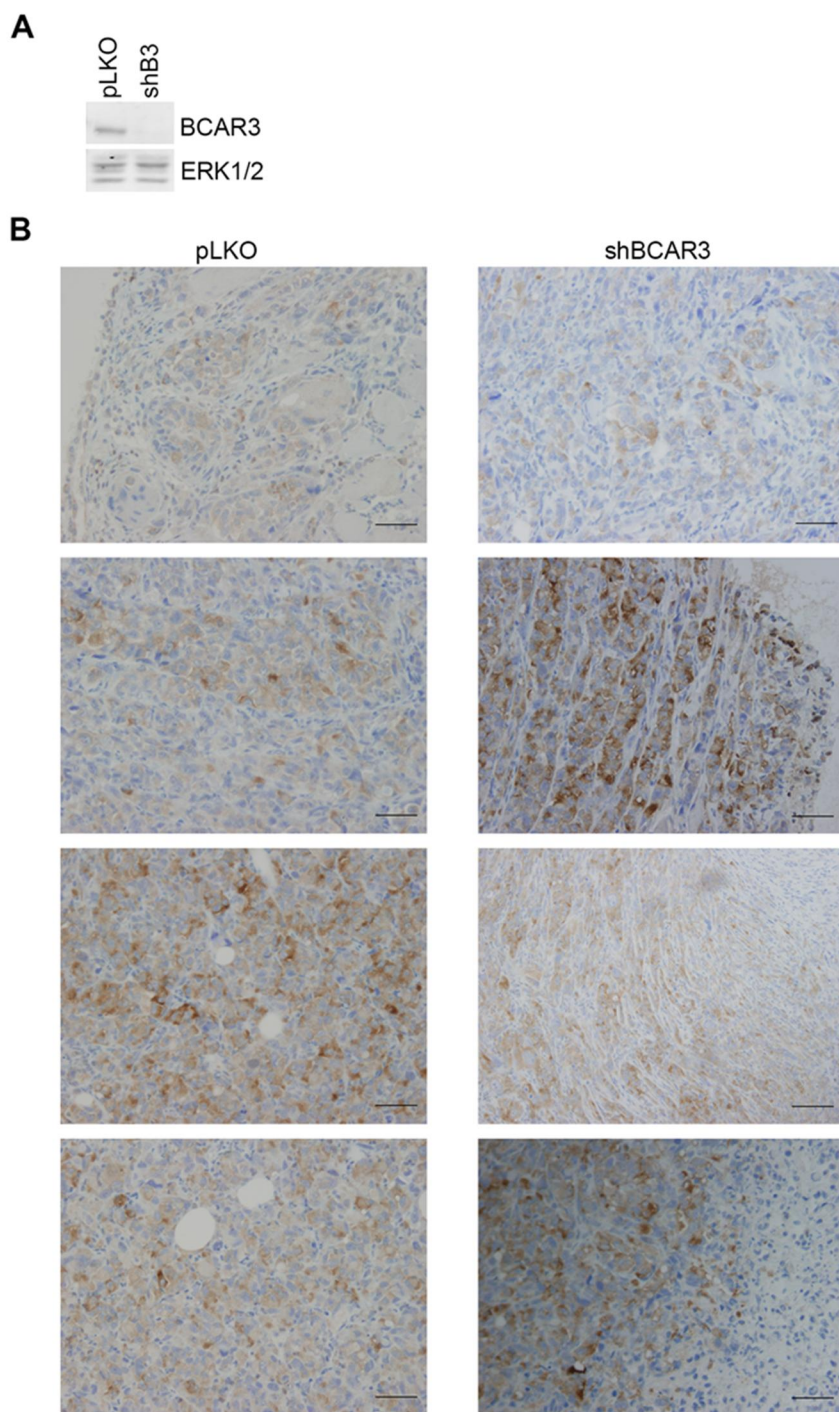


Figure 3.4. BCAR3 is expressed in tumors formed from shBCAR3-infected cells

(A) MDA-MB-231 cells stably expressing empty vector (pLKO) or BCAR3-targeted shRNA (shBCAR3) were lysed. Proteins were immunoblotted with antibodies recognizing the designated proteins. (B) Tumors formed in mammary gland 5 of nude mice were removed at week 12 or earlier (if tumor volume reached 1500mm³), fixed, and embedded in paraffin. Sections of tumor tissue from mice injected with the indicated cells were immunostained with BCAR3 antibodies. Scale bars=50µm.

efficient knockdown of BCAR3 in the original shBCAR3 cells, examination of the tumors by IHC revealed that BCAR3 protein was present in all tumors isolated from mice injected with the BCAR3-depleted cells (**Figure 3.4B**). The level of BCAR3 expression in these tumors appeared to be roughly comparable to the amount of BCAR3 present in tumors isolated from mice injected with control cells. These data indicate that there was a strong selection for BCAR3-expressing cells in the tumors that ultimately formed from the BCAR3-depleted cell populations.

3.3 Discussion

The upregulation of BCAR3 in invasive breast cancer cell lines has been shown to be a driver of migration and invasion in these cells. In addition to these functions, BCAR3 has been reported to regulate proliferation through cyclin D1 expression (Near *et al.*, 2007; Wallez *et al.*, 2014). In this study we aimed to elucidate the role of BCAR3 in controlling tumor growth. Our data demonstrate that BCAR3 is upregulated and differentially expressed during tumor progression in the MMTV-PyMT mouse model, and that BCAR3 promotes tumor formation and regulates total tumor burden in an MDA-MB-231 xenograft model of breast cancer.

These preliminary studies raise several questions. First, the data presented above do not provide insight into the mechanism of BCAR3-mediated tumor formation. Second, it is not clear whether BCAR3 loss in established tumors would result in a reduced tumor burden over time, or if BCAR3 is only required for the early events that determine tumor outgrowth in a xenograft transplantation model. Finally, though our preliminary studies focused on primary tumor burden, it will be important to determine if BCAR3 can promote metastasis *in vivo*.

3.3.1 How does BCAR3 regulate primary tumor formation?

The delay in time-to-tumor-appearance observed in mice injected with BCAR3-depleted cells, along with the observation that BCAR3 was found to be expressed in all of the tumors formed from shBCAR3-infected cells, argues that BCAR3 protein may be required to establish tumors in this xenograft model. The requirement for BCAR3 in this process could result from its function as a regulator of tumor cell proliferation. However, if BCAR3 regulates tumor outgrowth by controlling cell proliferation, this is likely not the only function of BCAR3 during this process. The observation that 30% of fat pads injected with BCAR3-depleted cells were cleared of luciferase-expressing tumor cells by day 28 post-injection argues that BCAR3 may also be important for cell survival. Interestingly, BCAR3-depleted MDA-MB-231 cells grown on plastic exhibit a slight decrease in doubling-time compared to control cells- (personal communication, Barbara Dziegielewska). Whether such a modest defect in cell proliferation and/or survival could account for the significant delay in tumor appearance observed in mice injected with BCAR3-depleted cells and the dramatic enrichment of BCAR3-expressing cells present in the tumors at later times remains to be determined. Notably, cell proliferation and survival rates are altered in the presence of stromal components and as a consequence of physiological properties of the tissue (e.g. stiffness, rigidity) (Provenzano *et al.*, 2009; Khamis *et al.*, 2012; Edmondson *et al.*, 2014). Stromal cells, including tumor-associated fibroblasts and macrophages, mediate tumor cell proliferation and survival through production of collagen, laminin, and fibronectin and through release of growth factors and cytokines (Wyckoff *et al.*, 2004; Khamis *et al.*, 2012; Hollmén *et al.*, 2015). In addition, increased matrix rigidity induced by changes in extracellular matrix composition promotes proliferation of epithelial cells (Provenzano *et al.*, 2009). Therefore, a modest impairment in cell proliferation or survival *in vitro* may be exacerbated *in vivo*.

Data presented in chapter 2 highlight the importance of BCAR3/Cas binding in promoting BCAR3-mediated adhesion turnover, migration, and invasion. Furthermore, Wallez *et al.* have shown that direct interaction between BCAR3 and Cas is required for BCAR3-dependent Src activity and Cas phosphorylation (Wallez *et al.*, 2014). The ability of BCAR3 to promote tumor formation *in vivo* may be similarly dependent upon its direct association with Cas. This can be tested by performing studies comparing the tumorigenicity of stable pLKO- and shBCAR3-expressing MDA-MB-231 cells with that of BCAR3-depleted cells re-expressing either shRNA-resistant WT or Cas-binding mutant BCAR3 proteins. If direct interaction between BCAR3/Cas is required for efficient BCAR3-mediated MDA-MB-231 tumor growth in mice, the cells re-expressing WT BCAR3 protein should form tumors at a similar rate to control cells, while cells re-expressing the Cas-binding mutant of BCAR3 should form tumors at a similar rate to the shBCAR3 cells.

To address the potential role of BCAR3 and the BCAR3/Cas complex in controlling tumor cell proliferation and survival, immunohistochemistry can be performed analyzing Ki67, cyclin D1, and cleaved caspase levels in early tumors. Importantly, the immune system is known to play role in breast cancer and, although nude mice lack T cells, these mice have B cells, macrophages, and natural killer cells (Rao *et al.*, 1977; Standish *et al.*, 2008; Belizário, 2009). Tumor cell survival and tumor growth could be altered if BCAR3 depletion in the tumor cells affects the immune response to the tumor. To test if the immune response to tumors is altered in the absence of BCAR3, the presence of immune cell infiltrate into the tumor can be analyzed.

3.3.2 Does BCAR3 regulate tumor growth in established tumors?

Because the outgrowth of tumors initiated from BCAR3-depleted cells was significantly delayed, it was difficult to determine whether BCAR3 might also have an effect on the growth rate of established tumors. This could be tested using conditional

knockdown approaches. If knockdown of BCAR3 once the tumors become palpable fails to reduce the rate of tumor growth, this would argue that BCAR3 is only required for early events in the transplantation model during the process of establishing the tumor. It would be important under these conditions to measure BCAR3 expression in the tumors that grow out to assure that knockdown was maintained. The alternative finding, where tumor growth would become significantly delayed once BCAR3 was knocked down, would be consistent with BCAR3 playing a sustained role in proliferation and/or survival. If this is found to be the case, the knockdown tumors might exhibit a second phase of rapid growth in parallel with overgrowth of cells that escaped BCAR3 knockdown. In addition, the conditional knockout model described in this section may be more amenable to the studies described above examining markers of proliferation, apoptosis, and immune cell infiltration, as it will be possible to more readily isolate tumors for analysis.

3.3.3 *Is there a role for BCAR3 in tumor metastasis?*

The tumor study presented above suggests that BCAR3 expression regulates primary tumor formation in a transplantable tumor model. As BCAR3 is known to control cell motility and invasion (Schrecengost *et al.*, 2007; Wilson *et al.*, 2013) (Chapter 2), two processes known to be important for metastasis, it is also interesting to consider the possibility that BCAR3 may play a role in driving metastasis. However, metastasis studies would be a challenge with the current model due to the marked difference in tumor burden observed in mice injected with control versus BCAR3-depleted cells, and the presence of BCAR3 in the tumors that ultimately formed from the BCAR3-depleted cells. To circumvent this problem, the conditional knockout cell lines described above would be ideal to study the role of BCAR3 in metastasis. For these studies, primary tumors would be allowed to reach 300-500mm³ at which point they would be surgically resected. Upon tumor resection, conditional knockdown of BCAR3 would be induced and tumor metastasis to

the lung monitored by IVIS imaging. As an alternative to tumor resection, tail vein injections could be used to study the ability of control and BCAR3-depleted cells to colonize the lung.

Overall, the data presented in this chapter suggest that BCAR3 plays an important role in controlling tumor formation and total tumor burden *in vivo*. Despite *in vitro* evidence showing that BCAR3 controls Src activity, cyclin D1 expression, and cell migration and invasion (Riggins *et al.*, 2003; Near *et al.*, 2007; Schrecengost *et al.*, 2007; Schuh *et al.*, 2010; Wilson *et al.*, 2013; Wallez *et al.*, 2014) (Chapter 2), however, the mechanism of BCAR3 control over tumor progression still remains to be clarified. Further studies are needed to gain a complete understanding of how BCAR3 controls tumor formation, if BCAR3 promotes growth of established tumors, and to determine if BCAR3 regulates metastases.

Chapter 4: BCAR3 is a potential negative regulator of normal mammary gland development

4.1 Introduction

Mammary gland development is a multistep process that begins during embryogenesis and continues through puberty and pregnancy. A rudimentary ductal tree is present at birth, and during puberty robust branching morphogenesis occurs in response to hormone signaling. During this period, branching begins as terminal end buds (TEBs) form at the tips of ducts and penetrate into the fat pad, repeatedly bifurcating and invading into the surrounding stroma (Hinck and Silberstein, 2005; Sternlicht, 2006; Lanigan *et al.*, 2007). During pregnancy, rapid proliferation of mammary epithelial cells within the ductal branches results in the formation of new lateral buds that differentiate into lobuloalveolar structures containing secretory epithelial cells. Following lactation, the secretory epithelial cells die by apoptosis and the gland is remodeled to resemble that of an adult virgin gland in a process called involution (Wiseman, 2002; Lanigan *et al.*, 2007).

The processes of mammary gland development and breast tumor progression are regulated by many of the same mechanisms and signaling pathways (Lanigan *et al.*, 2007) (**Figure 4.1**). Pubertal mammary gland development, along with the massive remodeling of the gland that occurs during pregnancy, involves proliferation of ductal epithelial cells and invasion of these cells into the surrounding fat pad. This proliferation and invasion, along with the signaling pathways that control these processes, are believed to have some similarities with processes that occur during breast cancer progression (Lanigan *et al.*, 2007). In breast cancer cell lines, BCAR3 has been reported to control proliferation through cyclin D1 expression and promote cellular migration and invasion through its association with Cas (Near *et al.*, 2007) (Chapter 2). Cyclin D1 expression is required for normal lobuloalveolar proliferation during pregnancy (Sicinski & Weinberg, 1997). The

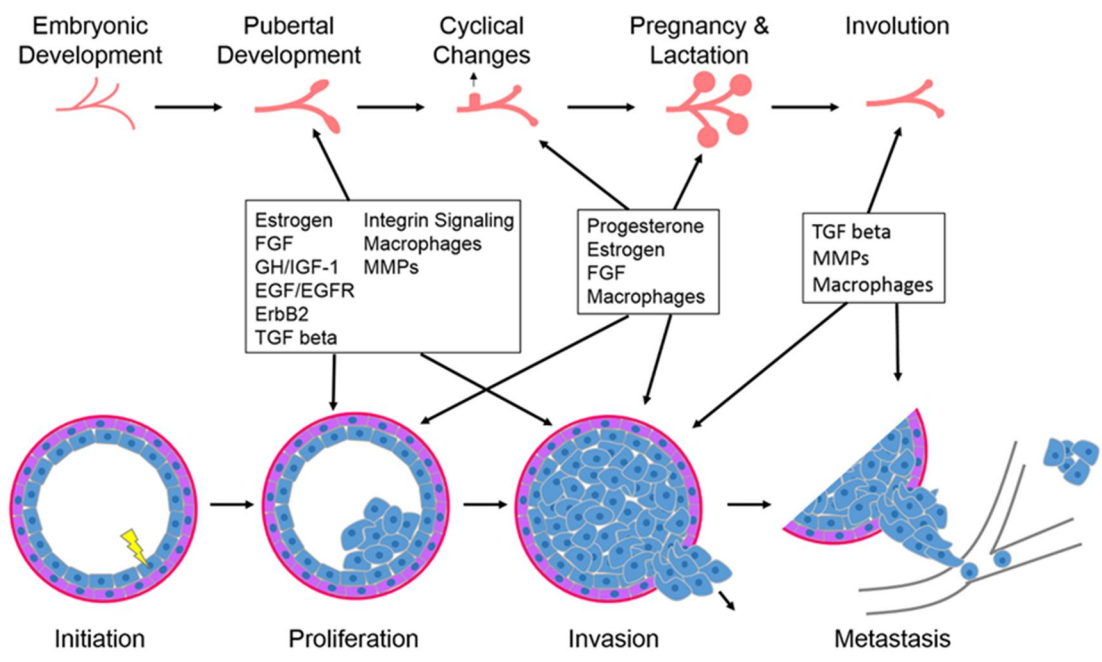


Figure 4.1. Similarities between mammary gland development and breast cancer progression

Many of the proteins, signaling pathways, and cell types that control normal mammary gland development also play a role in breast cancer progression. This diagram illustrates some of the molecular and cellular similarities between these two processes. Figure adapted from Lanigan *et al.* (Lanigan *et al.*, 2007).

role of Cas signaling in normal mammary development has not been well defined due to the fact that Cas depletion in mice results in prenatal lethality (Honda *et al.*, 1998). However, Src and Rac1 activity, both of which are upregulated upon BCAR3 interaction with Cas (Schuh *et al.*, 2010; Wallez *et al.*, 2014) (Chapter 2), play a role in mammary gland development. Studies in c-Src deficient mice have revealed a requirement for Src in promoting ductal outgrowth and TEB formation (Kim *et al.*, 2005), and *in vitro* studies suggest that Rac1 may promote initiation of ductal branching during normal mammary gland morphogenesis (Ewald *et al.*, 2008). Based on these data, we hypothesized that BCAR3 may also play a role in normal mammary gland development through its ability to promote cyclin D1 expression and Src and Rac1 activity.

Considering the established roles of BCAR3 in breast cancer cell proliferation, motility and invasion, we set out to determine if BCAR3 function was important for mammary gland morphogenesis. It has previously been reported that BCAR3 KO mice develop normally with the exception of a defect in the ocular lens (Near *et al.*, 2009). These mice were found to nurse normally and showed no defects in mammary gland development as analyzed by H&E staining of fixed glands. However, it was not clear that a thorough analysis of ductal elongation, TEB formation, and branch density was performed in the mammary glands of BCAR3 KO mice (Near *et al.*, 2009). Moreover, there are several instances described in the literature in which defects in mammary gland development do not affect the ability of the mice to nurse (Chen *et al.*, 2002; Lilla and Werb, 2010).

To better understand if BCAR3 is important for normal mammary gland development, we evaluated BCAR3 expression in developing mammary glands. BCAR3 expression was found to be upregulated during puberty and pregnancy. Preliminary studies analyzing whole mounts of mammary glands from WT and BCAR3 KO mice revealed altered mammary gland development in BCAR3 KO mice during puberty,

characterized by accelerated ductal outgrowth and a reduction in TEBs. To begin to understand the potential mechanisms of BCAR3 control over mammary gland development, we employed MCF10A acinar cultures to model mammary gland development *in vitro*. However, these studies failed to provide evidence for a role of BCAR3 in this process. It is possible that the phenotype observed in BCAR3 KO mice is the result of a function of BCAR3 in non-epithelial cells, which could explain why MCF10A cultures were not able to provide evidence for how BCAR3 regulates mammary gland development. Furthermore, there are many growth factors and hormones present in the developing mammary gland that are not present in MCF10A acinar cultures. It is possible that the function of BCAR3 in the developing gland is linked to signaling downstream of these factors.

4.2 Results

4.2.1 BCAR3 expression is upregulated during mammary gland development

To determine if BCAR3 plays a role in normal mammary gland morphogenesis, we first analyzed BCAR3 protein expression in mammary glands of mice during development. Mammary gland 4 was isolated from C57BL/6 mice during early puberty (4-6 weeks of age) and post-puberty (10+ weeks of age), and BCAR3 expression was analyzed by IHC. Individual ducts in glands from mice at different ages were scored blindly on a scale from 0 to 2+ for levels of BCAR3 expression (0 for no staining, 1+ for low staining, and 2+ for high staining). BCAR3 expression was significantly greater in mammary glands of mice during puberty compared to the older mice (**Figure 4.2A and B**). Surprisingly, this difference in BCAR3 expression between pubertal and mature mammary glands was not recapitulated by western blot analysis of mammary epithelial cell lysates; in this case, BCAR3 expression levels were similar between 5- and 12- week old mice (**Figure 4.2C**). This discrepancy could be due to the fact that BCAR3 expression was extremely

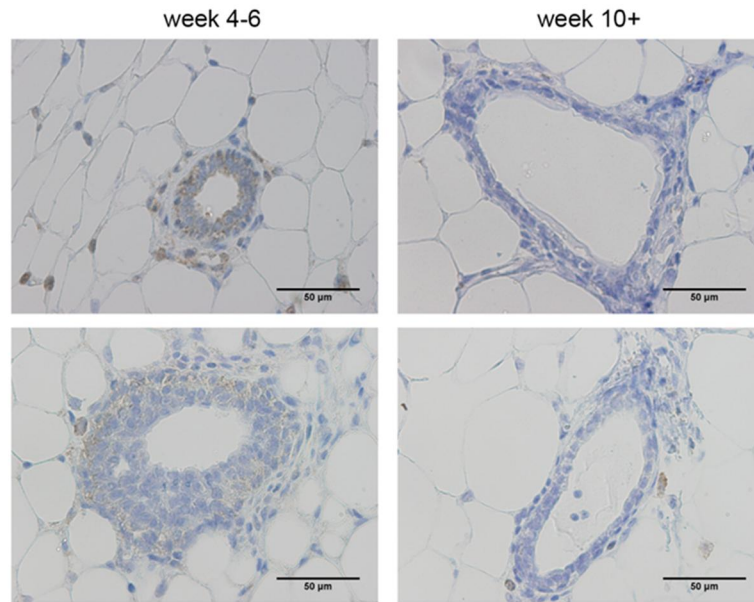
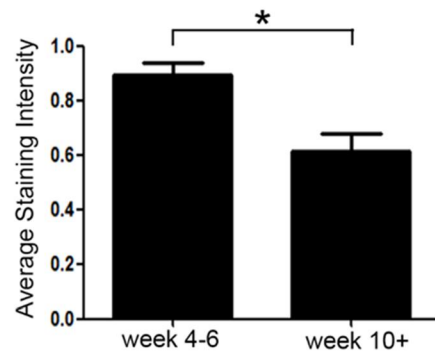
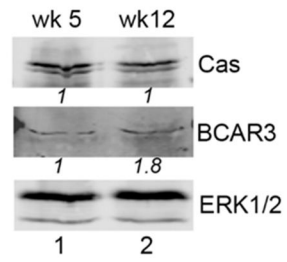
A**B****C**

Figure 4.2. BCAR3 expression is upregulated in mammary glands of mice during puberty

(A) Mammary gland 4 was isolated from C57BL/6 mice during early puberty (4-6 weeks of age) and post-puberty (10+ weeks of age) and BCAR3 expression was analyzed by IHC. (B) Levels of BCAR3 expression were scored on a 0-2+ scale (0 for no staining, 1+ for light staining, and 2+ for heavy staining). The average staining intensity was determined for 5-10 ducts per mouse. Data presented are the mean \pm SEM of 10 mice per age group. *, $p < 0.05$ by unpaired t-test. (C) Mammary epithelial cells were isolated from mammary glands 3, 4 and 5 of 4-7 mice at 5 and 12 weeks of age. Cells were lysed and proteins were immunoblotted with antibodies recognizing the designated proteins. Scale bars=50 μ M.

heterogeneous in the immature ducts (see left panels, **Figure 4.2A**); thus, although BCAR3 expression was clearly elevated in a subset of cells in the immature glands, the overall difference in BCAR3 expression between developing and fully formed glands may not be sufficient to detect by western blot analysis.

Following development of the mature mammary gland at the end of puberty, the next significant tissue remodeling that is seen occurs during pregnancy. The branching morphogenesis that occurs during this stage requires high levels of proliferation of ductal epithelial cells and invasion of newly formed branches into the surrounding fat pad (Lanigan *et al.*, 2007). As BCAR3 promotes cell migration, invasion, and proliferation (Near *et al.*, 2007; Schrecengost *et al.*, 2007; Wilson *et al.*, 2013), we hypothesized that BCAR3 would be upregulated again during pregnancy. Conversely, mammary gland involution involves massive amounts of cell death in the absence of proliferation and invasion; thus, we hypothesized that BCAR3 would be downregulated at this time. Mammary glands were isolated from WT C57Bl/6 mice during pregnancy, lactation, and involution and analyzed for BCAR3 expression by IHC. BCAR3 was expressed during pregnancy, predominantly in epithelial cells located at the outer edge of the ducts (**Figure 4.3A left panel**). In contrast, BCAR3 expression was low to non-existent during lactation and involution (**Figure 4.3A middle and right panels**). Since BCAR3 expression was not easily quantifiable in the glands of pregnant mice by IHC, western blot analysis was performed. However, as was the case during mammary gland development, total BCAR3 expression levels were similar in mammary epithelial cells isolated from mice during pregnancy compared to those of virgin mice (**Figure 4.3B**). This again may be due to the fact that BCAR3 appears to be upregulated in only a small fraction of mammary epithelial cells during pregnancy. Together, these data indicate that BCAR3 expression becomes elevated in a subset of ductal epithelial cells during both puberty and pregnancy,

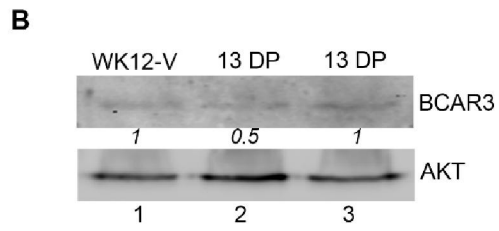
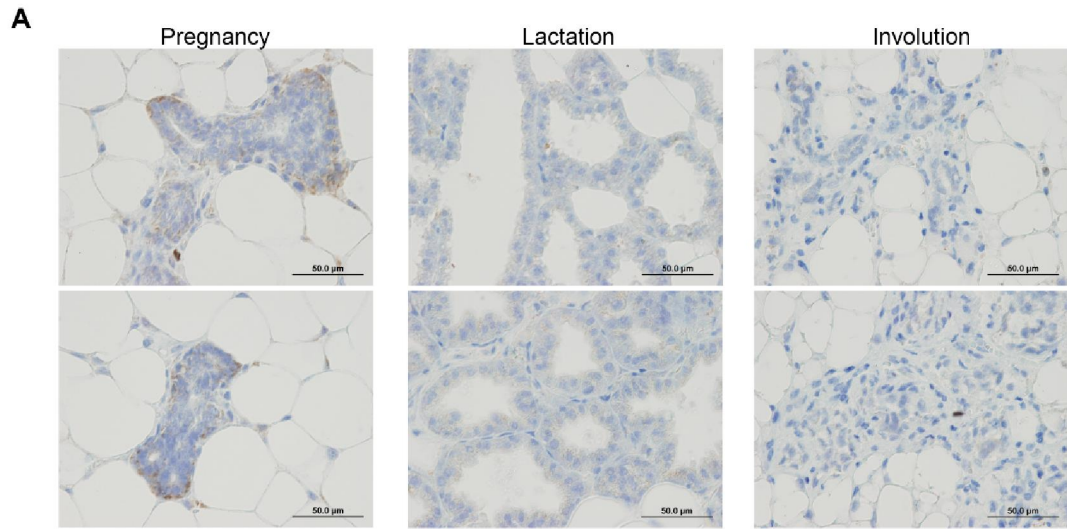


Figure 4.3. BCAR3 expression is upregulated in mammary glands of pregnant mice

(A) Mammary gland 4 was isolated from C57BL/6 mice during pregnancy, lactation, and involution, and BCAR3 expression was analyzed by IHC. (B) Mammary epithelial cells were isolated from mammary glands 3, 4, and 5 of 4 mice at 12 weeks of age and 2 mice at day 13 of pregnancy. Cells were lysed and proteins were immunoblotted with antibodies recognizing the designated proteins. DP=days pregnant. Scale bars=50 μ M.

suggesting that it may play a role in the proliferation and/or invasion of these cells during these stages of development.

4.2.2 BCAR3 is expressed but not upregulated during branching morphogenesis in mammary epithelial organoid cultures

In vitro systems can be used to model some of the processes of mammary development, including branching morphogenesis during pregnancy. To analyze BCAR3 expression during branching morphogenesis *in vitro*, mammary epithelial cells were isolated from 8 to 12 week old mice and embedded in Matrigel. Under these conditions, the cells form organoids which, when stimulated with growth factors such as fibroblast growth factor (FGF), undergo a growth and remodeling process to form branched structures similar to what is observed *in vivo* during alveologenesis (Mroue and Bissell, 2013) (**Figure 4.4A**). BCAR3 expression was measured in branching (+FGF) and non-branching (-FGF) mammary epithelial organoids by western blot analysis. BCAR3 was expressed at similar levels in branching and non-branching organoids (**Figure 4.4B**). To better determine if BCAR3 function is required for the branching observed upon FGF stimulation of mammary organoid cultures, it will be necessary to perform loss-of-function studies with cells isolated from BCAR3 KO mice.

4.2.3 BCAR3 knockout mice exhibit altered mammary gland development

The expression of BCAR3 in mammary epithelial cells during puberty and pregnancy suggests that BCAR3 may play a role in mammary gland development. To test this, mammary gland whole mounts were prepared from WT and BCAR3 KO mice. The glands were assessed for TEB numbers, extent of ductal outgrowth, and density of branching during puberty. Preliminary analysis was performed on mammary gland 4 from two WT and two BCAR3 KO mice at 6, 8, and 12 weeks of age (**Figure 4.5A**). The BCAR3

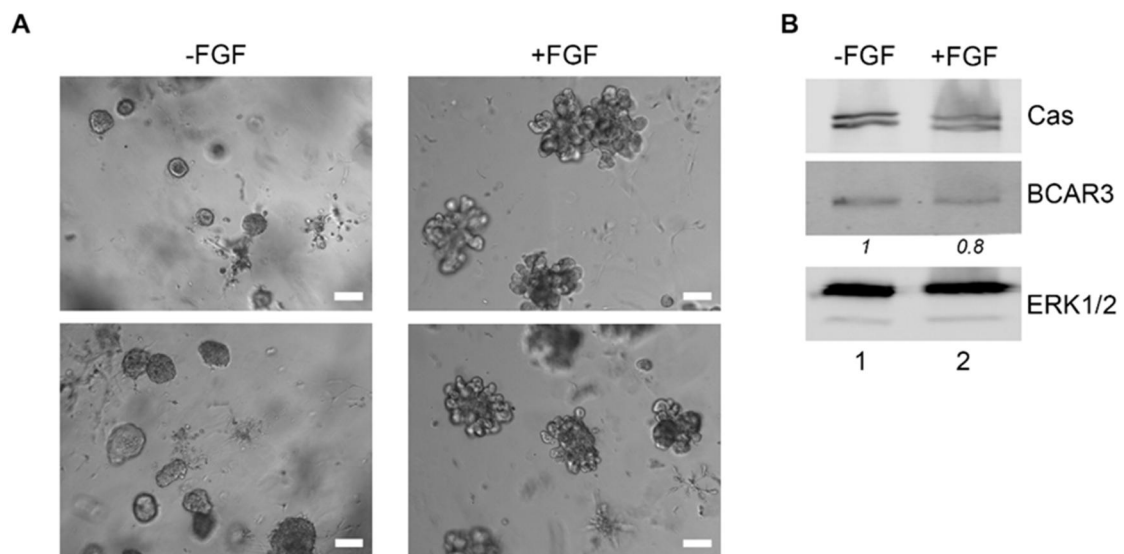


Figure 4.4. BCAR3 is expressed in mammary organoids but expression is not upregulated upon FGF-stimulated branching

(A) Mammary epithelial cells were isolated from 8- to 12-week old mice and embedded in Matrigel for 7 days in the absence (left panel) or presence (right panel) of 2.5nm FGF. (B) Mammary epithelial organoids were extracted from Matrigel and lysed. Proteins were immunoblotted with antibodies recognizing the designated proteins. Scare bars=100μM.

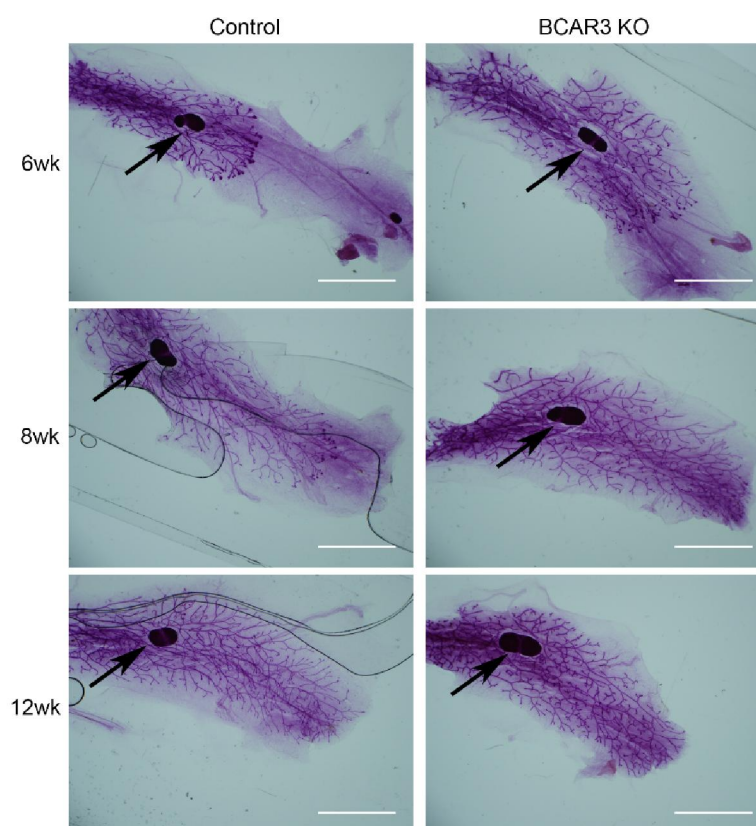
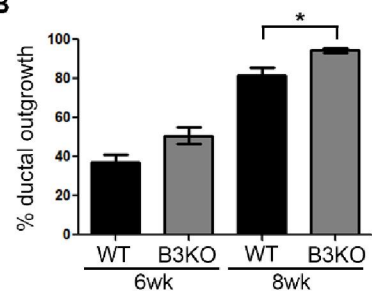
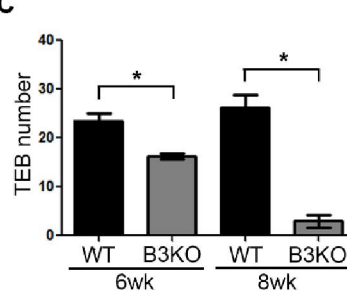
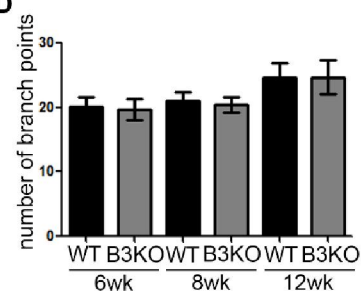
A**B****C****D**

Figure 4.5. BCAR3 knockout mice show altered mammary gland development during puberty

(A) Representative images of whole mounts of mammary gland 4 from wildtype and BCAR3 knockout mice. (B) Quantification of the percent of ductal outgrowth in mammary glands from 6 and 8 week old mice. Ductal outgrowth was measured as the distance from the lymph node (arrow) to the end of the longest branch divided by the distance from the lymph node to the end of the gland. (C) The number of TEBs present in glands of mice at 6 and 8 weeks of age was plotted. (D) The branching density of glands of 6, 8, and 12 week old mice was calculated by taking the average of the number of branch points present in two (6 week) or three (8 and 12 week) regions of interest per gland. Data presented are the mean \pm SEM of 4 glands per genotype. *, $p < 0.05$ by unpaired t-test. Scale bars= 0.5cm.

KO glands exhibited a trend toward greater ductal outgrowth at 6 weeks of age and a significant difference in ductal outgrowth at 8 weeks of age compared to glands from WT mice (**Figure 4.5B**). While the difference at week 6 was not statistically significant, it is likely that it will become significant with an increased sample size. This difference in ductal outgrowth was accompanied by a significant decrease in the number of TEBs present in glands of BCAR3 KO mice at 6 and 8 weeks of age (**Figure 4.5C**). No differences were observed in the density of branching in mammary glands at 6, 8, or 12 weeks of age between WT and BCAR3 KO mice (**Figure 4.5D**). These preliminary data suggest that BCAR3 may contribute to mammary gland morphogenesis. Whole mount analyses of additional glands during puberty as well as during pregnancy, lactation, and involution need to be performed to provide a more complete understanding of the role of BCAR3 in these processes.

4.2.4 BCAR3 is not required for MCF10A acini formation

To elucidate the mechanism behind BCAR3 regulation of mammary gland morphogenesis, an *in vitro* model of mammary gland development was used. When cultured on Matrigel, MCF10A mammary epithelial cells form growth-arrested acinar-like spheroids that closely resemble mammary gland alveoli *in vivo*. MCF10A acinar structures are characterized by the presence of a hollow lumen, apico-basal polarization of the cells making up the acini, and the basal deposition of basement membrane components (Debnath *et al.*, 2003) (**Figure 4.6**). The ability of MCF10A cells grown in 3D Matrigel culture to recapitulate many of features of breast epithelium *in vivo* makes this system ideal for examining a potential a role for BCAR3 in normal mammary development.

To investigate whether BCAR3 expression was differentially regulated during the formation of MCF10A acini, cells cultured under these conditions were isolated and lysed over a time course ranging from 4-12 days. Expression of both BCAR3 and its binding

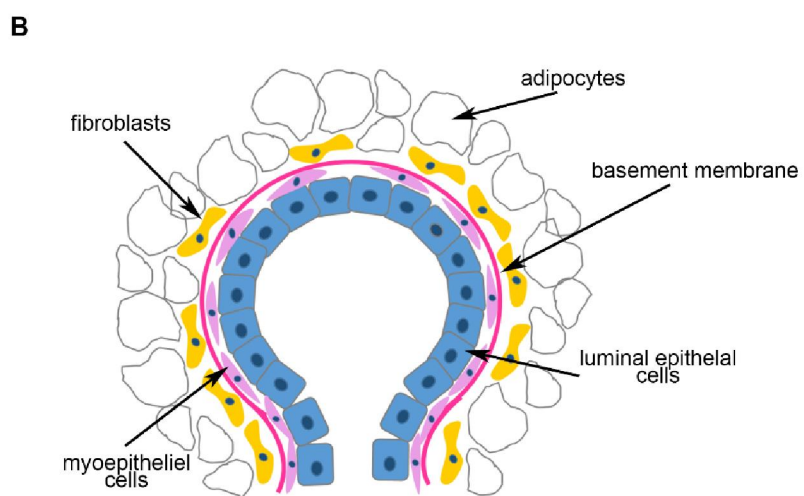
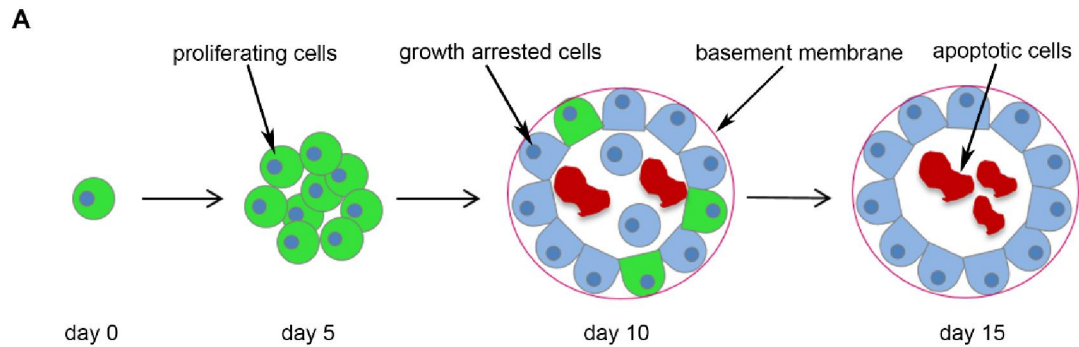


Figure 4.6. MCF10A acinar morphogenesis results in formation of structures *in vitro* that closely resemble mammary alveoli *in vivo*

(A) Schematic of MCF10A acinar morphogenesis. When seeded on Matrigel, MCF10A cells proliferate to form acini. The outer cells are in contact with basement membrane and become polarized and growth arrest. The inner cells, lacking contact with the basement membrane, die by apoptosis. The death of the inner cells results in the formation of a hollow lumen. (B) Schematic of alveoli *in vivo*. The mammary epithelia form polarized structures with hollow lumens. The lumen is surrounded by an inner layer of luminal epithelial cells. These luminal epithelial cells are bordered by a layer of myoepithelial cells that make contact with the surrounding basement membrane. The alveoli are embedded in the mammary stroma, which is made up of multiple cell types including fibroblast and adipocytes.

partner Cas was downregulated as the acini matured (**Figure 4.7A**). To determine if BCAR3 expression was required for the formation/maturation of MCF10A acini, MCF10A cells that were stably infected with an empty vector (pLKO) or a BCAR3-targeted shRNA (shBCAR3) were plated in 3D Matrigel culture. As before, BCAR3 and Cas expression was downregulated during the maturation process (**Figure 4.7B**). This was reminiscent of the downregulation of BCAR3 seen during mammary gland development in the mouse (**Figures 4.2A, B**).

To establish whether BCAR3 was required for acinar development or architecture, the size, extent of cell proliferation and cell death, and amount of luminal clearing were analyzed over time. Constitutive depletion of BCAR3 by shRNA resulted in a decrease in acinar size at day 5 that was overcome by day 10 (**Figure 4.7C, D**). MCF10A acini form from a single cell that proliferates to form a spheroid before undergoing polarization and growth arrest. Thus, we next asked whether the difference in acinar size observed at day 5 was a result of decreased proliferation in the BCAR3-depleted cells. However, the percentage of proliferating cells per acinus, as measured by enumerating Ki67-positive cells, was similar in acini formed from control and BCAR3 depleted cells at day 5 (**Figure 4.8A, B**). This suggests that the smaller acinar size observed in BCAR3-deleted acini was not due to a defect in proliferation in these cells at day 5. However, acini formed from BCAR3-depleted cells at day 10 contained significantly more Ki67-positive cells than did control acini (**Figure 4.8A, B**). This difference was also evident at day 15, when 80% of control acini but only 50% of BCAR3-depleted acini were considered to be growth-arrested, as defined by acini containing less than 2 Ki67-positive cells (**Figure 4.8C, D**). This was coincident with a trend towards a decrease in the percentage of BCAR3-depleted acini containing fully hollow lumens at day 15 in culture (**Figure 4.8E**). This failure to produce fully cleared acini at day 15 under conditions of BCAR3 depletion could be the result of increased proliferation, decreased luminal cell death, or both. However, analysis

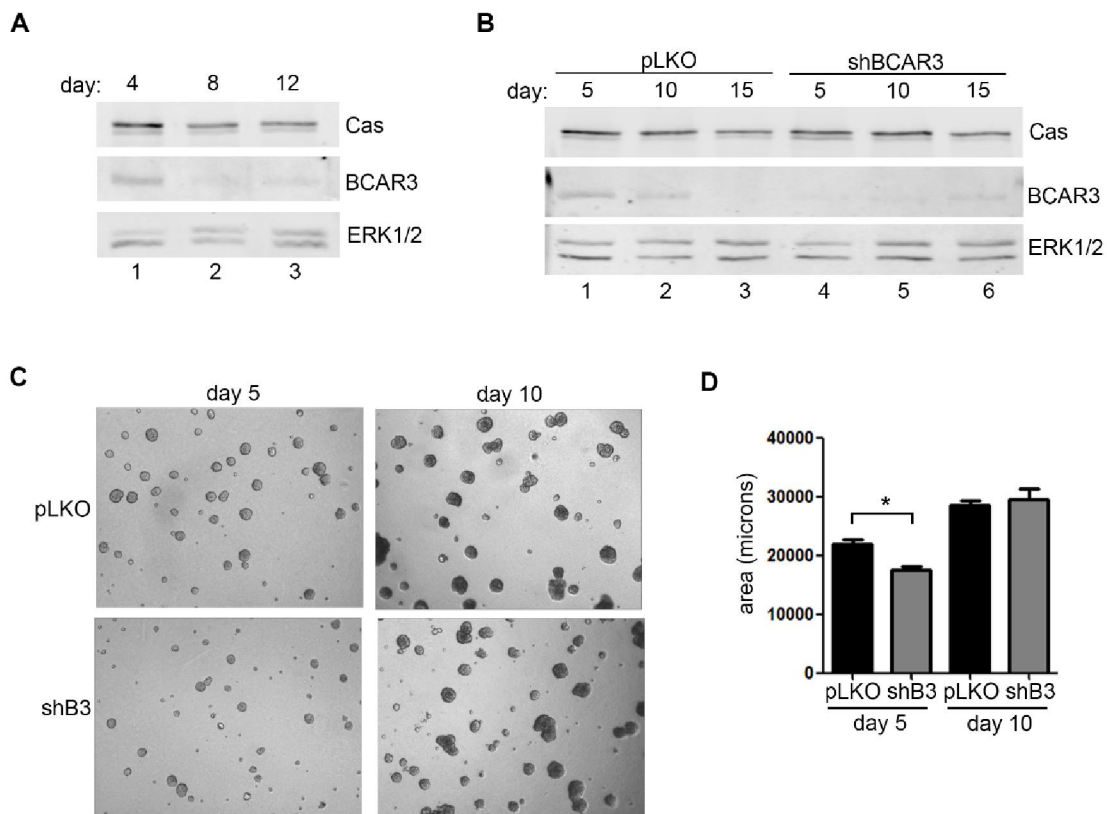


Figure 4.7. BCAR3 expression is highest during early acinar morphogenesis and regulates acinar size

(A) MCF10A epithelial cells were cultured on top of Matrigel, collected, and lysed at days 4, 8, and 12. Proteins were immunoblotted with antibodies recognizing the designated proteins. (B-D) MCF10A cells were stably infected with an empty vector (pLKO) or a virus encoding a BCAR3-targeted shRNA (shBCAR3) and plated in 3D Matrigel culture for up to 15 days. (B) Cells were collected and lysed at days 5, 10 and 15 to verify BCAR3 knockdown. Proteins were immunoblotted with antibodies recognizing the designated proteins. (C) Representative phase-contrast images are shown of acini formed from pLKO and shBCAR3 cells at day 5 and 10 in culture. (D) Acinar size was quantified from phase-contrast images. Data presented are the mean \pm SEM of 3 independent experiments. *, $p < 0.05$ by unpaired t-test.

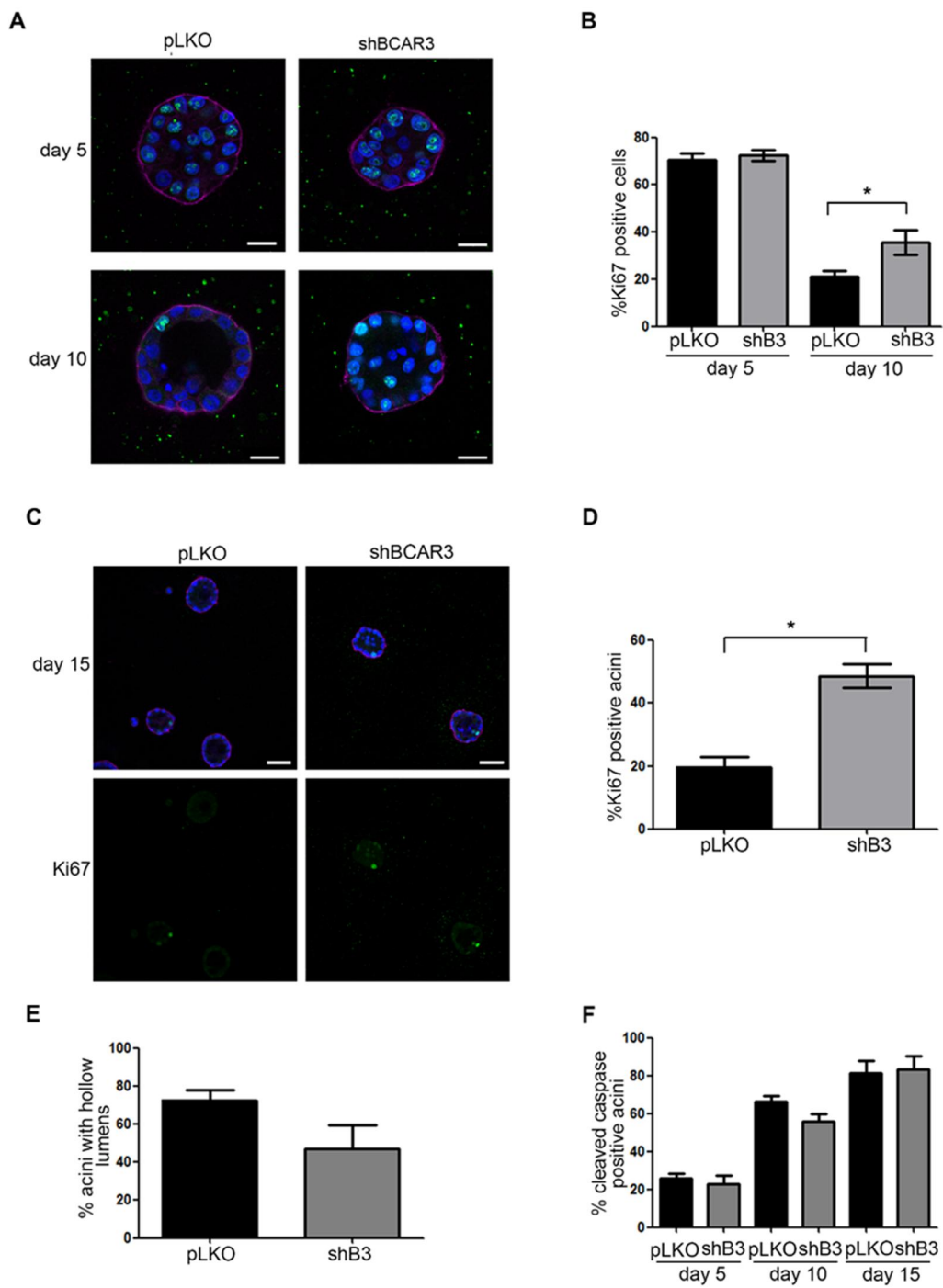


Figure 4.8. BCAR3 controls proliferation and luminal clearing, but not apoptosis, in MCF10A acini

MCF10A cells stably expressing an empty vector (pLKO) or BCAR3-targeted shRNA (shBCAR3) were plated on 3D Matrigel culture for up to 15 days. (A, C) Representative confocal images are shown of acini formed from pLKO and shBCAR3 cells at day 5 and 10 (A) and at day 15 (C) in culture. Blue=dapi, green=ki67, magenta= α 6 integrin. (A) Scale bars=20 μ M, (C) Scale bars=50 μ M. (B, D) Quantification of the percentage of Ki67-positive cells per acinus at day 5 and 10 in culture (B) and the percentage of Ki67-positive acini at day 15 (D). Acini were considered “Ki67-positive” if they contained more than 1 Ki67-positive cell. Data presented are the mean \pm SEM of 3-4 independent experiments. *, $p < 0.05$ by unpaired t-test. (E) Quantification of the percentage of acini from pLKO and shBCAR3 cells that contained cleared lumens at day 15. Acini were considered to have cleared lumens if less than 2 cells were present in the lumen. Data are representative of 2 independent experiments. (F) Quantification of the percentage of acini formed from pLKO and shBCAR3 cells containing cleaved caspase-positive cells at day 5, 10, and 15 in culture. Data presented are the mean \pm SEM of 2 (day 15) or 3 (day 5 and 10) independent experiments.

of cleaved caspase as a measure of apoptosis showed that the percentage of acini containing cleaved caspase-positive cells was similar between control and BCAR3-deleted conditions (**Figure 4.8F**).

Together, these data show that constitutive depletion of BCAR3 in MCF10A cells results in a decrease in acinar size at day 5 and an increase in proliferating cells at day 10 and 15 in culture. This suggests that BCAR3 may control the kinetics of MCF10A acini maturation such that, in the absence of BCAR3, acini maturation/growth arrest is slowed. Another possibility is that the increase in proliferating cells in BCAR3-depleted acini is specifically due to a requirement for BCAR3 in polarization-induced growth arrest. To distinguish between these possibilities, conditional knockout experiments were performed using MCF10A cells that were stably infected with empty vector (pLKO) or a tetracycline-inducible BCAR3-specific shRNA construct (shBCAR3) (**Figure 4.9A**). Cells were cultured for 4 days in Matrigel to allow acini to begin to form, after which BCAR3 expression was depleted by treatment with doxycycline. Under these conditions, there was no effect of BCAR3 depletion on the growth arrest of acini, as measured by Ki67 at days 10 and 15 (**Figure 4.9B, C**). This was in contrast to the increase in proliferating cells seen at these times when BCAR3 was depleted throughout the entire course of acini development and maturation (**Figure 4.8A-D**). These data show that BCAR3 is not required for polarization-induced growth arrest in MCF10A acini.

We next investigated whether acinar maturation was delayed under conditions of BCAR3 depletion due to changes in the expression of proteins that regulate cell cycle progression, proliferation, survival, and/or polarity. Expression of cyclin D1, cyclin A, p21CIP, phospho-AKT, phospho-ERK1/2, phospho-paxillin, and phospho-FAK was similar in day 3 acini formed from control and constitutive BCAR3-depleted cells (**Figure 4.10**). This prompted us to determine whether the effects initially observed in acini formed from constitutive BCAR3-depleted cells were recapitulated in the conditional knockdown

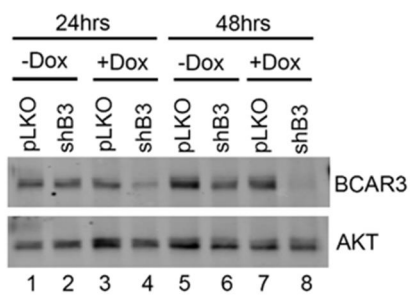
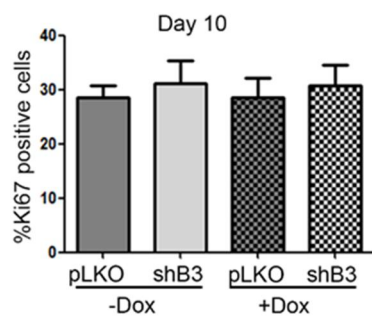
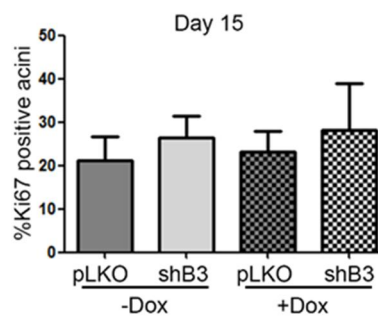
A**B****C**

Figure 4.9. Conditional knockdown of BCAR3 at day 4 in culture does not alter MCF10A cell proliferation in acinar structures

MCF10A cells were stably infected with tetracycline-inducible plasmids expressing empty vector (pLKO) or BCAR3-specific shRNA (shBCAR3). (A) Cells were cultured in the presence or absence of doxycycline (Dox) for 24 to 48 hours prior to lysing to confirm doxycycline-induced BCAR3 depletion. Proteins were immunoblotted with antibodies recognizing the designated proteins. (B, C) Cells were plated on top of Matrigel for up to 15 days. The percentage of Ki67-positive cells per acinus at day 10 (B) and the percentage of Ki67-positive acini at day 15 (C) are shown upon doxycycline addition at day 4 in culture. Data presented are the mean \pm SEM of 3 independent experiments.

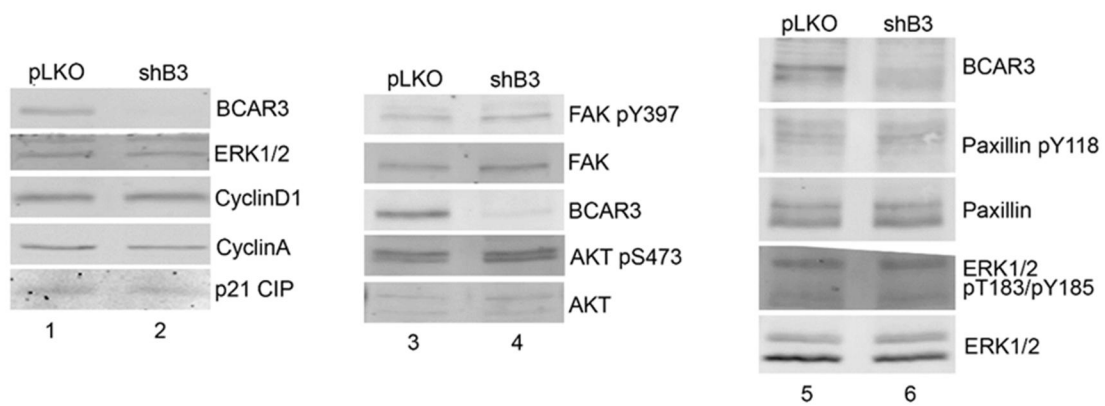


Figure 4.10. Constitutive depletion of BCAR3 in MCF10A acini does not affect expression of proteins that regulate cell cycle progression, proliferation, survival, and polarity

MCF10A cells stably expressing an empty vector (pLKO) or BCAR3-targeted shRNA (shBCAR3) were plated on 3D Matrigel culture. Following 3 days in culture, cells were collected and lysed. Proteins were immunoblotted with antibodies recognizing the designated proteins.

cells by depleting BCAR3 one day prior to plating them on Matrigel (day -1). In contrast to the constitutive knockdown cells, there were no differences in KI67 staining between acini formed from control or conditional BCAR3 knockdown cells at day 10 or 15 (**Figure 4.11**). These data suggest that the effects of constitutive BCAR3 knockdown on MCF10A acini were specific to that cell line and most likely do not reflect an inherent role for BCAR3 in controlling MCF10A acini morphogenesis.

4.3 Discussion

While a role for BCAR3 in mammary development remains unclear, data presented in this chapter suggest that BCAR3 may play a role in this process. BCAR3 expression was modestly elevated in mammary glands of pubertal mice compared to glands of mature virgin mice. During and following pregnancy, BCAR3 was most highly expressed at mid-pregnancy and subsequently downregulated during lactation and involution. These differences in BCAR3 expression were observed by IHC but were not recapitulated by western blot analysis; this disparity may be explained by the localized nature of BCAR3 upregulation. Analysis of BCAR3 KO mice revealed altered mammary gland development during puberty, characterized by an increase in the extent of ductal outgrowth coincident with a decrease in TEB numbers. Despite these data suggesting that BCAR3 may regulate mammary gland morphogenesis, however, the use of MCF10A acini cultures to mimic mammary gland development *in vitro* failed to elucidate a role for BCAR3 in acini development.

In breast cancer cell lines, BCAR3 has been shown to promote proliferation, cell motility, and invasion (Near *et al.*, 2007; Schrecengost *et al.*, 2007; Wilson *et al.*, 2013). Proliferation and invasion are important not only for driving cancer progression but also for promoting normal mammary gland development. Furthermore, the signaling pathways that control these processes are believed to be similar in normal and cancer development

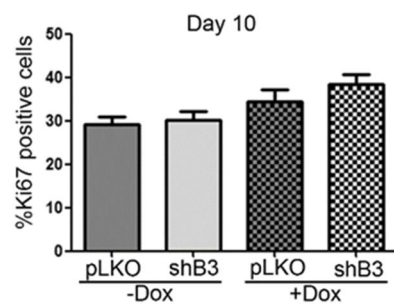
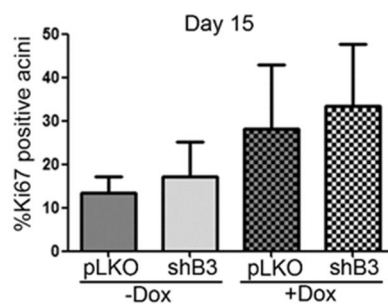
A**B**

Figure 4.11. Conditional knockdown of BCAR3 in MCF10A cells prior to plating on Matrigel does not replicate effects observed upon constitutive depletion of BCAR3 in MCF10A

Tetracycline-inducible pLKO and shBCAR3-expressing MCF10A cells were treated with doxycycline one day prior to plating on Matrigel culture. Cells were cultured on Matrigel for up to 15 days. The percentage of Ki67-positive cells per acinus at day 10 (A) and the percentage of Ki67-positive acini at day 15 (B) are shown. Data presented are the mean \pm SEM of 3 independent experiments.

(Lanigan *et al.*, 2007). Thus, we hypothesized that BCAR3 would promote normal mammary gland development by driving proliferation and invasion of epithelial cells. However, the data presented in this chapter failed to support this hypothesis and in fact, suggested instead that BCAR3 may serve as a negative regulator of mammary gland development. In particular, the increased ductal outgrowth and decreased number of TEBs observed in BCAR3 KO mice during puberty could be explained by accelerated mammary gland development in the absence of BCAR3. A more complete analysis using additional mice of different ages is needed to determine if BCAR3 KO mice do in fact undergo accelerated mammary gland development. It will be important to compare mammary glands of WT and BCAR3 KO mice at a time when the extent of ductal outgrowth into the fat pad is similar between the two genotypes. We would hypothesize that, if the difference in the number of TEBs observed between WT and BCAR3 KO mice is related to accelerated rates of ductal outgrowth, then WT and BCAR3 KO mice should have similar numbers of TEBs at times when the extent of ductal outgrowth is the same. In addition, the number of TEBs in mammary glands from BCAR3 KO mice isolated earlier during development (e.g. at weaning - 3 weeks) should be significantly elevated compared to WT mice due to increased proliferation at that time (Rudel *et al.*, 2011).

At first glance, the ability of BCAR3 to act as a negative regulatory of mammary gland development seems contradictory to the proliferation, migration, and invasion functions of BCAR3 in tumor cells *in vitro* (Near *et al.*, 2007; Schrecengost *et al.*, 2007; Wilson *et al.*, 2013). One possibility is that BCAR3 has different functions in normal mammary epithelial cells and breast cancer cells such that BCAR3 may slow/inhibit proliferation and invasion in normal cells while promoting these activities in tumor cells. Another possibility is that the accelerated rate of mammary gland development observed in BCAR3 KO mice is the result of loss of BCAR3 in stromal cells present in the fat pad since these mice contain a global genetic knockout of the gene encoding BCAR3. The

mammary epithelium is surrounded by fibroblasts, adipocytes, and immune cells that contribute to normal mammary gland development (Crowley, Bowtell, & Serra, 2005). The fibroblasts in the mammary gland secrete a variety of growth factors and express multiple growth factor receptors; signaling through these factors and receptors is important for mammary gland development (Crowley *et al.*, 2005). It is interesting to speculate that BCAR3 may function in these pathways if it is expressed in these cells. Macrophages, eosinophils, and mast cells have also been shown to be important for mammary gland morphogenesis (Reed and Schwertfeger, 2010). While a role for BCAR3 in immune cell function during mammary gland development has not been established, BCAR3 is expressed in macrophages in the lung (Human Protein Atlas) and has been reported to control macrophage functions, as depletion of BCAR3 in a mouse macrophage cell line was shown to impair IL6 production following treatment with LPS (Yang *et al.*, 2011). Taken together, it is formally possible that the suppressive function of BCAR3 revealed by our studies with BCAR3 KO mice could potentially stem from its function in the mammary stroma. This could also explain why BCAR3 depletion had no clear effect on the ability of MCF10A cells to form mature acini in 3D culture. Future studies with conditional knockout mice need to be performed to tease apart the potentially distinct functions of BCAR3 in different cells within the mammary gland stroma (see chapter 5).

Chapter 5: Perspectives

Breast cancer remains the second leading cause of cancer deaths among women despite advances in early detection and treatment options (American Cancer Society, 2016). To improve patient survival, a better understanding of the signaling pathways that promote tumor growth, progression, metastasis and therapeutic resistance is required. The work presented in this thesis focuses on understanding BCAR3 signaling in breast cancer progression and mammary gland morphogenesis. Previous work in the field has focused on understanding BCAR3 functions and determining whether interaction with its binding partner, Cas, is required for these functions (Vanden Borre *et al.*, 2011; Wallez *et al.*, 2014). The data presented in this thesis expands our knowledge of the importance of the BCAR3/Cas complex in BCAR3-mediated functions *in vitro* and provides the first *in vivo* study of BCAR3 in breast cancer. *In vitro*, we demonstrate that the ability of BCAR3 to promote adhesion turnover, migration, and invasion requires direct interaction with Cas. In the MMTV-PyMT mouse model of breast cancer, we show that BCAR3 expression is upregulated and differentially expressed during tumor progression. Finally, in an MDA-MB-231 xenograft tumor model, BCAR3 expression is found to promote tumor formation and control total tumor burden.

While this thesis contributes new insights into BCAR3 function, many questions remain to be answered. For example, the mechanisms and signaling pathways through which BCAR3 regulates breast tumor progression are still not well defined. Additionally, it remains unknown whether BCAR3 is capable of promoting metastasis. Moreover, despite the established functions of BCAR3 as a regulator of proliferation, migration, and invasion in breast cancer cells, preliminary studies in BCAR3 KO mice suggest that loss of BCAR3 accelerates ductal outgrowth during puberty. How BCAR3 functions to regulate mammary gland development is not yet understood. This chapter begins to address the next steps

that should be taken to tackle these key questions and explores the possibility that BCAR3 may serve as a biomarker and/or therapeutic target in breast cancer.

5.1 How does BCAR3 function as a negative regulator of mammary gland development?

Data presented in chapter 4 suggest that BCAR3 may act as a negative regulator of normal mammary gland development. Analysis of mammary glands of BCAR3 KO mice showed that, in the absence of BCAR3, mammary glands displayed increased ductal outgrowth and a reduction in the number of TEBs throughout puberty (**Figure 4.5**). Since TEBs regress once they reach the end of the fat pad (Rudel *et al.*, 2011), these observations suggest that loss of BCAR3 may accelerate mammary gland development during puberty. Further studies are needed to determine if this is the case. As discussed in chapter 4, mammary glands of WT and BCAR3 KO mice need to be compared when the extent of ductal outgrowth into the fat pad is similar between the two genotypes to determine if there is a difference in the number of TEBs at this time. If there is no difference, this would suggest that the process of ductal outgrowth is regulated by BCAR3 and the decrease in the number of TEBs observed in BCAR3 KO mice during puberty is the result of accelerated ductal outgrowth. Alternatively, a difference in the number of TEBs when ductal outgrowth is consistent between WT and BCAR3 KO mammary gland would suggest that BCAR3 plays some role in TEB formation and/or maintenance. However, this seems unlikely, as all published studies that report reduced TEB formation also show impaired ductal outgrowth (Lanigan *et al.*, 2007; Hynes and Watson, 2010; Macias and Hinck, 2012). In addition to measuring ductal outgrowth, it will be important to analyze epithelial cell proliferation in TEBs formed in BCAR3 KO mice compared to those formed in WT mice. As ductal outgrowth is believed to be regulated by massive proliferation of the epithelial cells in the TEBs that effectively pushes the TEBs into the fat

pad (Wiseman, 2002; Hinck and Silberstein, 2005), and BCAR3 loss augments ductal outgrowth, we would hypothesize that there may be greater proliferation within the TEBs of BCAR3 KO mice.

5.1.1 Is BCAR3 loss in epithelial or stromal cells responsible for the control of ductal outgrowth during mammary gland development?

The observation that BCAR3 may negatively regulate mammary gland development is contradictory to what we expected based upon the established proliferative, migratory, and invasive functions of BCAR3 *in vitro*. Because the mice used in these studies contain a global genetic knockout of the gene encoding BCAR3, the putative suppressive role of BCAR3 in mammary gland development could stem from its function in any of the cell types present in the mammary gland. Mammary organoid cultures and reciprocal transplantation techniques could be used to help determine which cell type is responsible for the suppressive function of BCAR3 in the developing mammary gland.

Branching morphogenesis can be modeled by culturing mammary epithelial cells (MECs) in different types of basement membrane and stimulating them with various growth factors (Mroue and Bissell, 2013). To model branching morphogenesis during puberty, MECs are embedded in collagen-I gels and stimulated with growth factors such as FGF (Mroue and Bissell, 2013). If the suppressive function of BCAR3 in mammary gland development is due to a function of BCAR3 in the epithelial cells, comparison of organoids formed from MECs isolated from WT and BCAR3 KO mice should show differences in branching. If the organoids formed from MECs isolated from WT and BCAR3 KO mice are similar under these conditions, this would suggest that the suppressive function of BCAR3 may be mediated by a stromal cell type present in the mammary gland rather than the epithelial cell.

A more complete analysis of the epithelial vs. stromal functions of BCAR3 could be performed using reciprocal transplantation techniques. For these studies, donor tissue from BCAR3 KO mice could be transplanted into WT hosts and donor tissue from WT mice could be transplanted into BCAR3 KO mice. The donor tissue is typically obtained by surgical dissection of the region of mammary gland 4 between the nipple and the lymph node of 6-day-old mice, which contains the rudimentary ductal tree. Mammary gland 4 of the transplant recipient is cleared by surgical removal of the region between the nipple and the lymph node at 3 weeks of age. The donor tissue is then transplanted into the surgically cleared fat pad and the mammary gland is allowed to develop for the desired period of time before harvesting for whole mount analysis (Brantley *et al.*, 2001). If the normal suppressive role of BCAR3 stems from a function of BCAR3 in the epithelial cells, we would expect to see accelerated ductal outgrowth coincident with a reduction in TEBs in WT mice implanted with BCAR3-null epithelial cells. On the other hand, if the suppressive role of BCAR3 stems from non-epithelial cells in the tumor stroma, we would expect WT epithelial cells to exhibit accelerated ductal outgrowth and a reduction in TEBs when implanted into BCAR3 KO mice. Future experiments with conditional KO mice are needed to tease apart the potentially distinct functions of BCAR3 in different cells within the mammary gland stroma.

5.1.2 How might BCAR3 function in epithelial cells to slow mammary gland development?

In breast cancer cell lines, BCAR3 has been shown to promote proliferation, migration and invasion through Cas signaling (Wilson *et al.*, 2013; Wallez *et al.*, 2014) (Chapter 2). Based on these established functions of BCAR3 *in vitro*, it seems somewhat paradoxical that BCAR3 would negatively regulate these processes in epithelial cells of the developing mammary gland. This could be potentially reconciled by examining BCAR3 signaling downstream of the insulin-like growth factor 1 receptor (IGF1R) during normal

mammary gland development. Insulin-like growth factor 1 (IGF1) is produced by both stromal and epithelial cells and is required for cell proliferation in the TEB, proper TEB formation, and ductal outgrowth (Hynes and Watson, 2010). Interestingly, in ER-positive breast cancer cells, BCAR3 overexpression was shown to promote the degradation of insulin receptor substrate 1 (IRS-1) (Yu *et al.*, 2006). IRS-1 is a critical adaptor molecule that functions downstream of IGFR1 to promote signaling through the Ras/Raf/MEK/ERK and PI3K/AKT pathways (Farabaugh *et al.*, 2015). Degradation of IRS-1 by BCAR3 could thus diminish signaling through IGF1R. If this is the case, loss of BCAR3 would be expected to enhance signaling downstream of IGF1R, promote proliferation of MECs in the TEB, and accelerate normal mammary gland development. This could be tested by measuring IRS-1 levels and PI3K, AKT, and ERK activity in mammary epithelial cells isolated from WT and BCAR3 KO mice; each of these should be elevated in KO relative to WT cells.

The downregulation of IGF1 signaling by BCAR3 might appear to be contradictory to its ability to enhance breast cancer cell proliferation, particularly in the multiple examples of breast cancer cells that exhibit elevated IGF1R levels (Davison *et al.*, 2011). Regulation of proliferation by BCAR3 is mediated at least in part to its ability to augment Cas/Src complexes and signaling (Wallez *et al.*, 2014). Potent activation of Cas/Src signaling by BCAR3 may override the negative effects of BCAR3 expression on IGF1R-mediated proliferation in breast cancer cells. In addition, it is possible that BCAR3 expression may have differential effects on proliferation depending on whether its signaling is in response to integrin, growth factor, or hormone receptor activation. Notably, *in vitro* studies are performed in the presence of rich media comprised of high levels of growth factors, hormones etc., and this could result in other signaling pathways masking differences in responses to IGF1.

5.1.3 How might BCAR3 function in stromal cells to slow mammary gland development?

The epithelial cells of the mammary gland are surrounded by fibroblasts, adipocytes, and immune cells that make up the mammary stroma (Crowley, Bowtell, & Serra, 2005). The immune cells that have been shown to regulate mammary gland morphogenesis include macrophages, eosinophils, and mast cells (Reed and Schwertfeger, 2010). While a role for BCAR3 in immune cell function during mammary gland development has not been established, BCAR3 is expressed in macrophages in the lung (Human Protein Atlas). During puberty, macrophages are found to localize to the neck of the TEB where they contribute to TEB formation, ductal elongation and branching. IL4 and IL13, which can polarize macrophages toward an anti-inflammatory M2 state, are present in the developing mammary gland and may regulate macrophage function in the gland (Brady *et al.*, 2016).

Signaling through the TGF- β receptor II in macrophages promotes expression of genes characteristic of M2 polarization (Gong *et al.*, 2012). As BCAR3 expression has been shown to inhibit TGF- β /Smad signaling in breast cancer cell lines (Guo *et al.*, 2014), BCAR3 loss may augment TGF- β signaling in these cells and promote polarization of M2 macrophages. Future experiments could employ double-labeling immunohistochemistry to characterize the polarization state of macrophages in situ. Macrophages that are M1-polarized can be identified by staining for CD68 or CD163 in combination with phospho-STAT1 or “recombination signal binding protein for immunoglobulin kappa j region” (RBP-J), while M2 macrophages can be identified by staining for CD68 or CD163 in combination with “musculoaponeurotic fibrosarcoma oncogene homolog” (c-MAF) (Barros *et al.*, 2013).

In addition to immune cells, fibroblasts in the mammary stroma play a critical role in mammary morphogenesis. Mammary gland fibroblasts express multiple growth factor receptors, and signaling through these receptors is required for normal mammary gland

development (Crowley *et al.*, 2005). It is interesting to speculate that BCAR3, if expressed in these cells, may control expression or signaling downstream of these growth factor receptors. One of the growth factor receptors normally expressed on fibroblasts is the TGF- β type II receptor. Deletion of this TGF- β receptor in mammary fibroblasts has been reported to impair TEB formation and ductal morphogenesis (Cheng *et al.*, 2005). As mentioned above, BCAR3 expression has been reported to impair TGF- β /Smad signaling in breast cancer cell lines. If BCAR3 is normally expressed in these cells during mammary gland development, it may inhibit TGF- β /Smad signaling downstream of TGF- β type II receptor. As suggested above for macrophages, BCAR3 depletion could thus augment TGF- β signaling in fibroblasts and enhance TEB formation and ductal outgrowth.

Understanding if and how BCAR3 functions in mammary stromal cells during development may provide important insights into novel stromal functions of BCAR3 during cancer progression. Most of the work studying BCAR3 function in breast cancer has been performed in the epithelial-derived cancer cells. It is possible that BCAR3 expression in stromal cells contributes to breast cancer progression in ways that are distinct from its functions in the cancer cells. Understanding this signaling will be important if BCAR3 is to be considered in the future as a therapeutic target in breast cancer.

5.1.4 Does BCAR3 regulate the mammary gland during pregnancy, lactation, and involution?

We have yet to analyze mammary glands of BCAR3 KO mice during pregnancy, lactation and involution. During pregnancy, massive proliferation within the ductal tree results in the formation of tertiary branches and alveolar buds. In mid-pregnancy, the newly developed alveolar buds progressively cleave and differentiate into distinct alveoli (Lanigan *et al.*, 2007). As BCAR3 appears to suppress proliferation and branching during

puberty, it is possible that BCAR3 KO mice would exhibit increased branching and alveoli number during pregnancy in comparison to WT mice. However, the signaling pathways that control proliferation and branching during puberty and pregnancy do not always overlap, and it is formally possible that loss of BCAR3 may have no effect on mammary gland morphogenesis during pregnancy despite having a role during puberty. It will also be informative to analyze mammary glands of BCAR3 KO mice during lactation and involution. We would hypothesize that BCAR3 protein may have no role in mammary gland remodeling during these stages because these processes are not dependent on proliferation, migration, and invasion of the epithelial cells. However, as suggested by the analysis of mammary glands from BCAR3 KO mice during puberty, we do not currently have a full appreciation for BCAR3 functions in the epithelial or non-epithelial cells of the breast. Therefore, analysis of glands during lactation and involution may provide further insight into these functions.

5.2 How does BCAR3 regulate tumor progression?

Data presented in chapter 3 include the first *in vivo* studies of BCAR3 in breast cancer models and demonstrate that BCAR3 expression promotes tumor formation in a MDA-MB-231 xenograft mouse model. The data presented in chapter 2 highlight the importance of BCAR3/Cas binding in controlling BCAR3-mediated adhesion turnover, migration, and invasion. Based on these data, together with data from Wallez *et al.* showing that direct interaction between BCAR3 and Cas is required for BCAR3-mediated Cas phosphorylation and Src activity (Wallez *et al.*, 2014), we hypothesize that direct interaction between BCAR3 and Cas is necessary to promote MDA-MB-231 tumor formation. As explained in chapter 3, this could be tested by comparing tumorigenesis of the stable pLKO- and shBCAR3-expressing MDA-MB-231 cells to the tumorigenesis of

BCAR3-depleted cells re-expressing shRNA-resistant WT and Cas binding mutant BCAR3 proteins.

Because the outgrowth of tumors formed from BCAR3-depleted cells was significantly delayed and the tumors that ultimately grew out exhibited robust expression of BCAR3, it was not possible to determine whether BCAR3 might also have an effect on the growth of established tumors. Conditional knockdown approaches could be used to investigate tumor growth as a function of BCAR3 by depleting BCAR3 expression after the tumors become palpable, as discussed in chapter 3. If BCAR3 is found to play a role in this process, the requirement for BCAR3/Cas interactions could be determined by re-expression of the WT and Cas-binding mutant BCAR3 protein at the time of conditional BCAR3 knockdown.

5.2.1 Is BCAR3-mediated tumor progression dependent on Src?

If BCAR3 interactions with Cas are found to be required for its ability to control tumor formation, one possibility is that this activity is ultimately driven by Src activity. It is well established that BCAR3-Cas interactions result in increased Cas/Src complexes and Src kinase activity (Riggins *et al.*, 2003; Schrecengost *et al.*, 2007). Src activity, in turn, controls many cellular functions associated with tumor growth, including cell growth, motility, and survival (Irby and Yeatman, 2000; Finn, 2008). Ablation of Src activity in MMTV-PyMT tumors delays tumor initiation in this model (Marcotte *et al.*, 2011). To determine if BCAR3 controls tumor formation through Cas-mediated Src activity, stable shBCAR3 and shCas expressing MDA-MB-231 could be engineered to re-express shRNA-resistant WT Cas or a Src-binding mutant of Cas (CasP642A/Y668/670F) (Riggins *et al.*, 2006) with or without re-expressed WT BCAR3. If the ability of BCAR3 to promote tumor formation is dependent on Cas-mediated Src activity, mice injected with the cells re-expressing BCAR3 and the Src-binding mutant Cas will exhibit delayed tumor formation

compared to those injected with cells re-expressing BCAR3 and WT Cas proteins. Furthermore, because BCAR3 expression increases Cas/Src interactions and these complexes significantly enhance Src activity, we would expect the cells re-expressing WT Cas in the absence of BCAR3 to exhibit delayed tumor formation compared to cells re-expressing both WT Cas and BCAR3.

If BCAR3 is found to augment the growth of established tumors through direct interaction with Cas, the importance of Src activity in this function can be elucidated by performing inhibitory studies with dasatinib. Dasatinib inhibits Src family members, as well as c-kit, PDGFR, and Bcr-Abl (Montero *et al.*, 2011). For these experiments, we would begin dasatinib treatment in mice inoculated with the conditional knockdown/re-expression cells at the same time that BCAR3 knockdown and re-expression of WT and mutant BCAR3 proteins is initiated. If the ability of BCAR3 to regulate tumor growth is dependent on Cas-mediated Src activation, dasatinib treatment should slow the growth of tumors established from control and BCAR3-depleted cells that re-express WT protein so that they are similar to the reduced growth rates exhibited by tumors from BCAR3-depleted cells or BCAR3-depleted cells re-expressing the Cas-binding mutant of BCAR3. It is important to note, however, that dasatinib may affect tumor growth regardless of BCAR3 expression since Src kinase activity is regulated in multiple ways and dasatinib has specificity for other tyrosine kinases (Mayer and Krop, 2010) (Irby and Yeatman, 2000).

In MMTV-PyMT mice, Src activity is elevated in primary tumors as well as in metastases, and Src expression is required for tumor formation in this model (Irby and Yeatman, 2000)(Guy *et al.*, 1994). In chapter 3, we show that BCAR3 is upregulated and differentially expressed during PyMT tumor development. Based on these data, we hypothesize that BCAR3 depletion might impair tumor growth in MMTV-PyMT mice through a mechanism that involves a reduction in Src activity. This could be tested by

crossing MMTV-PyMT mice with BCAR3 KO mice. The major caveat to this approach is the global nature of the BCAR3 knockout, which was discussed in detail in chapter 4. Thus, it will be important to generate conditional BCAR3 knockouts in the genetic background of the MMTV-PyMT mice to distinguish between cancer and stromal cell effects of BCAR3 depletion on PyMT progression. A role for Src in this process could then be investigated using dasatinib, as described above.

5.2.2 Could BCAR3 be a regulator of TGF- β signaling?

It is well established that BCAR3 promotes Cas/Src interactions and subsequent Src-mediate tyrosine phosphorylation of Cas (Riggins *et al.*, 2006; Schuh *et al.*, 2010; Wallez *et al.*, 2014). This Src-mediated phosphorylation of the substrate domain of Cas promotes Crk/Dock180 binding and Rac1 activation (Defilippi *et al.*, 2006). Additionally, elevated expression and tyrosine phosphorylation of Cas has been reported to regulate TGF- β signaling (Kim *et al.*, 2008; Wendt *et al.*, 2009; Kang *et al.*, 2013). However, despite the ability of BCAR3 to promote tyrosine phosphorylation of Cas, there is little published data addressing the role of BCAR3 in TGF- β signaling. It is possible that the ability of BCAR3 to promote tumor growth and metastasis *in vivo* may be dependent at least in part, on its regulation of TGF- β signaling.

5.2.2.1 Cas as a regulator of canonical and non-canonical TGF- β signaling

TGF- β binding to its receptors activates their serine kinase activity, leading to phosphorylation and activation of Smad2 and Smad3. This promotes the interaction of Smad2/3 with Smad4 and translocation of the complex into the nucleus, where it regulates transcription of many genes and ultimately impacts numerous cellular activities. Additionally, TGF- β signals in a Smad-independent manner. In this non-canonical

pathway, TGF- β induces activation of ERK, JNK, p38 MAPK, RhoA, and AKT-(Kim *et al.*, 2008; Zhang, 2009; Moses and Barcellos-Hoff, 2011). There is some evidence to suggest that the balance between the activity of canonical and non-canonical pathways may control the function of TGF- β as a tumor suppressor or a tumor promoter (Wendt *et al.*, 2009; Parvani *et al.*, 2011).

Cas expression has been reported to enhance the ability of TGF- β to act as tumor promoter by inhibiting TGF- β /Smad signaling and augmenting non-canonical signaling through p38 MAPK. Depletion of Cas in 4T1 breast cancer cells decreases TGF- β -induced invasion *in vitro* and impairs primary tumor growth in an orthotopic mouse model. Furthermore, in 4T1 cells overexpressing the TGF- β type II receptor (T β R-II), Cas depletion impairs metastasis *in vivo* (Wendt *et al.*, 2009). As BCAR3 enhances Cas phosphorylation and stabilization (Wallez *et al.*, 2014) (Appendix 1), it is interesting to speculate that the ability of Cas to augment non-canonical and impair canonical signaling downstream of TGF- β may be regulated by BCAR3. This is supported by a study that shows that BCAR3 expression mediates TGF- β signaling by inhibiting Smad3 phosphorylation in breast cancer cell lines (Guo *et al.*, 2014).

5.2.2.2 Does BCAR3 regulate canonical and non-canonical signaling downstream of TGF- β in cancer cells?

As mentioned above, the link between Cas and TGF- β signaling prompts the question of whether BCAR3 may also contribute to this pathway. Both *in vitro* and *in vivo* studies could be performed to determine if BCAR3 also regulates tumor progression by controlling canonical and/or non-canonical TGF- β signaling. First, the extent of Smad2/3, ERK, JNK, p38 MAPK, and AKT phosphorylation could be analyzed in the MDA-MB-231 cell variants used and described throughout this thesis over a time course of TGF- β

stimulation in 2D culture. If BCAR3, like Cas, promotes non-canonical TGF- β signaling, BCAR3 depletion would be expected to result in increased Smad phosphorylation and impaired phosphorylation of one or more of the proteins that are activated by non-canonical signaling following TGF- β stimulation. Furthermore, cells re-expressing WT BCAR3 protein would be expected to exhibit impaired Smad phosphorylation and elevated phosphorylation of proteins activated through the non-canonical signaling pathway. If direct interaction between BCAR3 and Cas is required for this phenotype, cells re-expressing the Cas-binding mutant of BCAR3 would behave like BCAR3-depleted cells. Interestingly, if BCAR3 expression is found to impair Smad signaling and promote non-canonical signaling, it is possible that MDA-MB-231 cells would become susceptible to TGF- β growth inhibition under conditions of BCAR3 depletion or blockade of the BCAR3/Cas interaction. This has been reported to be the case in Cas-depleted cells (Kang *et al.*, 2013).

If BCAR3 is found to impact the balance between canonical and non-canonical TGF- β signaling in MDA-MB-231 cell variants, we would next investigate whether the ability of BCAR3 to control tumor growth and/or metastasis is related to this function. First, Smad2/3, ERK, JNK, p38 MAPK, and AKT phosphorylation levels would be examined in tumors following conditional knockdown of BCAR3 and re-expression of the WT and Cas-binding mutant of BCAR3. Second, mice could be treated with TGF- β inhibitors to determine if the ability of BCAR3 to promote tumor growth and/or metastasis is dependent on this signaling pathway. It should be noted, however, that the effects of TGF- β inhibitors are often pleiotropic due to the complex nature of TGF- β signaling and the numerous cell types potentially impacted by the inhibitors (Barcellos-Hoff and Akhurst, 2009). To more directly test if BCAR3 expression contributes to TGF- β -driven tumor growth and metastasis, mouse studies could be performed using 4T1 breast cancer cells engineered

to express T β R-II. These cells exhibit significantly increased tumor growth and metastasis as compared to control cells (Gallagher-Beckley and Schiemann, 2008; Wendt *et al.*, 2009). Using this model, it will be possible to determine whether BCAR3 collaborates with TGF- β by comparing tumor growth and metastasis between mice injected with 4T1 control cells, 4T1 cells over-expressing T β R-II, and 4T1 cells over-expressing T β R-II and expressing shRNA to BCAR3. If BCAR3 mediates TGF- β -driven tumor growth and metastasis, we would expect 4T1 cells expressing T β R-II and shBCAR3 to behave as control cells and exhibit impaired tumor growth and metastasis in comparison to 4T1 cells expressing T β R-II.

5.2.2.3 TGF- β signaling in epithelial cells during mammary gland development

During normal mammary gland development, TGF- β signaling in epithelial cells inhibits proliferation and branching (Moses and Barcellos-Hoff, 2011). If BCAR3 inhibits TGF- β /Smad signaling in epithelial cells during development as has been reported for breast cancer cell lines (Guo *et al.*, 2014), we would expect that loss of BCAR3 would augment TGF- β /Smad signaling and impair proliferation and branching. However, in the absence of BCAR3, we observed accelerated ductal outgrowth during puberty (**Figure 4.5**). This suggests that BCAR3 might not be a key regulator of TGF- β signaling in mammary epithelial cells during development.

The possibility that there is a role for TGF- β -BCAR3 signaling in epithelial cells during tumorigenesis but not during mammary development could be reconciled if the function of BCAR3 in TGF- β signaling pathways involves crosstalk between TGF- β receptors and specific integrins. In support of this idea, the inhibition of Smad phosphorylation following TGF- β stimulation by Cas over-expression required integrin engagement to fibronectin; cells plated on poly-L-lysine showed no such inhibition (Kim *et*

et al., 2008). This suggests that the ability of Cas to impact TGF- β signaling is adhesion-dependent and may require engagement of distinct integrins. During mammary gland development, only a limited array of integrins are expressed on mammary epithelial cells (Lambert *et al.*, 2012). These integrins mediate the interaction between mammary epithelial cells and the basement membrane, which is composed mainly of laminin and collagen (Zhu *et al.*, 2014). The basement membrane functions to block interactions between these cells and the stromal matrix, which is rich in fibronectin and fibrillar collagen (Zhu *et al.*, 2014). In contrast, breast tumor cells often express a large variety of integrins and, in a process known as integrin switching, downregulate integrins that mediate adhesions to the basement membrane and upregulate integrins that promote growth invasion and survival in the stroma (Lanigan *et al.*, 2007; Lambert *et al.*, 2012). These dramatic differences in adhesion signaling could account for how adhesion molecules like BCAR3 might regulate TGF- β signaling in cancer cells but not in normal mammary epithelial cells.

5.2.3 How could BCAR3 promote tumor progression independently of Src activity?

Work presented in this thesis, as well as other published work, supports that idea that BCAR3 functions through the BCAR3/Cas/Src complex (Riggins *et al.*, 2003; Schuh *et al.*, 2010; Wallez *et al.*, 2014) (Chapter 2). However, it is important to consider that the ability of BCAR3 to promote tumor progression may also be due to functions that are independent of the BCAR3/Cas/Src complex and Src activity. BCAR3 is a scaffolding molecule, and in addition to binding to Cas, it has been shown to bind to PTP α through its SH2 domain (Sun *et al.*, 2012). In fact, interacting with PTP α may be another route with which BCAR3 activates Src, as one of the substrates of PTP α is the inhibitory phosphate on tyrosine 527 of Src (Harder *et al.*, 1998; Pallen, 2003). However, the ability of PTP α to

function as a Src activator does not require phosphorylation of the tyrosine residue that mediates binding to the BCAR3 SH2 domain (Tyr 789) (Sun *et al.*, 2012). It is not clear whether other PTP α substrates might coordinate with BCAR3 to promote tumorigenesis. A similar argument could be made for Cas, in that BCAR3 may function by promoting signaling downstream of Cas or its other family members in a manner that is independent of Src. Finally, there may be additional as yet unidentified binding proteins that could contribute to the ability of BCAR3 to promote tumor progression.

5.3 Does BCAR3 promote metastasis?

In addition to studying the role of BCAR3 in regulating tumor growth, it will be important to determine if BCAR3 expression promotes metastasis. As discussed in chapter 1, most breast cancer deaths are the result of metastatic disease (Wiechmann and Kuerer, 2008). BCAR3 is known to promote breast cancer cell migration and invasion (Schrecengost *et al.*, 2007; Wilson *et al.*, 2013) (Chapter 2), two processes that are critical elements of the metastatic process. In order to determine whether BCAR3 promotes metastasis, conditional knockout cell lines can be used as discussed in chapter 3. Briefly, primary tumors would be allowed to reach 300-500mm³ at which point they would be surgically resected. Upon tumor resection, BCAR3 knockdown would be initiated, and tumor metastasis to the lung would be monitored by IVIS imaging.

If BCAR3 is found to regulate metastasis, the importance of the interaction between BCAR3 and Cas in this function should again be analyzed with the conditional BCAR3 knockdown and re-expression systems described earlier in this chapter. BCAR3 knockdown and re-expression could be initiated following tumor resection, and metastasis monitored by IVIS imaging. If BCAR3 is found to promote tumor metastasis through direct interaction with Cas, a role for Src activity could be determined by treatment with dasatinib at the time of tumor resection.

Several studies have shown that tumor cells disseminate early during primary tumor growth, independently of primary tumor size (Hüsemann *et al.*, 2008). Furthermore, in spontaneous mouse models of breast cancer, mammary epithelial cells have been detected in metastatic sites when the mammary gland appears histologically normal or in a premalignant stage (Weng *et al.*, 2012). The ability of tumor cells to disseminate early and from small tumors may make it difficult to observe differences in tumor metastasis in the experiments described above. As an alternative to studying metastasis following primary tumor resection, tail vein injections can be performed using control and BCAR3-depleted cells re-expressing the WT or Cas binding mutant of BCAR3. These studies would specifically address the ability of BCAR3 to promote colonization and growth in the lung.

The ability of BCAR3 to promote metastasis can also be tested in the MMTV- PyMT mouse model of breast cancer. MMTV-PyMT mice form spontaneous metastases in the lung and depletion of Src suppresses these lung metastases (Lin *et al.*, 2003) (Wang *et al.*, 2009). The MMTV-PyMT/BCAR3 conditional KO mice described above could be used to determine if BCAR3 expression regulates the formation of lung metastases in this mouse model. The added advantage of this model is that it will measure metastasis in the presence of an intact immune system.

5.4 Can BCAR3 serve as a potential biomarker and/or therapeutic target in breast cancer patients?

BCAR3 has been shown to promote proliferation, migration, and invasion of breast cancer cell lines (Near *et al.*, 2007; Schrecengost *et al.*, 2007; Wilson *et al.*, 2013; Wallez *et al.*, 2014) (Chapter 2). On the molecular level, BCAR3 expression regulates Cas protein phosphorylation and Src kinase activity (Riggins *et al.*, 2003; Wallez *et al.*, 2014). In this thesis, we show for the first time that BCAR3 regulates tumor formation *in vivo*. It remains

to be determined if BCAR3 regulates tumor growth of established tumors or if BCAR3 promotes metastasis, but the established *in vitro* functions of BCAR3 suggest that it may. In this regard, BCAR3 may serve as a potential therapeutic target for breast cancer. Furthermore, analysis of clinical samples may show that BCAR3 expression can be used as a biomarker for metastasis and/or response to specific therapies.

5.4.1 BCAR3 as a biomarker

Clinical data analyzing BCAR3 protein expression in patients is lacking. Preliminary studies have shown that BCAR3 protein is expressed in a multiple subtypes of breast cancers (**Chapter 2, Figure 2.12**). Analysis of a much larger number of clinical samples is needed to determine if there is a correlation between BCAR3 expression and tumor subtype, tumor grade, metastasis, therapeutic response, and relapse-free and overall survival. If BCAR3 protein expression is found to track with any of these endpoints, it may serve as a biomarker that can help in the clinical management of the disease. The ability of BCAR3 to predict metastasis and/or overall survival may be dependent on the subtype of the tumor. For example, BCAR3 expression may serve as a biomarker for metastasis in basal-like or claudin-low tumors but not luminal A and B tumors or vice versa. Interestingly, preliminary data suggest that BCAR3 expression may be highest in high-grade DCIS (Dr. Ashley Wilson, personal communication). High-grade DCIS, when compared to low-grade DCIS, is more likely to progress to invasive disease (Makki, 2015); based on these preliminary results, it is possible that BCAR3 could serve as a biomarker for patients who present with DCIS and are likely to develop invasive disease.

BCAR3 expression may also correlate with response to specific therapeutic treatments. BCAR3 was originally identified as a gene that, when overexpressed in cell lines, conferred resistance to antiestrogens (VanAgthoven *et al.*, 1998). However, one study reported that high BCAR3 mRNA levels associated with increased progression-free

survival in a cohort of ER+ breast cancer patients receiving tamoxifen treatment (Guo *et al.*, 2014). This is potentially contradictory to what we know about BCAR3 function *in vitro*. However, this study analyzed BCAR3 mRNA levels and did not measure protein expression. It will therefore be important to independently assess whether BCAR3 protein expression serves as a biomarker for patients who will or will not respond to antiestrogens. Furthermore, as discussed in section 5.2.2, it is possible that BCAR3 may regulate TGF- β signaling in breast cancers. There are several TGF- β inhibitors currently in clinical trials (Buijs *et al.*, 2012), and if BCAR3 is found to regulate TGF- β signaling, BCAR3 expression may serve as a biomarker for patients who would benefit from treatment with these inhibitors.

Finally, BCAR3 may serve as a biomarker for patients who would benefit from treatment with Src kinase inhibitors. Several Src inhibitors have been developed and are in preclinical and clinical trials for various cancers, including breast cancer. One of Src inhibitors currently in clinical trials for breast cancer is dasatinib (Mayer and Krop, 2010). Despite *in vitro* data indicating that triple negative breast cancer (TNBC) cells are uniquely sensitive to dasatinib-induced growth inhibition (Huang *et al.*, 2007; Finn, 2008), a phase-II clinical trial showed only limited effectiveness (objective response rate of 4.7%) of dasatinib as a single-agent therapy for patients with advanced or metastatic TNBC (Finn *et al.*, 2011). Importantly, TNBC is a highly heterogeneous disease, and it is possible that only a subset of patients will benefit from dasatinib treatment. However, there are currently no biomarkers to predict dasatinib-responsive tumors (Finn *et al.*, 2011). Considering BCAR3 is highly expressed in TNBC cell lines and augments Src activity, we suggest that BCAR3 may serve as a biomarker for patients who would benefit from treatment with dasatinib or other Src kinase inhibitors.

Despite *in vitro* data demonstrating that BCAR3 promotes Src activity, further studies are needed to help determine if BCAR3 could serve as biomarker for dasatinib sensitivity. *In vitro* studies can be performed to determine if BCAR3 over-expression in dasatinib-resistant cell lines renders the cells more sensitive to treatment, and if BCAR3 knockdown in sensitive cells renders them more resistant to treatment. Performing these studies in 3D cell culture would allow the cells to interact with the ECM and provide a more physiological system for studying drug sensitivity (Chavez *et al.*, 2010). Additionally, the *in vivo* studies proposed above to determine whether dasatinib treatment impairs BCAR3-mediated primary tumor progression and metastasis (sections 5.2.1 and 5.3) would provide valuable insight into the ability of BCAR3 to impact dasatinib responsiveness. Finally, as dasatinib has been used in clinical trials for breast cancer, tumor samples from patients who responded or did not respond to dasatinib treatment could be analyzed for levels of BCAR3 protein expression to determine if there is a correlation between BCAR3 expression and response.

5.4.2 BCAR3 as a therapeutic target

If BCAR3 is found to be a biomarker for tumor grade, metastasis, therapeutic response, and/or relapse-free and overall survival, this could suggest that inhibiting BCAR3 signaling may be a successful treatment option for some breast cancer patients. However, in order to be a good therapeutic target, BCAR3 must serve as a driver or amplifier of tumor growth and progression. Several approaches could be used to inhibit BCAR3 signaling in breast tumors. BCAR3 could be directly targeted clinically using siRNA. Alternatively, as many of the functions of BCAR3 require direct interaction between BCAR3 and Cas (Wallez *et al.*, 2014) (Chapter 2), inhibitors that block this interaction may prove beneficial in tumors that express these proteins. Finally, since Src

and potentially TGF- β are effectors of the Cas/BCAR3 complex, inhibiting these molecules as described above could be a viable approach to blocking BCAR3 functions.

Treatment with a BCAR3 specific siRNA or disrupting the BCAR3/Cas interaction could be an effective way to impair Src signaling and potentially inhibit TGF- β signaling. Notably, Src and TGF- β inhibitors are in clinical trials but these proteins have many physiological functions and thus therapeutic targeting of these proteins can have adverse effects (Finn, 2008; Finn *et al.*, 2011; Connolly *et al.*, 2012). Due to the fact that BCAR3 expression appears to be fairly low in normal tissue (Chapter 2) and largely dispensable for normal development (Near *et al.*, 2009), inhibiting BCAR3 expression or BCAR3/Cas interactions may provide a more directed way to impair TGF- β and Src signaling in tumor tissues. Furthermore, as BCAR3 was originally identified as a gene whose overexpression conferred antiestrogen resistance in breast cancer cell lines (VanAgthoven *et al.*, 1998), treatment with a BCAR3-specific siRNA or inhibition of BCAR3/Cas interactions may make tumors more susceptible to antiestrogens.

siRNA oligonucleotides regulate protein expression through degradation of the mRNA molecule. Though siRNA molecules are widely available and capable of regulating protein expression in cell lines, effective use of these molecules as treatment options in cancer patients has proven challenging (Resnier *et al.*, 2013; Shen *et al.*, 2013). The barriers to the use of siRNAs as cancer therapeutics include inefficient cell delivery, off-target effects, and unwanted immune system stimulation (Xu and Wang, 2015). Packaging of siRNA molecules into nanoparticles helps to overcome some of these problems. Currently, several nanoparticle-packaged siRNA molecules are in clinical trials for different cancers (Xu and Wang, 2015).

Intracellular protein-protein interactions (PPIs) can be inhibited using competitive peptides and small molecules. One of the challenges in developing inhibitors for PPIs is

the absence of well-defined binding pockets (Arkin and Wells, 2004; Nero *et al.*, 2014; Sable and Jois, 2015). However, the crystal structure of BCAR3 has been solved and the binding interface of BCAR3 and Cas has been modeled by Mace *et al.* (Mace *et al.*, 2011). The binding interface between BCAR3 and Cas is characterized as a globular interface as it is composed of 1,192 Å² of buried surface, has two discontinuous binding motifs, and requires tertiary structure on both sides of the interface (Mace *et al.*, 2011; Arkin *et al.*, 2014). Notably, inhibition of globular interfaces is challenging, but identification of 'hot spots' or high affinity binding sites within the globular interface can make these interfaces more druggable (Arkin and Wells, 2004; Arkin *et al.*, 2014). Hot spots in the BCAR3/Cas interface have been identified by mutational studies performed by Mace *et al.*, which demonstrated that the BCAR3 residues leucine 744 and arginine 748 and Cas residues leucine 787, phenylalanine 794 and aspartic acid 797 are specifically required for interaction between these two proteins (Mace *et al.*, 2011). This work can provide critical information for the development of peptides or small molecules that block the interaction between BCAR3 and Cas. Inhibitors of PPIs have shown promise clinically and a couple of inhibitors are on the market for use in cardiovascular disease and HIV (Ivanov *et al.*, 2013; Nero *et al.*, 2014). In recent years, several anti-cancer PPI inhibitors have entered clinical trials including inhibitors to the MDM2 (mouse protein double minute 2)/p53 interaction and Smac (second mitochondria-derived activator of caspase) mimetics capable of binding to XIAP (X-linked inhibitor of apoptosis protein) and preventing its binding to and inhibition of pro-apoptotic caspase-9 (Ivanov *et al.*, 2013).

It will be important to identify the patients who will respond favorably to treatment with siRNA to BCAR3 or BCAR3/Cas PPI inhibitors. This can be determined by analyzing the correlation between BCAR3 expression and tumor subtype, tumor grade, metastasis, and overall survival in breast cancer patients. As mentioned previously, high levels of BCAR3 mRNA in patients treated with tamoxifen were found to correlate with increased

progression-free survival (Guo *et al.*, 2014). Therefore it remains possible that, at least in some patients, inhibition of BCAR3 or the BCAR3/Cas complex could enhance tumor growth or metastasis. Furthermore, our developmental studies raise the question of whether BCAR3 functions in other as yet unidentified ways in normal epithelial and/or stromal cells. A thorough understanding of BCAR3 function is necessary to determine if the use of siBCAR3 oligonucleotides or BCAR3/Cas PPI inhibitors could have unforeseen negative side effects. Finally, it is important to remember that cancer cells are often able to take advantage of signaling pathway redundancies and cross-talk to alter their signaling circuitry following drug treatment (Logue and Morrison, 2012). Therefore, inhibition of BCAR3 or the BCAR3/Cas complex alone may not be sufficient for long-term Src and/or TGF- β inhibition and combination therapy may be required.

The work presented in this thesis adds important information to the understanding of BCAR3 and the BCAR3/Cas complex in breast cancer. This work highlights the importance of the BCAR3/Cas complex in BCAR3 mediated functions and provides the first analysis of BCAR3 function in mouse models of breast cancer. Furthermore, the analysis of BCAR3 function in normal mammary gland development highlights the fact that BCAR3 may have additional as-yet-unknown functions in epithelial and non-epithelial cells. Many questions remain, but the data presented herein suggest that BCAR3 may be a promising biomarker and/or therapeutic target for breast cancer patients.

Chapter 6: Materials and Methods

6.1 Antibodies and reagents

Monoclonal antibodies were obtained from the following sources: β -Actin (Sigma-Aldrich, A3854); β -tubulin (Sigma-Aldrich, T4026); α -actinin (Sigma-Aldrich, A5044); talin (Sigma-Aldrich, T3287); phospho-ERK1/2-T183/Y185 (Sigma-Aldrich, M8159); Cyclin A (Cell Signaling, 4656); AKT (Cell Signaling, 2920); phospho-AKT-S473 (Cell Signaling, 9018); phospho-FAK-Y397 (Cell Signaling, 8556); Cyclin D1 (Millipore, 05-362) (AbCam, ab134175); p21CIP (Millipore, 05655); α 6 integrin (Millipore, MAB1378); Ki67 (AbCam, ab92742); Paxillin (BD Biosciences, 610052); FAK (BD Biosciences, 610087). Polyclonal antibodies were obtained from the following sources: BCAR3 (Bethyl Laboratories, Inc., A301-671A); BCAR3 (for IHC) (Sigma Aldrich, HPA014858); GFP (Abcam, AB6673); ERK (Cell Signaling Technology, Inc., 9102); AKT (Cell Signaling, 9272); Cleaved Caspase 3 (Cell Signaling, 9661); Texas red-conjugated goat anti-rabbit (Jackson ImmunoResearch Laboratories Inc., 111-075-144); CasB (Bouton and Burnham, 1997); phosphor-paxillin-Y118 (Invitrogen, 44-722G); anti-Rat Alexa Fluor 647 (Life Technologies, A21472); anti-Rabbit Alexa Fluor 594 (Life Technologies, A11037); anti-Rabbit Fitc (Jackson ImmunoResearch, 111-095-144). Dapi was purchased from Sigma-Aldrich (D9542). Additional reagents included fibronectin (Sigma-Aldrich, F1141), EGF (Peprotech, AF-100-15), FGF-basic (Peprotech, 100-18B), and Matrigel (Corning, 354230).

6.2 Expression vectors

BCAR3 cDNA was cloned into the EcoRI and XbaI sites of pEGFP-C1 (Clontech Laboratories, Inc) to generate pEGFP-BCAR3 (WT GFP-BCAR3). Cas cDNA was cloned into the XbaI and BamHI sites of pm-Cherry-C1 to generate pm-Cherry-Cas.

Mutant R171V, L744E/R748E, and R171V/L744E/R748E GFP-BCAR3 proteins were created using the QuickChange II Lightning Site-Directed Mutagenesis Kit (Agilent Technologies). The following primers were used (changed nucleotides are underlined, and all constructs were confirmed by sequencing):

R171V Forward:

5'-CGAGATGGTGA^{CTTCCTAGTT}GTCGACTCTCTGTCCAGCCCTGGG-3'

R171V Reverse:

5'-CCCAGGGCTGGACAGAGAGTCGACAACTAGGAAGTCACCATCTCG-3'

L744E/R748E Forward:

5'-CATGCTGAACCATGAGGCAACAGCGGAAATTCATGGCCGAGGCTGC-3'

L744E/R748E Reverse:

5'-GCAGCCTCGGCCATGAATTCCGCTGTTGCCCTCATGGTTCAGCATG-3'

shRNA oligonucleotides targeting BCAR3 and cloned into the TRC2-pLKO-puro vector were purchased from Sigma Aldrich. Hairpin sequences were as follows:

shBCAR3-1 shRNA ID: TRCN0000364816, sequence:

5'-CCGGTAACTGCCCTCTCGCGTAAATCTCGAGATTTACGCGAGAGGGCAGTTATTTTTG-3'

shBCAR3-2 shRNA ID: TRCN0000376503, sequence:

5'-CCGGTCGGCATTGCAGTGGACATTCTCGAGGAATGTCCACTGCAATGCCGATTTTTG-3'

shBCAR3-3 shRNA ID: TRCN0000369682, sequence:

5'-CCGGGCGCCTGGACATAATTGAAAGCTCGAGCTTTCAATTATGTCCAGGCGCTTTTTG-3'

Wobble mutants of BCAR3 were generated in the pLV-Venus vector. WT and L744E/R748E BCAR3 cDNA were cloned into the NotI and SpeI sites of the pLV-Venus vector. Site directed mutagenesis was performed using the QuickChange II XL Site-Directed Mutagenesis Kit (Agilent Technologies) to eliminate targeting by shBCAR3-1 without altering the amino acid sequence of the resultant BCAR3 protein. The following

primers were used (changed nucleotides are underlined, and all constructs were confirmed by sequencing):

shB3wobble1 Forward:

5'-CCAGATTTTAACTGCGCTGTCCCGAAAATTGGAACCTCCTCCTG-3',

shB3wobble1 Reverse:

5'-CAGGAGGAGGTTCCAATTTTCGGGACAGCGCAGTTAAAATCTGG-3'

For conditional knockdown experiments, the shBCAR3-1 oligo was cloned into a Tet-pLKO-puro vector provided by Dr. Kevin Janes (UVA). For *in vivo* mouse experiments, stable luciferase expressing cells were created by infection with the pLenti-PGK-BLAST-V5-Luc vector (Addgene).

6.3 Cell culture

BT549 and MDA-MB-231 cells (American Type Tissue Culture) were cultured as previously described (Schrecengost *et al.*, 2007). Hs578T cells (provided by Dr. Kevin Janes), were cultured in Dulbecco's Modified Eagle's Medium (DMEM) containing 10% FBS, 0.01mg/ml bovine insulin, and 1% Penicillin/Streptomycin. SUM159PT cells (provided by Dr. Kevin Janes) were cultured in Ham's F-12 containing 5% FBS, 10mM HEPES, 5µg/ml Insulin, 1µg/ml Hydrocortisone, and 1% Penicillin/Streptomycin. MDA-MB-436 cells (provided by Dr. Kevin Janes) were cultured in Leibovitz's L-15 medium contained 10 µg/ml insulin, 16 µg/ml glutathione, 10% FBS, and 1% Penicillin/Streptomycin. The metastatic 231/LM2-4 variant cell line was provided by Dr. Robert Kerbel (Sunnybrook Research Institute) and cultured in RPMI 1640 containing 5% FBS and 1% Penicillin/Streptomycin. MCF10A cells (provided by Dr. Kevin Janes) were cultured in DMEM/F12 in containing 5% horse serum, 20ng/ml EGF, 0.5mg/ml hydrocortisone, 100ng/ml cholera toxin, 10ug/ml insulin, and 1% Penicillin/Streptomycin.

6.3.1 3D cell culture

For 3D culture of MDA-MB-231 and Hs578T cells, Matrigel (50 μ l) (Corning) was spread evenly on the bottom of 8-well chamber slides. Cells grown in 2D monolayer culture were trypsinized and plated in the chamber slides with DMEM containing 2% (MDA-MB-231) or 10% (Hs578T) serum, 2% Matrigel, 5ng/ml EGF, and 0.5 μ g/ml (MDA-MB-231) or 1 μ g/ml (Hs578T) puromycin. Cells were grown for 6-8 days with media changes every 4 days. Phase images of representative fields were captured using an Olympus CKX41 or Zeiss Axiovert 40 CFL inverted scope.

MCF10A acinar cultures were performed as described by Debnath *et al.* (Debnath *et al.*, 2003). Briefly, Matrigel (50 μ l) was spread evenly on the bottom of 8-well chamber slides. Cells grown in 2D monolayer culture were trypsinized and plated at 4,000 cells/well in the chamber slides with assay media (DMEM/F12 containing 2% horse serum, 0.5mg/ml hydrocortisone, 100ng/ml cholera toxin, 10 μ g/ml insulin, and 1% Penicillin/Streptomycin without EGF). 5ng/ml EGF and 2% Matrigel was added fresh to the assay media at time of seeding. Media was changed every 4 days. Immunofluorescence staining of MCF10A acinar cultures was performed as described by Debnath *et al.* (Debnath *et al.*, 2003).

6.3.2 Mammary epithelial organoid culture

Mammary organoid cultures were performed as described by Dr. Andrew Ewald (Ewald, 2013). Briefly, mammary glands 3, 4, and 5 were dissected from mice, minced, and digested with a collagenase/trypsin mixture (.2% trypsin, .2% collagenase type IV, 5% FBS, 5 μ g/ml Insulin, 50 μ g/ml gentamycin, in 50ml DMEM/F12). Following digestion of the glands, the collagenase/trypsin/cell mixture was centrifuged and treated with DNase. Epithelial pieces were separated from the single cells through differential centrifugation

and plated in Matrigel. Organoid media (DMEM/F12 containing 1% Penicillin/Streptomycin and ITS media supplement) was added after Matrigel solidified and media changes were performed every 2 days. Media was supplemented with 2.5nM FGF2 when indicated. Phase images of representative fields were captured using an Olympus CKX41 or Zeiss Axiovert 40 CFL inverted scope.

6.4 Plasmid transfection, lentivirus production and infection

Transfections were performed using Lipofectamine 2000 (Invitrogen, 11668019) following manufacturer's specifications.

Lentiviral particles were produced by calcium phosphate transfection of HEK293T cells with a mixture of the transfer vector, packaging vector (psPAX2), and envelope vector (pMD2.G). Medium containing lentivirus was collected 48 hours post-transfection, filtered through 0.45µm filter, and used immediately or frozen at -80°C. Cells were infected with lentivirus in the presence of 8µg/ml polybrene.

6.5 Immunoprecipitation, immunoblotting and immunofluorescence

Cells grown in 2D were lysed in ice-cold radioimmune precipitation assay (RIPA) buffer supplemented with protease inhibitors and protein concentrations determined as previously described (Schrecengost *et al.*, 2007) or when indicated, in a non-denaturing lysis buffer (50mM Tris-HCl, pH 7.5, 120mM NaCl, 1% Triton X-100, 2mM EDTA, 5% glycerol, 1mM sodium orthovanadate, 1mM sodium fluoride, 1mg/ml aprotinin, 1mg/ml leupeptin, and 1 mM phenylmethylsulfonyl fluoride). Immunoprecipitations, immunoblotting and immunofluorescence of 2D cultures were performed as previously described (Schrecengost *et al.*, 2007). For serial immunoprecipitations (IP), 10% of the lysate was collected prior to immunoprecipitations (the pre-IP lysate) and an aliquot

representing an equal percentage of the total preparation was collected and saved after each subsequent IP (the post-IP lysate).

For immunoblotting of non-phosphorylated proteins from 3D culture, cells were washed with 250µl of 0.25% trypsin before adding a fresh 125µl of trypsin to each well. Wells were scraped with the end of a sterile plunger and the cells and Matrigel were collected. An additional 125µl of trypsin was added to the wells and the combined cell/Matrigel mixture was pipetted several times to break up the Matrigel and incubated for 30 minutes at 37°C. Cells were collected by centrifugation at 150 x g for 3 minutes, washed 1X in DMEM, re-suspended in phosphate buffered saline (PBS), and then pelleted by spinning for 3 minutes at 2000 rpm in a micro-centrifuge. The pellet was re-suspended in ice-cold RIPA buffer supplemented with protease inhibitors and protein concentrations determined as previously described (Schrecengost *et al.*, 2007). For immunoblotting of phosphoproteins, cells grown in 3D were washed with PBS containing protease inhibitors and lysed directly in the well by adding RIPA. Following a 15 minute incubation at 4°C, the Matrigel and acini in lysis buffer was collected and pulled through a 27-gauge needle several times. The mixture was incubated for another 15 minutes at 4°C before clearing the lysate by centrifugation. The supernatant was collected for analysis by immunoblot.

For immunofluorescence of MCF10A acinar cultures, staining was completed as described by Debnath *et al.* (Debnath *et al.*, 2003) and fluorescent microscopy was performed on a Zeiss LSM 710 Multiphoton confocal microscope.

6.6 Live-cell imaging and adhesion turnover analysis

BT549 cells were plated on acid-washed 2µg/ml fibronectin-coated glass bottom TIRF dishes (MatTek Corporation, Ashland, MA) and incubated for 30-40 minutes at 37°C, pH 7.4 in CCM1 media (Hyclone). Images were captured using an inverted TIRF microscope (1X70; Olympus) with a 60X objective (±1.5X magnification), a cool charged-

couple device camera (Retiga Exi; Qimaging), and heated objective/stage (Bioprotechs). Images were captured every 5 seconds for 10-12 minutes using MetaMorph software. To quantify adhesion turnover, adhesions at peripheral, protruding edges were manually selected for analysis. Complete fluorescence intensity time tracings for individual adhesions were (1) normalized, (2) corrected for background intensity by subtracting an average intensity value corresponding to a background region away from the cell, and (3) plotted. Both the increase (incorporation/assembly) and decrease (dissociation/disassembly) in fluorescence intensity were linear as a function of time on semi-logarithmic plots, and rate constants were determined from the slopes of these graphs. Rate constant measurements were obtained for a minimum of 13 individual adhesions on 2-5 cells.

6.7 Rac activity assays

To measure GTP-Rac1 levels, BT549 cells were transfected with plasmids encoding GFP, WT GFP-BCAR3, or L744E/R748E GFP-BCAR3. Cells were incubated for 24 hours, trypsinized, held in suspension for 90 minutes, and then plated on 10 μ g/ml fibronectin for 1 hour. Cells were lysed and GTP-bound Rac1 was isolated by incubation with PAK-1-binding domain agarose (Millipore, 14-325) following manufacturer's instructions.

6.8 Transwell migration assays

For migration assays, the lower chamber of a modified Boyden chamber (6.5 mm, 8.0- μ m Transwell Costar membrane; Corning Incorporated) was pre-incubated with 10% FBS in DMEM for 2 hours. MDA-MB-231 (2.5×10^4) cells were plated in the top chamber in DMEM without serum and allowed to migrate toward 10% serum for 6 h at 37°C. Following migration, the non-migratory cells were removed from the top of the membrane

with cotton swabs. The underside of the membrane was fixed, stained using Protocol HEMA 3 stain set (Fisher Scientific, 122-911), and mounted onto coverslips using Cytoseal-60 (Thermo Scientific, 8310). The total number of migrated cells was determined by light microscopy.

6.9 Protein degradation studies

BT549 cells were infected with lentiviruses encoding control (Venus), WT-Venus BCAR3, or L744E/R748E (L/R) Venus-BCAR3 and plated in 6 well dishes at 100,000 cells per well. One day after plating, cells were treated with 25ug/ml cyclohexamide (CHX) for indicated times. Cells were lysed at each time point and protein concentrations were determined by BCA. Protein levels were normalized to the 0 hour time point and graphed using an exponential decay non-linear regression. A representative blot and graph is shown. Experiments were repeated 2 times.

6.10 Mice

MMTV-PyMT C57Bl/6 mice were obtained from Dr. Tom Parsons (UVA). The presence of the PyMT transgene was confirmed by PCR. To confirm mouse genotype, the following primers were used;

PyMT-1: 5'-TGTGCACAGCGTGTATAATCC-3',

PyMT-2: 5'-CAGAATAGGTCGGGTTGCTC-3'

The expected product for MMTV-PyMT C57Bl/6 mice was a 200bp fragment. The wildtype C57Bl/6 mice used in these studies were transgene negative MMTV-PyMT C57Bl/6 mice.

For xenograft tumor models, J:Nu mice were purchased from Jackson Laboratories (007850).

BCAR3 knockout mice were generously provided by Richard Near (Near *et al.*, 2009). To confirm mouse genotypes, the following primers were used;

5PRGenNeoko 5'-TACCGGTGGATGAGGAATGTG TGCGAG-3'

KOIIWT3PR 5'-GGAAAGGTAGAGGGTGACTIONTGGAGG-3'

KOIIWT5PR 5'-GTGTGGTAATACATGGAGTGG AGAG-3'

Wildtype was assayed with primers, KOIIWT5' and KOIIWT3', yielding a 2.4 kb fragment whereas BCAR3 knockout was assayed with 5' GenNeoko and KOIIWT3' yielding a 2.0 kb fragment.

6.11 Whole mounts

Mammary whole mounts were performed as described by Plante *et al.* following dissection of mammary gland 4 (Plante *et al.*, 2011).

6.12 Immunohistochemistry

For human breast tumor staining, sequential sections of breast tissue were received from the University of Virginia Biorepository and Tissue Research Facility (BTRF). Sections were stained with hematoxylin and eosin (H&E) or immunostained with BCAR3 or Cas antibodies by the Biorepository and Tissue Research Facility (BTRF). For mouse mammary gland staining, mammary gland 4 was isolated, paraffin embedded, sectioned, and immunostained with the designated antibodies by the BTRF. For mouse tumor staining, xenograft tumors were dissected from nude mice and similarly processed and immunostained by the BTRF.

6.13 IVIS Imaging

Mouse were IP injected with 200µl D-Luciferin (15mg/ml) (Gold Bio, LUCNA-1) and imaged on the Caliper IVIS Spectrum bioluminescence and fluorescence scanner.

6.14 Statistical analysis

Statistical analyses were conducting using GraphPad Prism and the statistical test used in each experiment is specified in the figure legends.

Appendix 1: Control of Cas expression by BCAR3

A1.1 Introduction

The physical association between BCAR3 and Cas has been shown to be critical for many of the functions of BCAR3 (Wallez *et al.*, 2014) (Chapter 2). In chapter 2, we highlighted the relevance of this complex in breast cancer cells by demonstrating that all of the BCAR3 present in these cells is in complex with Cas. The direct interaction between BCAR3 and Cas promotes Src-dependent tyrosine phosphorylation of the substrate domain of Cas and stabilization of Cas protein (Schuh *et al.*, 2010; Wallez *et al.*, 2014).

As discussed in Chapter 5, BCAR3 and the BCAR3/Cas complex may serve as potential therapeutic targets for breast cancer. Gaining a better understanding of how these proteins regulate one another will be helpful in determining the best ways to target them for possible future therapies. To investigate the contribution of direct binding between BCAR3 and Cas to the stabilization of Cas, protein degradation studies were performed in the presence of WT BCAR3 or a mutant of BCAR3 that was unable to bind to Cas. As expected based on published work (Wallez *et al.*, 2014), BCAR3 promoted Cas protein stabilization only when it was directly bound to Cas. Furthermore we found that, in some breast cancer cell lines, expression of Cas protein was dependent on BCAR3 expression, as depletion of BCAR3 by shRNA resulted in a concomitant loss in Cas protein expression. Further studies are needed to understand how BCAR3 controls Cas expression and why this regulation is cell line-specific.

A1.2 Results

A.1.2.1 BCAR3 promotes Cas stabilization through direct binding

Work by Wallez *et al.* and Near *et al.* showed that Cas protein levels are higher in cells transiently transfected with BCAR3 (Near *et al.*, 2007; Wallez *et al.*, 2014). Wallez

et al. demonstrated that this increase in Cas protein levels was dependent on interactions between BCAR3 and Cas (Wallez *et al.*, 2014). Both of these previous studies attributed the increase in Cas protein levels to stabilization of Cas by BCAR3 at one time point following transient overexpression of BCAR3. To explore this process further, Cas and BCAR3 protein levels were measured following cyclohexamide treatment to block protein translation in the presence of the WT and Cas-binding mutant of BCAR3. BT549 cells were infected with lentiviruses encoding Venus protein (control), WT-Venus BCAR3 or L744E/R748E (L/R)-Venus BCAR3 and treated with 25µg/ml cyclohexamide (CHX). Analysis of protein lysates over a 3-day time course of CHX treatment showed that, in the absence of exogenous BCAR3, the Cas protein present in BT549 cells had an estimated half-life of 35 to 42 hours (**Figure A1.1**). In the presence of overexpressed WT BCAR3, the estimated half-life of Cas increased to over 100 hours (**Figure A1.1A**). This increase in the half-life of endogenous Cas was not observed when the Cas-binding mutant of BCAR3 was overexpressed; in fact, the half-life of Cas was reduced to about 25 hours (**Figure A1.1B**).

A.1.2.2 Cell line-specific control of Cas protein expression by BCAR3

Although the data presented above together with the work by Wallez *et al.* show a strong relationship between BCAR3/Cas interactions and Cas protein stability, BCAR3 has not previously been shown to be required for Cas protein expression (Wallez *et al.*, 2014). Depletion of BCAR3 by siRNA in breast cancer cell lines results loss of Cas phosphorylation but not a complete loss of Cas protein expression (Schuh *et al.*, 2010). However, we found that depletion of BCAR3 by multiple different shRNAs in BT549 cells resulted in a significant loss of Cas protein expression (**Figure A1.2A**). The extent of Cas protein loss was directly related to the efficiency of the shRNA in depleting BCAR3 expression (compare Cas and BCAR3 expression levels in lanes 2-4). Interestingly, this

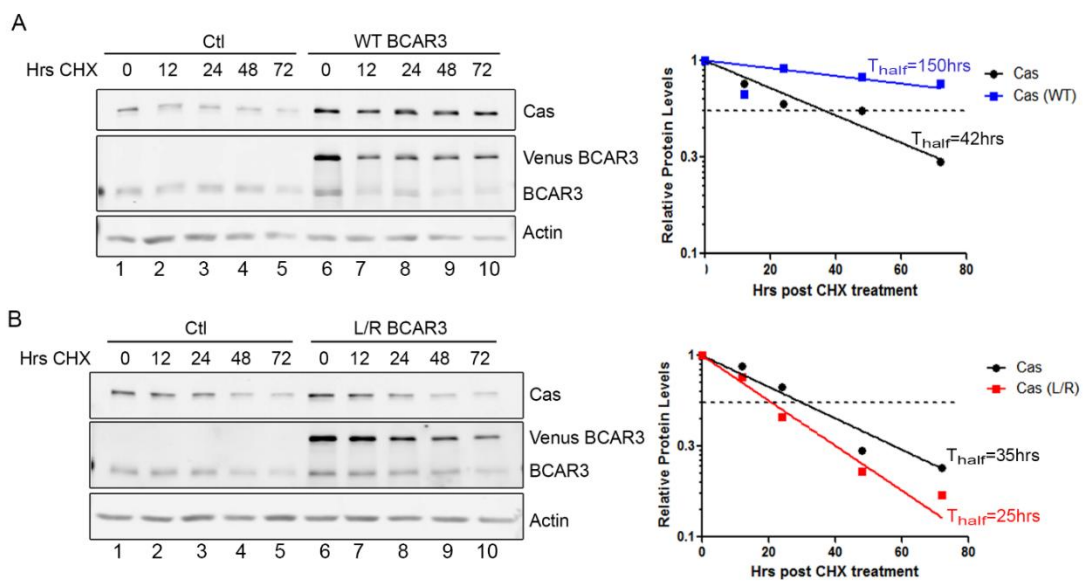
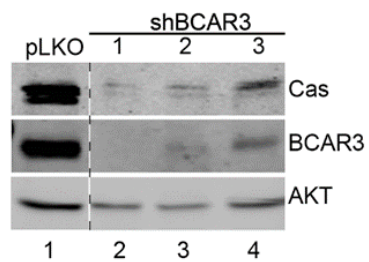


Figure A1.1. BCAR3 promotes Cas stabilization through direct binding

BT549 cells were infected with lentiviruses encoding Venus alone (Ctl) and WT Venus-BCAR3 (A) or L744E/R748E (L/R) Venus-BCAR3 (B) and plated in 6-well dishes at 100,000 cells per well. One day after plating, cells were treated with 25 μ g/ml cyclohexamide (CHX) and lysed at the indicated times. Proteins were immunoblotted with antibodies recognizing the designated proteins. Representative blots are shown. Protein levels from the representative blots were normalized to the 0 hour time point and plotted as an exponential decay nonlinear regression.

A



B

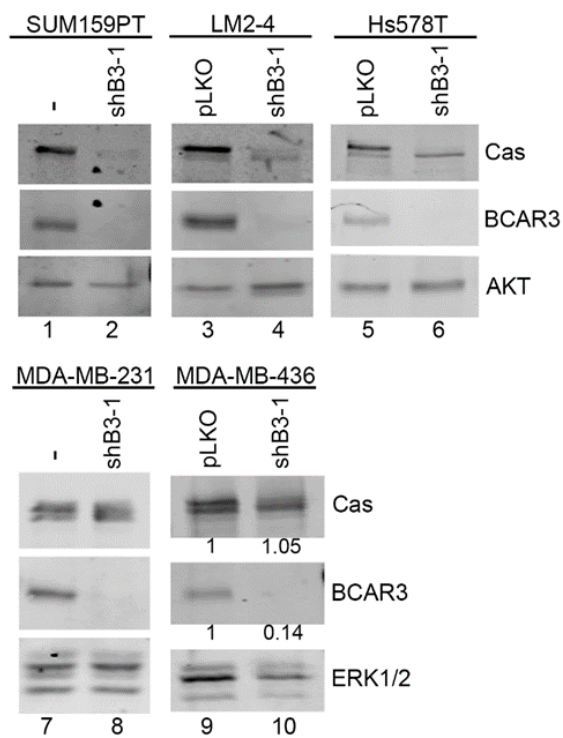


Figure A1.2. The control of Cas expression by BCAR3 is cell line specific

(A) Lysates from BT549 cells stably expressing empty vector (pLKO), shBCAR3-1, shBCAR3-2, or shBCAR3-3 were immunoblotted with antibodies recognizing the designated proteins. (B) Lysates from uninfected (-) cells or SUM159PT, LM2-4, Hs579T, MDA-MB-231, and MDA-MB-436 cells expressing empty vector (pLKO) or shBCAR3-1 were immunoblotted with antibodies recognizing the designated proteins.

dependence of Cas protein expression on BCAR3 was cell line-specific. For example, depletion of BCAR3 protein by shRNA resulted in loss of Cas protein expression in BT549, SUM159PT, and LM2-4 cells but not in MDA-MB-231 and MDA-MB-436 cells (**Figure A1.2A, B compare lanes 1-4 and 7-10**). Hs578T cells exhibited an intermediate phenotype where depletion of BCAR3 by shRNA resulted in a reduction but not significant loss in Cas protein levels (**Figure A1.2B, lanes 5-6**). This cell line-specific dependence of Cas protein expression on BCAR3 has not been previously published.

A1.3 Discussion

It has been reported in the literature that transient transfection of BCAR3 promotes an increase in Cas protein levels. This increase in protein expression was dependent on BCAR3 interaction with Cas (Near *et al.*, 2007; Wallez *et al.*, 2014). The work presented above supports these findings by demonstrating that the estimated half-life of Cas protein is increased in the presence of WT BCAR3 protein but not in the presence of a Cas-binding mutant of BCAR3. Furthermore, we show a novel cell line-specific dependence between Cas and BCAR3 protein expression.

A1.3.1 Control of BCAR3 expression by Cas

In chapter 2 we show that all of the BCAR3 present in breast cancer cells is in complex with Cas (**Figure 2.1**). As discussed in chapter 2, this interaction is required for many BCAR3-mediated functions. Interestingly, Cas protein is required for stable BCAR3 expression, as Cas depletion by siRNA in breast cancer cell lines results in concomitant loss of BCAR3 (Dr. Michael Guerrero, personal communication). The mechanism through which Cas controls BCAR3 expression still remains uncertain. However, studies analyzing newly synthesized protein by labeling with an amino acid analog of methionine suggested that Cas may regulate BCAR3 protein synthesis (Dr. Michael Guerrero, personal

communication). These data, together with work presented above, suggest the presence of a positive feedback loop in which Cas controls BCAR3 expression, which in turn helps to stabilize Cas and augment its signaling.

A1.3.2 The mechanism of Cas stabilization by BCAR3

In this study, we show that the half-life of endogenous Cas is greatly increased upon exogenous expression of WT BCAR3 (**Figure A1.1A**). We fail to observe this increase upon exogenous expression of a Cas-binding mutant of BCAR3, demonstrating that direct interaction is required for Cas stabilization (**Figure A1.1B**). BCAR3 promotes Cas/Src interactions, resulting in Src-dependent tyrosine phosphorylation of the substrate domain of Cas (Schuh *et al.*, 2010). The ability of BCAR3 to promote Cas/Src interactions and Src activity requires direct interaction with Cas (Wallez *et al.*, 2014). Taken together, these data suggest that one possible explanation for the stabilization of Cas upon direct binding with BCAR3 is enhanced Cas phosphorylation by Src.

Another possibility is that the binding of BCAR3 to Cas directly impairs Cas protein degradation. For example, the binding between BCAR3 and Cas may prevent the interaction between Cas and ubiquitin ligases that target it for degradation. Ubiquitin ligases interact with the carboxy-terminal domain of Cas, the same domain through which BCAR3 binds to Cas. The interaction of Cas with ubiquitin ligases, including AIP4 and APC/C-CDH1, results in proteolytic degradation of Cas (Di Stefano *et al.*, 2011; Wallez *et al.*, 2012). If BCAR3 interaction with Cas prevents the binding of ubiquitin ligases to Cas, this could explain the stabilization of Cas protein observed upon expression of WT but not Cas binding mutants of BCAR3. Finally, BCAR3 may inhibit Cas degradation by altering Cas localization. It is possible that direct binding between BCAR3 and Cas localizes Cas to a region of the cell where the signals and/or machinery that control Cas degradation may not be accessible.

A1.3.3 Differences in BCAR3 shRNA vs siRNA knockdown on Cas protein levels

In some breast cancer cell lines, we observe a loss of Cas protein upon shRNA depletion of BCAR3 (**Figure A1.2**). Interestingly, this loss of Cas protein is not observed upon siRNA knockdown of BCAR3, at least for certain cell lines like BT549 (Schuh *et al.*, 2010). One possible explanation for this difference is that long-term depletion of BCAR3 in stable shRNA lines has a pronounced effect on Cas that is not observed in the more limited time course of transient transfection with siRNAs. As shown above, Cas is a very stable protein with a half-life of approximately 35 hours (**Figure A1.1**).

A1.3.4 Cell line-specific control of Cas protein expression by BCAR3

We show here that BCAR3 depletion by shRNA results in the loss of Cas protein in some breast cancer cell lines, while other cell lines fail to show this relationship between BCAR3 and Cas (**Figure A1.2**). It is yet to be determined how BCAR3 regulates Cas protein differently in multiple cell lines. One possibility is the presence or absence of other BCAR3 family members. BCAR3 is a member of the novel Src homology 2 (SH2)-containing protein (NSP) family that includes two other proteins; NSP1 and NSP3. Transient transfection of all three NSP family members increases levels of Cas proteins in MCF7 cells (Near *et al.*, 2007). As different breast cancer cell lines have different levels of mRNA and protein expression of the three NSP family members, it is possible that BCAR3 strongly controls Cas expression in those cell lines where BCAR3 is the only or most dominantly expressed NSP family member (Near *et al.*, 2007; Vervoort *et al.*, 2007). Additionally, Cas is a scaffolding molecule that binds and interacts with many different proteins inside the cell (Defilippi *et al.*, 2006). The cell line-specific dependence of Cas protein expression on BCAR3 may be explained by the presence or absence of other Cas binding proteins outside of the NSP family members.

List of References

- Akakura, S., Kar, B., Singh, S., Cho, L., Tibrewal, N., Sanokawa-Akakura, R., Reichman, C., Ravichandran, K. S., and Birge, R. B. (2005). C-terminal SH3 domain of CrkII regulates the assembly and function of the DOCK180/ELMO Rac-GEF. *J. Cell. Physiol.* *204*, 344–351.
- Arkin, M. R., Tang, Y., and Wells, J. A. (2014). Small-molecule inhibitors of protein-protein interactions: progressing toward the reality. *Chem. Biol.* *21*, 1102–1114.
- Arkin, M. R., and Wells, J. A. (2004). Small-molecule inhibitors of protein-protein interactions: progressing towards the dream. *Nat. Rev. Drug Discov.* *3*, 301–317.
- Barcellos-Hoff, M. H., and Akhurst, R. J. (2009). Transforming growth factor-beta in breast cancer: too much, too late. *Breast Cancer Res.* *11*, 202.
- Barros, M. H. M., Hauck, F., Dreyer, J. H., Kempkes, B., and Niedobitek, G. (2013). Macrophage polarisation: an immunohistochemical approach for identifying M1 and M2 macrophages. *PLoS One* *8*, e80908.
- Belizário, J. E. (2009). Immunodeficient Mouse Models: An Overview. *Open Immunol. J.* *2*, 79–85.
- Bombonati, A., and Sgroi, D. C. (2011). The molecular pathology of breast cancer progression. *J. Pathol.* *223*, 307–317.
- Vanden Borre, P., Near, R. I., Makkinje, A., Mostoslavsky, G., and Lerner, A. (2011). BCAR3/AND-34 can signal independent of complex formation with CAS family members or the presence of p130Cas. *Cell. Signal.* *23*, 1030–1040.
- Bourdeanu, L., and Liu, E. A. (2015). Systemic treatment for breast cancer: chemotherapy and biotherapy agents. *Semin. Oncol. Nurs.* *31*, 156–162.
- Bouton, A. H., and Burnham, M. R. (1997). Detection of distinct pools of the adapter protein p130CAS using a panel of monoclonal antibodies. *Hybridoma* *16*, 403–411.
- Bouton, A. H., Riggins, R. B., and Bruce-Staskal, P. J. (2001). Functions of the adapter protein Cas: signal convergence and the determination of cellular responses. *Oncogene* *20*, 6448–6458.
- Brady, N. J., Chuntova, P., and Schwertfeger, K. L. (2016). Macrophages: Regulators of the Inflammatory Microenvironment during Mammary Gland Development and Breast Cancer. *2016*.
- Brantley, D. M., Chen, C. L., Muraoka, R. S., Bushdid, P. B., Bradberry, J. L., Kittrell, F., Medina, D., Matrisian, L. M., Kerr, L. D., and Yull, F. E. (2001). Nuclear factor-kappaB (NF-kappaB) regulates proliferation and branching in mouse mammary epithelium. *Mol. Biol. Cell* *12*, 1445–1455.

Braunstein, L. Z., and Taghian, A. G. (2016). Molecular Phenotype, Multigene Assays, and the Locoregional Management of Breast Cancer. *Semin. Radiat. Oncol.* *26*, 9–16.

Broussard, J. A., Webb, D. J., and Kaverina, I. (2008). Asymmetric focal adhesion disassembly in motile cells. *Curr. Opin. Cell Biol.* *20*, 85–90.

Buijs, J. T., Stayrook, K. R., and Guise, T. A. (2012). The role of TGF- β in bone metastasis: novel therapeutic perspectives. *Bonekey Rep.* *1*, 96.

Burnham, M. R., Bruce-Staskal, P. J., Harte, M. T., Weidow, C. L., Ma, A., Weed, S. A., and Bouton, A. H. (2000). Regulation of c-SRC activity and function by the adapter protein CAS. *Mol. Cell. Biol.* *20*, 5865–5878.

Cabodi, S. *et al.* (2006). p130Cas as a new regulator of mammary epithelial cell proliferation, survival, and HER2-neu oncogene-dependent breast tumorigenesis. *Cancer Res.* *66*, 4672–4680.

Cabodi, S., del Pilar Camacho-Leal, M., Di Stefano, P., and Defilippi, P. (2010). Integrin signalling adaptors: not only figurants in the cancer story. *Nat. Rev. Cancer* *10*, 858–870.

Cerami, E. *et al.* (2012). The cBio cancer genomics portal: an open platform for exploring multidimensional cancer genomics data. *Cancer Discov.* *2*, 401–404.

Chavez, K. J., Garimella, S. V, and Lipkowitz, S. (2010). Triple negative breast cancer cell lines: one tool in the search for better treatment of triple negative breast cancer. *Breast Dis.* *32*, 35–48.

Chen, J., Diacovo, T. G., Grenache, D. G., Santoro, S. A., and Zutter, M. M. (2002). The $\alpha 2$ Integrin Subunit-Deficient Mouse. *Am. J. Pathol.* *161*, 337–344.

Cheng, N., Bhowmick, N. A., Chytil, A., Gorksa, A. E., Brown, K. A., Muraoka, R., Arteaga, C. L., Neilson, E. G., Hayward, S. W., and Moses, H. L. (2005). Loss of TGF-beta type II receptor in fibroblasts promotes mammary carcinoma growth and invasion through upregulation of TGF-alpha-, MSP- and HGF-mediated signaling networks. *Oncogene* *24*, 5053–5068.

Condamine, T., Ramachandran, I., Youn, J.-I., and Gabrilovich, D. I. (2015). Regulation of tumor metastasis by myeloid-derived suppressor cells. *Annu. Rev. Med.* *66*, 97–110.

Connolly, E. C., Freimuth, J., and Akhurst, R. J. (2012). Complexities of TGF- β targeted cancer therapy. *Int. J. Biol. Sci.* *8*, 964–978.

Crowley, M. R., Bowtell, D., and Serra, R. (2005). TGF-beta, c-Cbl, and PDGFR-alpha the in mammary stroma. *Dev. Biol.* *279*, 58–72.

Dai, X., Li, T., Bai, Z., Yang, Y., Liu, X., Zhan, J., and Shi, B. (2015). Breast cancer intrinsic subtype classification, clinical use and future trends. *Am. J. Cancer Res.* *5*, 2929–2943.

Dalton, L. W., Page, D. L., and Dupont, W. D. (1994). Histologic grading of breast carcinoma. A reproducibility study. *Cancer* 73, 2765–2770.

Davison, Z., de Blacquièrre, G. E., Westley, B. R., and May, F. E. B. (2011). Insulin-like growth factor-dependent proliferation and survival of triple-negative breast cancer cells: implications for therapy. *Neoplasia* 13, 504–515.

Debnath, J., Muthuswamy, S. K., and Brugge, J. S. (2003). Morphogenesis and oncogenesis of MCF-10A mammary epithelial acini grown in three-dimensional basement membrane cultures. *Methods* 30, 256–268.

Defilippi, P., Di Stefano, P., and Cabodi, S. (2006). p130Cas: a versatile scaffold in signaling networks. *Trends Cell Biol.* 16, 257–263.

Dorssers, L. C. J. *et al.* (2004). The prognostic value of BCAR1 in patients with primary breast cancer. *Clin. Cancer Res.* 10, 6194–6202.

Edmondson, R., Broglie, J. J., Adcock, A. F., and Yang, L. (2014). Three-dimensional cell culture systems and their applications in drug discovery and cell-based biosensors. *Assay Drug Dev. Technol.* 12, 207–218.

Elsberger, B., Tan, B. A., Mitchell, T. J., Brown, S. B. F., Mallon, E. A., Tovey, S. M., Cooke, T. G., Brunton, V. G., and Edwards, J. (2009). Is expression or activation of Src kinase associated with cancer-specific survival in ER-, PR- and HER2-negative breast cancer patients? *Am. J. Pathol.* 175, 1389–1397.

Elston, C. W., and Ellis, I. O. (1991). pathological prognostic factors in breast cancer. I. The value of histological grade in breast cancer: experience from a large study with long-term follow-up. *Histopathology* 19, 403–410.

Ewald, A. J. (2013). Isolation of mouse mammary organoids for long-term time-lapse imaging. *Cold Spring Harb. Protoc.* 2013, 130–133.

Ewald, A. J., Brenot, A., Duong, M., Chan, B. S., and Werb, Z. (2008). Collective epithelial migration and cell rearrangements drive mammary branching morphogenesis. *Dev. Cell* 14, 570–581.

Farabaugh, S. M., Boone, D. N., and Lee, A. V (2015). Role of IGF1R in Breast Cancer Subtypes, Stemness, and Lineage Differentiation. *Front. Endocrinol. (Lausanne).* 6, 59.

Finn, R. S. (2008). Targeting Src in breast cancer. *Ann. Oncol.* 19, 1379–1386.

Finn, R. S., Bengala, C., Ibrahim, N., Roché, H., Sparano, J., Strauss, L. C., Fairchild, J., Sy, O., and Goldstein, L. J. (2011). Dasatinib as a single agent in triple-negative breast cancer: results of an open-label phase 2 study. *Clin. Cancer Res.* 17, 6905–6913.

Galliher-Beckley, A. J., and Schiemann, W. P. (2008). Grb2 binding to Tyr284 in TbetaR-II is essential for mammary tumor growth and metastasis stimulated by TGF-beta. *Carcinogenesis* 29, 244–251.

- Gao, J. *et al.* (2013). Integrative analysis of complex cancer genomics and clinical profiles using the cBioPortal. *Sci. Signal.* 6, p11.
- Gong, D., Shi, W., Yi, S., Chen, H., Groffen, J., and Heisterkamp, N. (2012). TGF β signaling plays a critical role in promoting alternative macrophage activation. *BMC Immunol.* 13, 31.
- Guerrero, M. S., Parsons, J. T., and Bouton, A. H. (2012). Cas and NEDD9 Contribute to Tumor Progression through Dynamic Regulation of the Cytoskeleton. *Genes Cancer* 3, 371–381.
- Guo, J. *et al.* (2014). Breast Cancer Anti-Estrogen Resistance-3 inhibits transforming growth factor- β /Smad signaling and associates with favorable breast cancer disease outcomes. *Breast Cancer Res.* 16, 476.
- Guy, C. T., Muthuswamy, S. K., Cardiff, R. D., Soriano, P., and Muller, W. J. (1994). Activation of the c-Src tyrosine kinase is required for the induction of mammary tumors in transgenic mice. *Genes Dev.* 8, 23–32.
- Hansen, R. K., and Bissell, M. J. (2000). Tissue architecture and breast cancer: the role of extracellular matrix and steroid hormones. *Endocr. Relat. Cancer* 7, 95–113.
- Harder, K. W., Moller, N. P. H., Peacock, J. W., and Jirik, F. R. (1998). Protein-tyrosine Phosphatase Regulates Src Family Kinases and Alters Cell-Substratum Adhesion. *J. Biol. Chem.* 273, 31890–31900.
- Harunaga, J. S., and Yamada, K. M. (2011). Cell-matrix adhesions in 3D. *Matrix Biol.* 30, 363–368.
- Hens, J. R., and Wysolmerski, J. J. (2005). Key stages of mammary gland development: molecular mechanisms involved in the formation of the embryonic mammary gland. *Breast Cancer Res.* 7, 220–224.
- Hinck, L., and Silberstein, G. B. (2005). Key stages in mammary gland development: the mammary end bud as a motile organ. *Breast Cancer Res.* 7, 245–251.
- Hollmén, M., Roudnicky, F., Karaman, S., and Detmar, M. (2015). Characterization of macrophage--cancer cell crosstalk in estrogen receptor positive and triple-negative breast cancer. *Sci. Rep.* 5, 9188.
- Honda, H. *et al.* (1998). Cardiovascular anomaly, impaired actin bundling and resistance to Src-induced transformation in mice lacking p130Cas. *Nat. Genet.* 19, 361–365.
- Huang, F., Reeves, K., Han, X., Fairchild, C., Platero, S., Wong, T. W., Lee, F., Shaw, P., and Clark, E. (2007). Identification of candidate molecular markers predicting sensitivity in solid tumors to dasatinib: rationale for patient selection. *Cancer Res.* 67, 2226–2238.
- Hüsemann, Y. *et al.* (2008). Systemic spread is an early step in breast cancer. *Cancer Cell* 13, 58–68.

Hynes, N. E., and Watson, C. J. (2010). Mammary Gland Growth Factors: Roles in Normal Development and in Cancer. *Cold Spring Harb. Perspect. Biol.* 2, a003186.

Irby, R. B., and Yeatman, T. J. (2000). Role of Src expression and activation in human cancer. *Oncogene* 19, 5636–5642.

Ivanov, A. A., Khuri, F. R., and Fu, H. (2013). Targeting protein-protein interactions as an anticancer strategy. *Trends Pharmacol. Sci.* 34, 393–400.

Kang, Y. S., Jeong, D. E., Lee, E. K., Song, W. K., and Kim, W. (2013). p130Cas controls the susceptibility of cancer cells to TGF- β -induced growth inhibition. *Biochem. Biophys. Res. Commun.* 438, 116–121.

Kenny, P. A. *et al.* (2007). The morphologies of breast cancer cell lines in three-dimensional assays correlate with their profiles of gene expression. *Mol. Oncol.* 1, 84–96.

Khamis, Z. I., Sahab, Z. J., and Sang, Q.-X. A. (2012). Active roles of tumor stroma in breast cancer metastasis. *Int. J. Breast Cancer* 2012, 574025.

Kim, H., Laing, M., and Muller, W. (2005). c-Src-null mice exhibit defects in normal mammary gland development and ER α signaling. *Oncogene* 24, 5629–5636.

Kim, W., Seok Kang, Y., Soo Kim, J., Shin, N.-Y., Hanks, S. K., and Song, W. K. (2008). The integrin-coupled signaling adaptor p130Cas suppresses Smad3 function in transforming growth factor-beta signaling. *Mol. Biol. Cell* 19, 2135–2146.

Kittaneh, M., Montero, A. J., and Glück, S. (2013). Molecular profiling for breast cancer: a comprehensive review. *Biomark. Cancer* 5, 61–70.

Klemke, R. L., Leng, J., Molander, R., Brooks, P. C., Vuori, K., and Cheresch, D. A. (1998). CAS/Crk coupling serves as a “molecular switch” for induction of cell migration. *J. Cell Biol.* 140, 961–972.

Kumbrink, J., de la Cueva, A., Soni, S., Sailer, N., and Kirsch, K. H. (2016). A truncated phosphorylated p130Cas substrate domain is sufficient to drive breast cancer growth and metastasis formation in vivo. *Tumour Biol.*

Lambert, A. W., Ozturk, S., and Thiagalingam, S. (2012). Integrin Signaling in Mammary Epithelial Cells and Breast Cancer. *ISRN Oncol.* 2012, 1–9.

Lanigan, F., Martin, F., and Gallagher, M. (2007). Molecular links between mammary gland development and breast cancer. *Cell. Mol. Life Sci.* 64, 3159–3184.

Leonard, G. D., and Swain, S. M. (2004). Ductal Carcinoma In Situ, Complexities and Challenges. *JNCI J. Natl. Cancer Inst.* 96, 906–920.

Lilla, J. N., and Werb, Z. (2010). Mast cells contribute to the stromal microenvironment in mammary gland branching morphogenesis. *Dev. Biol.* 337, 124–133.

- Lin, E. Y., Jones, J. G., Li, P., Zhu, L., Whitney, K. D., Muller, W. J., and Pollard, J. W. (2003). Progression to malignancy in the polyoma middle T oncoprotein mouse breast cancer model provides a reliable model for human diseases. *Am. J. Pathol.* *163*, 2113–2126.
- Liu, W. *et al.* (2015). The proto-oncogene c-Src and its downstream signaling pathways are inhibited by the metastasis suppressor, NDRG1. *Oncotarget* *6*, 8851–8874.
- Logue, J. S., and Morrison, D. K. (2012). Complexity in the signaling network: insights from the use of targeted inhibitors in cancer therapy. *Genes Dev.* *26*, 641–650.
- Lu, J. *et al.* (2009). Breast cancer metastasis: challenges and opportunities. *Cancer Res.* *69*, 4951–4953.
- Mace, P. D., Wallez, Y., Dobaczewska, M. K., Lee, J. J., Robinson, H., Pasquale, E. B., and Riedl, S. J. (2011). NSP-Cas protein structures reveal a promiscuous interaction module in cell signaling. *Nat. Struct. Mol. Biol.* *18*, 1381–1387.
- Macias, H., and Hinck, L. (2012). Mammary gland development. *Wiley Interdiscip. Rev. Dev. Biol.* *1*, 533–557.
- Mahyar-Roemer, M., and Roemer, K. (2001). p21 Waf1/Cip1 can protect human colon carcinoma cells against p53-dependent and p53-independent apoptosis induced by natural chemopreventive and therapeutic agents. *Oncogene* *20*, 3387–3398.
- Maier, T., Güell, M., and Serrano, L. (2009). Correlation of mRNA and protein in complex biological samples. *FEBS Lett.* *583*, 3966–3973.
- Makki, J. (2015). Diversity of Breast Carcinoma: Histological Subtypes and Clinical Relevance. 23–31.
- Makkinje, A., Near, R. I., Infusini, G., Vanden Borre, P., Bloom, A., Cai, D., Costello, C. E., and Lerner, A. (2009). AND-34/BCAR3 regulates adhesion-dependent p130Cas serine phosphorylation and breast cancer cell growth pattern. *Cell. Signal.* *21*, 1423–1435.
- Marcotte, R., Smith, H. W., Sanguin-gendreau, V., Mcdonough, R. V, and Muller, W. J. (2011). Mammary epithelial-specific disruption of c-Src impairs cell cycle progression and tumorigenesis.
- Mayer, E. L., and Krop, I. E. (2010). Advances in targeting SRC in the treatment of breast cancer and other solid malignancies. *Clin. Cancer Res.* *16*, 3526–3532.
- Mohamed, A., Krajewski, K., Cakar, B., and Ma, C. X. (2013). Targeted therapy for breast cancer. *Am. J. Pathol.* *183*, 1096–1112.
- Montero, J. C., Seoane, S., Ocaña, A., and Pandiella, A. (2011). Inhibition of SRC family kinases and receptor tyrosine kinases by dasatinib: possible combinations in solid tumors. *Clin. Cancer Res.* *17*, 5546–5552.

Moses, H., and Barcellos-Hoff, M. H. (2011). TGF-beta biology in mammary development and breast cancer. *Cold Spring Harb. Perspect. Biol.* 3, a003277.

Mroue, R., and Bissell, M. J. (2013). Three-dimensional cultures of mouse mammary epithelial cells. *Methods Mol. Biol.* 945, 221–250.

Myoui, A., Nishimura, R., Williams, P. J., Hiraga, T., Tamura, D., Michigami, T., Mundy, G. R., and Yoneda, T. (2003). C-SRC tyrosine kinase activity is associated with tumor colonization in bone and lung in an animal model of human breast cancer metastasis. *Cancer Res.* 63, 5028–5033.

Near, R. I., Smith, R. S., Toselli, P. A., Freddo, T. F., Bloom, A. B., Vanden Borre, P., Seldin, D. C., and Lerner, A. (2009). Loss of AND-34/BCAR3 expression in mice results in rupture of the adult lens. *Mol. Vis.* 15, 685–699.

Near, R. I., Zhang, Y., Makkinje, A., Vanden Borre, P., and Lerner, A. (2007). AND-34/BCAR3 differs from other NSP homologs in induction of anti-estrogen resistance, cyclin D1 promoter activation and altered breast cancer cell morphology. *J. Cell. Physiol.* 212, 655–665.

Nero, T. L., Morton, C. J., Holien, J. K., Wielens, J., and Parker, M. W. (2014). Oncogenic protein interfaces: small molecules, big challenges. *Nat. Rev. Cancer* 14, 248–262.

Oakes, S. R., Hilton, H. N., and Ormandy, C. J. (2006). The alveolar switch: coordinating the proliferative cues and cell fate decisions that drive the formation of lobuloalveoli from ductal epithelium. *Breast Cancer Res.* 8, 207.

Pallen, C. J. (2003). Protein tyrosine phosphatase alpha (PTPalpha): a Src family kinase activator and mediator of multiple biological effects. *Curr. Top. Med. Chem.* 3, 821–835.

Parsons, J. T., Horwitz, A. R., and Schwartz, M. A. (2010). Cell adhesion: integrating cytoskeletal dynamics and cellular tension. *Nat. Rev. Mol. Cell Biol.* 11, 633–643.

Parvani, J. G., Taylor, M. A., and Schiemann, W. P. (2011). Noncanonical TGF- β signaling during mammary tumorigenesis. *J. Mammary Gland Biol. Neoplasia* 16, 127–146.

Pencavel, T. D., and Hayes, A. (2009). Breast sarcoma—a review of diagnosis and management. *Int. J. Surg.* 7, 20–23.

Perou, C. M. *et al.* (2000). Molecular portraits of human breast tumours. *Nature* 406, 747–752.

Petrie, R. J., and Yamada, K. M. (2012). At the leading edge of three-dimensional cell migration. *J. Cell Sci.* 125, 5917–5926.

Plante, I., Stewart, M. K. G., and Laird, D. W. (2011). Evaluation of mammary gland development and function in mouse models. *J. Vis. Exp.*, 2–6.

- Prat, A., and Perou, C. M. (2011). Deconstructing the molecular portraits of breast cancer. *Mol. Oncol.* 5, 5–23.
- Provenzano, P. P., Inman, D. R., Eliceiri, K. W., and Keely, P. J. (2009). Matrix density-induced mechanoregulation of breast cell phenotype, signaling and gene expression through a FAK-ERK linkage. *Oncogene* 28, 4326–4343.
- Psaila, B., and Lyden, D. (2009). The metastatic niche: adapting the foreign soil. *Nat. Rev. Cancer* 9, 285–293.
- Pylayeva, Y., Gillen, K. M., Gerald, W., Beggs, H. E., Reichardt, L. F., and Giancotti, F. G. (2009). Ras- and PI3K-dependent breast tumorigenesis in mice and humans requires focal adhesion kinase signaling. *J. Clin. Invest.* 119, 252–266.
- Quail, D. F., and Joyce, J. A. (2013). Microenvironmental regulation of tumor progression and metastasis. *Nat. Med.* 19, 1423–1437.
- Raftopoulou, M., and Hall, A. (2004). Cell migration: Rho GTPases lead the way. *Dev. Biol.* 265, 23–32.
- Ramaswamy, S., Ross, K. N., Lander, E. S., and Golub, T. R. (2003). A molecular signature of metastasis in primary solid tumors. *Nat. Genet.* 33, 49–54.
- Rao, G. R., Rawls, W. E., Perey, D. Y., and Tompkins, W. A. (1977). Macrophage activation in congenitally athymic mice raised under conventional or germ-free conditions. *J. Reticuloendothel. Soc.* 21, 13–20.
- Reed, J. R., and Schwertfeger, K. L. (2010). Immune cell location and function during post-natal mammary gland development. *J. Mammary Gland Biol. Neoplasia* 15, 329–339.
- Resnier, P., Montier, T., Mathieu, V., Benoit, J.-P., and Passirani, C. (2013). A review of the current status of siRNA nanomedicines in the treatment of cancer. *Biomaterials* 34, 6429–6443.
- Riggins, R. B. *et al.* (2006). Physical and functional interactions between Cas and c-Src induce tamoxifen resistance of breast cancer cells through pathways involving epidermal growth factor receptor and signal transducer and activator of transcription 5b. *Cancer Res.* 66, 7007–7015.
- Riggins, R. B., Quilliam, L. A., and Bouton, A. H. (2003). Synergistic promotion of c-Src activation and cell migration by Cas and AND-34/BCAR3. *J. Biol. Chem.* 278, 28264–28273.
- Roskoski, R. (2004). Src protein-tyrosine kinase structure and regulation. *Biochem. Biophys. Res. Commun.* 324, 1155–1164.

- Rudel, R. A., Fenton, S. E., Ackerman, J. M., Euling, S. Y., and Makris, S. L. (2011). Environmental exposures and mammary gland development: state of the science, public health implications, and research recommendations. *Environ. Health Perspect.* *119*, 1053–1061.
- Sable, R., and Jois, S. (2015). Surfing the protein-protein interaction surface using docking methods: Application to the design of PPI inhibitors. *Molecules* *20*, 11569–11603.
- Schrecengost, R. S., Riggins, R. B., Thomas, K. S., Guerrero, M. S., and Bouton, A. H. (2007). Breast cancer antiestrogen resistance-3 expression regulates breast cancer cell migration through promotion of p130Cas membrane localization and membrane ruffling. *Cancer Res.* *67*, 6174–6182.
- Schuh, N. R., Guerrero, M. S., Schrecengost, R. S., and Bouton, A. H. (2010). BCAR3 regulates Src/p130 Cas association, Src kinase activity, and breast cancer adhesion signaling. *J. Biol. Chem.* *285*, 2309–2317.
- Scully, O. J., Bay, B.-H., Yip, G., and Yu, Y. (2012). Breast Cancer Metastasis. *Cancer Genomics Proteomics* *9*, 311–320.
- Sgroi, D. C. (2010). Preinvasive breast cancer. *Annu. Rev. Pathol.* *5*, 193–221.
- Shen, H., Mittal, V., Ferrari, M., and Chang, J. (2013). Delivery of gene silencing agents for breast cancer therapy. *Breast Cancer Res.* *15*, 205.
- Sicinski, P., and Weinberg, R. A. (1997). A Specific Role for Cyclin D1 in Mammary Gland Development. *J. Mammary Gland Biol. Neoplasia* *2*, 335–342.
- Sleeman, J. P., Christofori, G., Fodde, R., Collard, J. G., Berx, G., Decraene, C., and Rüegg, C. (2012). Concepts of metastasis in flux: the stromal progression model. *Semin. Cancer Biol.* *22*, 174–186.
- Soni, A., Ren, Z., Hameed, O., Chanda, D., Morgan, C. J., Siegal, G. P., and Wei, S. (2015). Breast cancer subtypes predispose the site of distant metastases. *Am. J. Clin. Pathol.* *143*, 471–478.
- Sørli, T. *et al.* (2001). Gene expression patterns of breast carcinomas distinguish tumor subclasses with clinical implications. *Proc. Natl. Acad. Sci. U. S. A.* *98*, 10869–10874.
- Standish, L. J., Sweet, E. S., Novack, J., Wenner, C. A., Bridge, C., Nelson, A., Martzen, M., and Torkelson, C. (2008). Breast cancer and the immune system. *J. Soc. Integr. Oncol.* *6*, 158–168.
- Di Stefano, P. *et al.* (2011). The adaptor proteins p140CAP and p130CAS as molecular hubs in cell migration and invasion of cancer cells. *Am. J. Cancer Res.* *1*, 663–673.
- Sternlicht, M. D. (2006). Key stages in mammary gland development: the cues that regulate ductal branching morphogenesis. *Breast Cancer Res.* *8*, 201.

Sternlicht, M. D., Kouros-Mehr, H., Lu, P., and Werb, Z. (2006). Hormonal and local control of mammary branching morphogenesis. *Differentiation* 74, 365–381.

Sun, G., Cheng, S. Y. S., Chen, M., Lim, C. J., and Pallen, C. J. (2012). Protein tyrosine phosphatase α phosphotyrosyl-789 binds BCAR3 to position Cas for activation at integrin-mediated focal adhesions. *Mol. Cell. Biol.* 32, 3776–3789.

Tornillo, G., Defilippi, P., and Cabodi, S. (2014). Cas proteins: dodgy scaffolding in breast cancer. *Breast Cancer Res.* 16, 443.

VanAgthoven, T., VanAgthoven, T. L., Dekker, A., VanderSpek, P. J., Vreede, L., and Dorssers, L. C. (1998). Identification of BCAR3 by a random search for genes involved in antiestrogen resistance of human breast cancer cells. *EMBO J.* 17, 2799–2808.

Vervoort, V. S., Roselli, S., Oshima, R. G., and Pasquale, E. B. (2007). Splice variants and expression patterns of SHEP1, BCAR3 and NSP1, a gene family involved in integrin and receptor tyrosine kinase signaling. *Gene* 391, 161–170.

Vogelstein, B., Papadopoulos, N., Velculescu, V. E., Zhou, S., Diaz, L. A., and Kinzler, K. W. (2013). Cancer genome landscapes. *Science* 339, 1546–1558.

Wallden, B. *et al.* (2015). Development and verification of the PAM50-based Prosigna breast cancer gene signature assay. *BMC Med. Genomics* 8, 54.

Wallez, Y., Mace, P. D., Pasquale, E. B., and Riedl, S. J. (2012). NSP-CAS Protein Complexes: Emerging Signaling Modules in Cancer. *Genes Cancer* 3, 382–393.

Wallez, Y., Riedl, S. J., and Pasquale, E. B. (2014). Association of the breast cancer antiestrogen resistance protein 1 (BCAR1) and BCAR3 scaffolding proteins in cell signaling and antiestrogen resistance. *J. Biol. Chem.* 289, 10431–10444.

Wang, S., Yuan, Y., Liao, L., Kuang, S.-Q., Tien, J. C.-Y., O'Malley, B. W., and Xu, J. (2009). Disruption of the SRC-1 gene in mice suppresses breast cancer metastasis without affecting primary tumor formation. *Proc. Natl. Acad. Sci. U. S. A.* 106, 151–156.

Webb, D. J., Donais, K., Whitmore, L. A., Thomas, S. M., Turner, C. E., Parsons, J. T., and Horwitz, A. F. (2004). FAK-Src signalling through paxillin, ERK and MLCK regulates adhesion disassembly. *Nat. Cell Biol.* 6, 154–161.

Weigelt, B., Glas, A. M., Wessels, L. F. A., Witteveen, A. T., Peterse, J. L., and van't Veer, L. J. (2003). Gene expression profiles of primary breast tumors maintained in distant metastases. *Proc. Natl. Acad. Sci.* 100, 15901–15905.

Weigelt, B., Peterse, J. L., and van 't Veer, L. J. (2005). Breast cancer metastasis: markers and models. *Nat. Rev. Cancer* 5, 591–602.

Wendt, M. K., Smith, J. A., and Schiemann, W. P. (2009). p130Cas is required for mammary tumor growth and transforming growth factor- β -mediated metastasis through regulation of Smad2/3 activity. *J. Biol. Chem.* 284, 34145–34156.

- Weng, D., Penzner, J. H., Song, B., Koido, S., Calderwood, S. K., and Gong, J. (2012). Metastasis is an early event in mouse mammary carcinomas and is associated with cells bearing stem cell markers. *Breast Cancer Res.* *14*, R18.
- Wiechmann, L., and Kuerer, H. M. (2008). The molecular journey from ductal carcinoma in situ to invasive breast cancer. *Cancer* *112*, 2130–2142.
- Wilson, A. L., Schrecengost, R. S., Guerrero, M. S., Thomas, K. S., and Bouton, A. H. (2013). Breast cancer antiestrogen resistance 3 (BCAR3) promotes cell motility by regulating actin cytoskeletal and adhesion remodeling in invasive breast cancer cells. *PLoS One* *8*, e65678.
- Wiseman, B. S. (2002). Stromal Effects on Mammary Gland Development and Breast Cancer. *Science* (80-.). *296*, 1046–1049.
- Wyckoff, J., Wang, W., Lin, E. Y., Wang, Y., Pixley, F., Stanley, E. R., Graf, T., Pollard, J. W., Segall, J., and Condeelis, J. (2004). A paracrine loop between tumor cells and macrophages is required for tumor cell migration in mammary tumors. *Cancer Res.* *64*, 7022–7029.
- Xu, C., and Wang, J. (2015). Delivery systems for siRNA drug development in cancer therapy. *Asian J. Pharm. Sci.* *10*, 1–12.
- Yamazaki, D., Kurisu, S., and Takenawa, T. (2009). Involvement of Rac and Rho signaling in cancer cell motility in 3D substrates. *Oncogene* *28*, 1570–1583.
- Yang, I. V, Jiang, W., Rutledge, H. R., Lackford, B., Warg, L. A., De Arras, L., Alper, S., Schwartz, D. A., and Pisetsky, D. S. (2011). Identification of novel innate immune genes by transcriptional profiling of macrophages stimulated with TLR ligands. *Mol. Immunol.* *48*, 1886–1895.
- Yu, Y., Hao, Y., and Feig, L. A. (2006). The R-Ras GTPase mediates cross talk between estrogen and insulin signaling in breast cancer cells. *Mol. Cell. Biol.* *26*, 6372–6380.
- Zhang, Y. E. (2009). Non-Smad pathways in TGF-beta signaling. *Cell Res.* *19*, 128–139.
- Zhao, Y., Kumbrink, J., Lin, B.-T., Bouton, A. H., Yang, S., Toselli, P. A., and Kirsch, K. H. (2013). Expression of a phosphorylated substrate domain of p130Cas promotes PyMT-induced c-Src-dependent murine breast cancer progression. *Carcinogenesis* *34*, 2880–2890.
- Zhu, J., Xiong, G., Trinkle, C., and Xu, R. (2014). Integrated extracellular matrix signaling in mammary gland development and breast cancer progression. *Histol. Histopathol.* *29*, 1083–1092.